REGULATION OF MEMBRANE ASYMMETRY BY GOLGI P4-ATPASES AND THEIR INTERACTORS

By

Mehmet Takar

Dissertation

Submitted to the Faculty

of the Graduate School of Vanderbilt University

in partial fulfillment of the requirements

for the degree of

DOCTOR OF PHILOSOPHY

in

Biological Sciences

December 15, 2018

Nashville, Tennessee

Approved:

Brandt Eichman, Ph.D.

Katherine L. Friedman, Ph.D.

Todd R. Graham, Ph.D

Kathleen L. Gould, Ph.D.

John D. York, Ph.D.

DEDICATION

This work is dedicated to Nergis Kara and Ela Takar,

who make my life wonderful

ACKNOWLEDGEMENTS

This work was made possible by the support of many. Foremost, I want to thank Todd for giving me the opportunity to join his lab. Todd has influenced me as a scientist in countless ways, but perhaps the greatest lesson he taught me is the art of mentorship. Very early in my training, Todd identified my strengths and weaknesses and thereby created an environment that fostered not only my analytical and scientific skills, but also my independence and resilience. I have been so lucky to have a mentor who is so passionate and motivated as much as Todd.

I also want to thank my committee members, Brandt Eichman, Katherine L. Friedman, Kathleen L. Gould, and John D. York. I'm grateful for their sharing of time and expertise, particularly for their positive criticisms and valuable guidance. I also want to thank Jason MacGurn and his lab members for technical guidance. I want to thank our collaborator Charles Boone (University of Toronto) for the opportunity of participating in their exciting projects.

I would like to thank my current and former fellow lab members Jordan Best, Hannah Hankins, Ryan Baldridge, especially two incredible postdocs Bart Roland and Peng Xu for both their conceptual and technical guidance throughout my graduate studies. I also want to thank my incredibly talented mentee Yannan Huang for her great contributions. Without any of them, there would not have been a stimulating, productive and exciting work environment with a lots of laughs. Lastly, I would like to thank my Turkish friend, Gokhan Unlu who always provide me with constructive criticisms as well as great support my life .

I would like to also thank my mom, whose endless sacrifices in her life helped me transform me from being a illiterate kid to a scientist. I also cannot thank my dad and my sisters for their endless support. Again, I thank my wife Nergis Kara for her endless love and support.

TABLE OF CONTENTS

Page

DEDICATION ..... **ii**

ACKNOWLEDGEMENTS ..... **iii**

ABBREVIATIONS ..... **viii**

CHAPTER I **1**

INTRODUCTION **1**
- **Thesis Overview** **1**
- **Membrane Asymmetry** **2**
- **The Aminophospholipid Translocase** **3**
- **Division of Labor Among P4-ATPases in Budding Yeast** **5**
  - P-type ATPases and the P4-ATPases 5
  - The P4-ATPase Giant Substrate problem and potential transport mechanisms 10
  - What is the purpose of pumping PL across the membrane? 16
  - Concluding remarks 23
- **Neo1 Regulatory Network** **24**

CHAPTER II **32**

THE ESSENTIAL NEO1 FROM BUDDING YEAST PLAYS A ROLE IN ESTABLISHING AMINOPHOSPHOLIPID ASYMMETRY OF THE PLASMA MEMBRANE[1] **32**
- **Abstract** **32**
- **Introduction** **33**
- **Results** **37**
  - Inactivation of Neo1 causes a loss of membrane asymmetry 36
  - Exposure of PE and PS on *neo1*^{ts} cells is not a secondary effect of Drs2/Dnf mislocalization or loss of activity at the plasma membrane 38
  - Relationship between P4-ATPases that potentially flip PE 46
- **Discussion** **52**
- **Materials and Methods** **56**
  - Reagents 56
  - Strains and plasmid construction 57
  - Sensitivity Assays 58
  - Quinacrine staining 58
  - Lipid uptake assay 58
  - Fluorescence microscopy 59
  - Vacuolar staining 59
  - Western blot analysis 59
  - Subcellular fractionation 59
- **Acknowledgements** **60**

CHAPTER III **63**

NEO1-ANY1-DRS2 AXIS IS REQUIRED FOR VIABILITY AND **63**

PLASMA MEMBRANE ASYMMETRY **63**
- **Abstract** **63**

Introduction **64**
Materials and Methods **67**
Reagents 67
Toxin Sensitivity assays 68
Lipid uptake assays 68
Fluorescence microscopy 69
Immunoprecipitation and Western blot analysis 69
Results **70**
PS flippase activity is required in *any1* deficient Golgi membranes 70
Overexpression of Any1 is toxic to P4-ATPase mutants. 74
Neo1[Y222S] is a dominant gain of function mutation that suppresses *drs2*Δ defects 77
The gain of function phenotype of Neo1[Y222S] is dependent on Any1 80
Interaction between Neo1 and Any1 83
Discussion **83**

CHAPTER IV **95**

CONCLUSIONS AND FUTURE DIRECTIONS **95**
The Essential Neo1 protein from Budding Yeast Plays a Role in Establishing Aminophospholipid Asymmetry of the Plasma Membrane **95**
Neo1-Any1-Drs2 axis is required for viability and plasma membrane asymmetry **100**
Future Directions **108**

APPENDIX **109**
Appendix 1. Strains and plasmids used in Chapter 2. ..... **109**
Appendix 2. Strains and plasmids used in Chapter 3. ..... **112**

REFERENCES **116**

LIST OF TABLES

Table Page

Table 1-1: Human and yeast P4-ATPases with their ß-subunits and localizations. 7

Table 2-1: Approximate IC_{50} values for strains treated with cytotoxic peptides at the indicated temperatures 61

Table 3-1: Survey of Neo1 mutants for growth. 77

Table 4-1: Physical interactors of Any1 and Neo1 from the SGD 105

LIST OF FIGURES

Figure Page

Figure 1-1: Membrane topology diagram of a P4-ATPase. 9

Figure 1-2: Post-Alber's cycle of P4-ATPase. 11

Figure 1-3: Intrinsic and extrinsic regulators of P4-ATPase activity in *S. cerevisiae.* 20

Figure 1-4: Negative extrinsic regulators of Golgi P4-ATPases Drs2 and Neo1 22

Figure 2-1: *neo1*^{ts} cells display a loss of membrane asymmetry. 36

Figure 2-2: Inactivation of Neo1 does not lead to significant changes in the distribution or expression of Drs2/Dnf P4-ATPases, but does increase Dnf1 and Dnf2 plasma membrane flippase activity. 39

Figure 2-3: *neo1*^{ts} mutants display a dramatic loss of membrane asymmetry at growth temperatures that do not disrupt protein trafficking. 40

Figure 2-4: *NEO1* exerts an essential function that cannot be provided by *DNF1* or *DRS2* 44

Figure 2-5: Moderate overexpression of *DNF1* or *DRS2* failed to suppress loss of membrane asymmetry in *neo1-1* cells 48

Figure 2-6: *NEO1* overexpression weakly suppresses *drs2*Δ, but not *dnf1,2,3*Δ. 50

Figure 2-7: Moderate overexpression of *NEO1* can partially suppress loss of PE and PS asymmetry in *drs2*Δ cells, but not in *dnf1,2*Δ cells 54

Figure 3-1: PS-flip in the Golgi membranes is required for viability. 71

Figure 3-2: Any1 is in strong genetic interaction with Neo1, but not other P4-ATPases 74

Figure 3-3: Overexpression of *ANY1* partially inhibits the growth of *drs2*Δ

and *dnf1,2*Δ mutants, but it is detrimental to *neo1*^{ts}, *dop1*^{ts} and *mon2*Δ mutants 76

Figure 3-4: Overexpression of *ANY1* induces partial loss of PE asymmetry,but not loss of PS asymmetry in wild-type and *drs2*Δ cells. 80

Figure 3.5: Neo1[Y222S] is a gain-of-function mutant that can suppress both growth and membrane asymmetry defects of *drs2*Δ mutant 82

Figure 3-6: Reciprocal Dnf1[S243Y] mutant failed to complement the Dnf1 function, but it gained an ability to transport PS... 84

Figure 3-7: Neo1[Y222S] is a dominant gain-of-function mutant that can partially suppress both growth and membrane asymmetry defects of *drs2*Δ mutant cells in the presence of wild-type Neo1 86

Figure 3-8: Loss of Any1 abolishes the gain-of-function phenotype of Neo1[Y222S]... 88

Figure 3-9: Neo1[Y222S] mutant is significantly more enriched in Drs2-positive compartments than wild-type Neo1 90

Figure 3-10: Any1 physically interacts with Neo1 in the Golgi-enriched membranes 92

ABBREVIATIONS

PS	Phosphatidylserine
PE	Phosphatidylethanolamine
PC	Phosphatidylcholine
PI	Phosphatidylinositol
SM	Sphingomyelin
IPC	Inositolphosphoryl-ceramide
NBD	7-nitro-2-1,3-benzoxadiazol-4-yl
PapA	Papuamide A
5-FOA	5-fluoroorotic acid
P4-ATPase	Type IV P-type ATPase or flippase
PI(4)P	Phosphatidylinsotiol-4-phosphate
ER	Endoplasmic reticulum
TGN	*trans*-Golgi network
PM	Plasma membrane
WT	Wild type
AP-1	Adaptor protein 1
GGA	Golgi-localized, γ-ear containing, Arf-binding family of proteins
Arf1	ADP ribosylation factor
COPI	Coatomer protein 1
Snx3	Sorting nexin-3
CHAPS	3-[(3-Cholamidopropyl)Dimethylammonio]-1-Propanesulfanate

CHAPTER I

INTRODUCTION

Thesis Overview

Neo1 was discovered in a multi-copy suppressor screen in *Saccharomyces cerevisiae* to search for factors conferring resistance against an aminoglycoside antibiotic, neomycin (1). Aminoglycoside antibiotics, used to treat bacterial infections by interfering with proofreading during protein synthesis, cause hearing loss in genetically susceptible individuals. It remains unclear why Neo1 overexpression confers resistance to neomycin. Among the yeast P4-ATPases, Neo1 is the only essential P4-ATPase and it has critical roles in COPI-mediated retrograde transport as well as Golgi glycosylation (2,3). In addition, *neo1*^{ts} mutants display hyperacidification of Golgi membranes and this defect is tightly associated with Neo1's role in Golgi glycosylation (4). My thesis research studies revealed that Neo1 regulates phosphatidylethanolamine (PE) and phosphatidylserine (PS) asymmetry of the plasma membrane, supporting its proposed function as a phospholipid flippase (5). I provided evidence for the regulation of plasma membrane asymmetry directly by Neo1 rather than indirectly by influencing the activity of Drs2/Dnf P4-ATPases (5). Neo1 also regulates the vacuole fusion machinery and our data suggest this occurs through the enrichment of PE on the cytosolic leaflet of the vacuole membrane (6). The Neo1 homolog Tat-5 in *C. elegans* was also associated with PE transport activity during embryonic development (7). Together these studies suggest PE is the primary transport substrate for the Neo1/Tat-5/ATP9 orthologs. Unlike Drs2/Dnf P4-ATPases, Neo1 and its human orthologues (Atp9a and Atp9b) do not require a Cdc50-related beta-subunit for either its ER exit nor for its function in vivo (8-11). Evidence others and we have accumulated strongly

support the hypothesized role of Neo1 as a phospholipid transporter, but it is still unclear how Neo1 activity is regulated in the Golgi/endosomal membranes.

In the second part of my thesis, we discovered a novel factor antagonizing the Golgi flippase activity called *A*ntagonize*s N*eo1 *Y*east phospholipid flippase (*ANY1)* in a collaborative study with Charles Boone's research group. We found that *any1*Δ completely suppresses the defects that occur from loss of Neo1 and its interaction partners Dop1 and Mon2. Our collaborative study showed that overexpression of Any1 redistributes PS pools from the plasma membrane to internal organelles. On the contrary, overexpression of Any1 only leads to the partial loss of PE asymmetry, but not PS asymmetry. I further identified an essential requirement for a PS flippase activity in the Golgi membranes in the absence of Any1. Serendipitously, I determined that a mutation in transmembrane segment 2 of Neo1 (Neo1[Y222S]) can suppress *drs2*Δ growth and membrane asymmetry defects. More interestingly, I revealed that the gain of function phenotype is dependent on Any1. Molecular interaction studies performed by immunoprecipitation and proteomics also determined that Neo1 and Any1 physically interact with each other in the Golgi membranes, but it is not clear whether the GOF phenotype of Neo1[Y222S] is due to the loss of Any1 and Neo1 interaction. In summary, Any1 has been introduced as a regulator of lipid landscape in the Golgi/endosomal system.

Membrane Asymmetry

When formed spontaneously from a mixture of phospholipids dissolved in water, artificial membrane bilayers typically display symmetric leaflets of nearly the same composition. A phospholipid molecule can diffuse freely throughout one leaflet of a bilayer, but its translocation or "flipping" between leaflets is restricted due to the polar headgroup and extremely hydrophobic core of the membrane (12,13). Thus, spontaneous flipping or transerve movement of

phospholipids are rare events in artificial membranes (12). In contrast, the plasma membrane of most eukaryotic cells is strikingly asymmetric (14). For instance, phosphatidylcholine (PC) and sphingolipids (Sph) are confined to the exofacial leaflet, while phosphatidylserine (PS) and phosphatidylethanolamine (PE) are enriched in the cytofacial leaflet (15-19). This asymmetric structure generates different chemical environments on opposing membrane leaflets that are vital for integral membrane protein function, signal transduction and cell-cell interactions (20). Controlled disruption of plasma membrane asymmetry plays key roles in physiological processes such as apoptosis, blood clotting, cytokinesis and some host-pathogen interactions (21-23). How is membrane asymmetry at the plasma membrane maintained despite of the low spontaneous phospholipid flipping rate? Mark Bretscher first suggested the requirement for energy dependent "flippases" to establish membrane asymmetry at the plasma membrane (14).

The Aminophospholipid Translocase

An energy-dependent aminophospholipid translocase (APLT) activity was first discovered in human erythrocytes and this discovery provided an insightful mechanism for the establishment of an asymmetric plasma membrane (24) Initial experiments showed that spin-labeled aminophospholipids (PE and PS) can be rapidly incorporated into the cytosolic leaflet of the erythrocytes, while spin-labeled PC remained in the extracellular leaflet (24). The aminophospholipid-specific incorporation into the cytosolic leaflet of the erythrocytes was also dependent on ATP and inhibited by the presence of the P-type ATPase inhibitor orthovanadate (24) This study provided some evidence that a P-type ATPase contribute to the APLT activity in human erythrocytes. Other reports described phospholipid translocase activities in bovine chromaffin granules (25), platelets (26) and yeast (27).

The identity of factors contributing to the APLT activity in erythrocytes and bovine chromaffin granules was a mystery for several years. This mystery was unraveled by the partial purification of 115kD ATPase from the bovine chromaffin ganules called "ATPase II" (28). The ATPase activity of ATPase II was shown to be stimulated significantly by PS and partially by PE (28,29). Previous attempts to reconstitute APLT activity in artificial membranes failed to identify the factor contributing to the APLT activity. Cloning of ATPase II (now called ATP8A1) from bovine chromaffin granules not only validated ATPase II as a P-type ATPase, but also facilitated the discovery of large family enzymes contributing the APLT activity (30), now referred to as type IV P-type ATPases or P4-ATPases. Identification of ATPase II led to the identification of homologs (Drs2 and Atp8b1) from different species and the yeast protein Drs2 shares about 50% sequence identity with ATPase II (30,31). Although Drs2 activity was associated with the plasma membrane APLT activity (30), later reports showed that disruption of *DRS2* has a negligible influence on the plasma membrane flippase activity (32,33). Disruption of *DRS2* leads to defects in various protein trafficking pathways and these defects provide a link of Drs2 APLT activity in the endomembrane system.

Loss of function studies in *S, cerevisiae* provide some evidence that P4-ATPases contribute to APLT activity in the cells. For instance, Dnf1 and Dnf2 are required for the translocation of fluorescent NBD-PC and NBD-PE at the plasma membrane in *S. cerevisiae* (34). All of the Drs2/Dnf families of P4-ATPases contribute to the establishment and maintenance of membrane asymmetry (11,34). Purified *trans*-Golgi network (TGN) membranes containing temperature sensitive allele of Drs2 were shown to have a decrease in the NBD-PS activity upon the inactivation of the mutant allele (35). Although genetic and cell biological results provide supportive evidence for APLT activity of P4-ATPases, *in vitro* reconstitution of P4-ATPases is required to show that P4-ATPases can flip phospholipid substrates by itself. Our lab showed for

the first time that *in vitro* reconstituted yeast Drs2 protein can catalyze the NBD-PS transport by itself (36). Independently, Molday and his coworkers showed that proteoliposomes containing Atp8a2 can translocate NBD-PS in the presence of ATP (37). These two seminal studies showed how Drs2 and Atp8a1 couple its ATPase activity with its aminophospholipid (NBD-PS and NBD-PE) translocation activities (36,37).

Division of Labor Among P4-ATPases in Budding Yeast

P-type ATPases and the P4-ATPases

The P-type ATPase superfamily provides an instructive example for how a common structural unit can evolve over time to provide a great diversity of integral membrane, ATP-powered pumps that transport different substrates across biological membranes. A phylogenetic grouping of P-type ATPases indicates five major divisions, designated P1 to P5, and subdivisions that often align with substrate specificity (38,39). For example, P1A-ATPases are primarily prokaryotic K^+ pumps, while the P1B clade is found in all three domains of life and are heavy metal transporters. The P2-ATPase group includes the well studied Na^+/K^+ ATPase (P2C) and Ca^{++} ATPases (P2A and B), and P3-ATPases include H^+ and Mg^{++} transporters. P4-ATPases are only found in eukaryotes and transport phospholipid, while no substrate has been identified yet for the P5-ATPases (40).

The biochemical, cell biological and physiological functions of P4-ATPases are becoming better defined. These enzymes harness energy from ATP hydrolysis to flip phospholipid from the extracellular leaflet of the plasma membrane, or lumenal leaflet of internal organelles, to the cytosolic leaflet against the prevailing concentration gradient (24,30,36,37,41,42). Because transport is unidirectional and specific for particular phospholipids, these flippases generate a membrane that is asymmetric in lipid composition between the two

leaflets. Membrane asymmetry is important for numerous cellular processes. For instance, phosphatidylserine (PS) is mainly enriched on the cytosolic leaflet of the *trans*-Golgi network, endosomes and plasma membrane (PM) by P4-ATPases, but regulated exposure of PS in the extracellular leaflet is an early apoptotic response that serves as a mark of death (43-46). Within endosomal and Golgi membranes, P4-ATPase-mediated transport of PS imparts negative charge and curvature to the cytosolic leaflet, which facilitate recruitment of peripheral membrane proteins and the budding of transport vesicles (15,47-49).

Mammals express ~14 P4-ATPases (ATP8A1 - ATP11C) (50) and mutations in individual genes cause liver disease (ATP8B1) (31,50), neurological disease (ATP8A2) (51,52), B-cell deficiency and anemia (ATP11C)(53-56), and are linked to obesity, type 2 diabetes and increased risk of myocardial infarction (ATP10A and 10D)(57-61). P4-ATPases are evolutionarily conserved in all eukaryotes and these enzymes have been studied in a variety of model organisms including plants, nematodes, fruit flies, and most extensively in yeast (15). There are five P4-ATPases in *Saccharomyces cerevisiae* (Dnf1, Dnf2, Dnf3, Drs2 and Neo1) (2), which transport phospholipid with specificities comparable to their mammalian counterparts (Table 1.1). Drs2 is nearly 50% identical in amino acid sequence to ATP8A1 and ATP8A2, and all three proteins flip PS and display a weaker activity towards phosphatidylethanolamine (PE) (35,37,62-64). Dnf1 and Dnf2 transport phosphatidylcholine (PC)

and PE and appear to strongly prefer the lyso-PC and lyso-PE molecular species lacking the sn2 fatty acyl chain (34,65,66). The mammalian orthologs of the Dnf P4-ATPases are less clear, but Dnf1 and Dnf2 appear most similar to ATP10A (PC flippase), 10B (substrate unknown), and 10D (substrate unknown)(67). ATP8B1 and 8B2 can also flip PC, although it

Table 1-1. Human and yeast P4-ATPases with their ß-subunits and localizations

Mammalian P4-ATPase	Substrate	ß-subunit	Localization	Reference	Yeast P4-ATPase	Substrate	ß-subunit	Localization	Reference
ATP8A1	PS, PE	CDC50A	Plasma membrane, endosomes	(1,2)	Drs2	PS, PE	Cdc50	Golgi, endosomes	(3,4)
ATP8A2	PS, PE	CDC50A	Plasma membrane, endosomes	(1,2)					
ATP10A	PC	CDC50A	Plasma membrane	(5)	Dnf1	Lyso-PC, Lyso-PE	Lem3	Plasma membrane, endosomes	(3,6)
ATP10B	?	CDC50A	Late endosome, lysosome	(5)	Dnf2	Lyso-PC, Lyso-PE	Lem3	Plasma membrane, endosome	(3,6)
ATP10D	?	CDC50A	Plasma membrane	(5)					
ATP8B1	PC	CDC50A	Plasma membrane	(2)					
ATP8B2	PC	CDC50B	Plasma membrane	(2)					
ATP11A	PS, PE	CDC50A	Plasma membrane	(2)	Dnf3	PS, PE, PC	Crf1	Golgi	(3,4)
ATP11B	PS, PE	CDC50A	Plasma membrane	(2)					
ATP11C	PS, PE	CDC50A	Plasma membrane	(2)					
ATP9A	?	?	Endosomes	(7)	Neo1	PS, PE	?	Golgi, endosomes	(3,8)
ATP9B	?	?	Plasma membrane	(9)					

isn't known if the mammalian proteins prefer lyso-PC or diacyl-PC (68). Dnf3 is understudied, but it appears to flip PS, PE and PC and may be most similar ATP11A, 11B and 11C PS/PE flippases (64). The substrate specificity of Neo1 and closely related ATP9A and 9B is uncertain; however, these proteins likely transport PE and to a lesser extent PS (7,69). P4-ATPase phospholipid flippase activity is now well established for most of these enzymes, but how these enzymes recognize and transport their phospholipid substrates to cytosolic leaflet is an ongoing question.

P-type ATPases couple large cytosolic domain movements driven by ATP binding and hydrolysis to conformational changes in the membrane domain that move transport substrate across the membrane (40). No high-resolution structure of a P4-ATPase is currently available. However, structural similarity between P1, P2 and P3-ATPases along with homology modeling efforts suggests a similar domain architecture for P4-ATPases (70,71). These pumps are large integral membrane proteins consisting of cytosolic domains called the nucleotide-binding (N), phosphorylation (P), and actuator (A) domains. The N- and C-termini face the cytosol and in some cases contain regulatory (R) domains (40). The membrane (M) domain of P4-ATPases consists of 10 transmembrane segments that mediate recognition and interleaflet transport of phospholipid substrate (Figure 1.1) (15,72). For most P4-ATPases, the catalytic α–subunit associates with a noncatalytic β-subunit in the Cdc50 family of proteins (10,50,73,74). The β-subunits have 2 transmembrane segments and a large extracellular (or luminal) domain that is glycosylated. The Neo1/ATP9 orthologs are exceptions that appear to function without a ß-subunit from the CDC50 family (8). The β-subunits clearly play a role in chaperoning the α-subunit from the ER and may also influence the catalytic cycle (75).

P4-ATPases appear to use a classical Post-Albers (E1-E2) catalytic cycle defined first for the Na^+/K^+ ATPase, but with interesting differences. The E1 conformational state allows ATP binding to the N-domain, followed by transfer of the γ-phosphate to a conserved aspartate within the P-domain, which defines the E1 to E1P transition (63,71). Na^+/K^+ ATPases couple phosphorylation with Na^+ ion binding and pump Na^+ out of the cell during the E1P→E2P conformational transition (40). On the contrary, P4-ATPases are not dependent on their

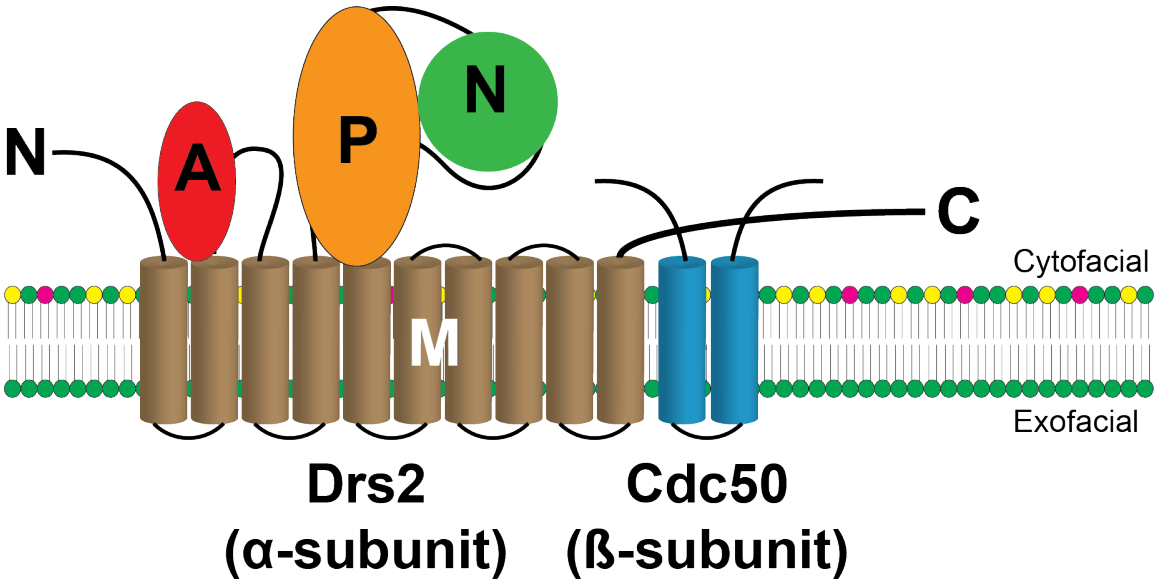

Figure 3-1. Membrane topology diagram of a P4-ATPase. P4-ATPase have four main structural domains: Actuator (A), phosphorylation (P), nucleotide-binding (N) and transmembrane (M) domains. Some P4-ATPases associate with a co-chaperone (Cdc50).

phospholipid substrate to form E1P or transition into the E2P state (63,71), but instead require phospholipid substrate to dephosphorylate E2P and return to the E1 conformational state (15,63,71,76).These E2P→E2→E1 conformational movements appear to be coupled to translocation of the phospholipid from the exofacial leaflet to the cytosolic leaflet, comparable to the transport of K^+ into the cell by the Na^+/K^+ ATPase (40) (Figure 1.2).

The mechanism of substrate recognition and transport by a P-type ATPase M domain is best understood for the Ca^{++}-ATPase (SERCA1). In the E1-ATP conformation, two Ca^{++} ions from the cytosol gain access to binding sites in the center of the M domain formed from resides within M4, M5, M6, and M8. Ca^{++} binding induces phosphorylation (E1P) and enclosure of the ions in an occluded state within the center of the M domain. Opening of access to the ER lumenal space accompanies the E1P→E2P transition allowing exchange of Ca^{++} ions for protons (40,77,78). Proton binding stimulates dephosphorylation and passage through an occluded state before the protons are released in the cytosol (E2P→E2→E1). The P1, P2 and P3-ATPases all appear to use this canonical transport pathway with subtle changes in the architecture of the binding site conferring differences in substrate specificity (40,79).

The P4-ATPase Giant Substrate problem and potential transport mechanisms

The P4-ATPases, by contrast, are faced with the challenge of transporting a substrate that is about 100-fold larger by volume (10-fold by mass) than a pair of Ca^{++} ions (Fig. 1). This issue is often described as the P4-ATPase "giant substrate problem" and raises many questions. Did the canonical binding site and transport mechanism evolve to accommodate this much larger and more complex substrate? Did the P4-ATPases evolve a new, noncanonical mode of substrate

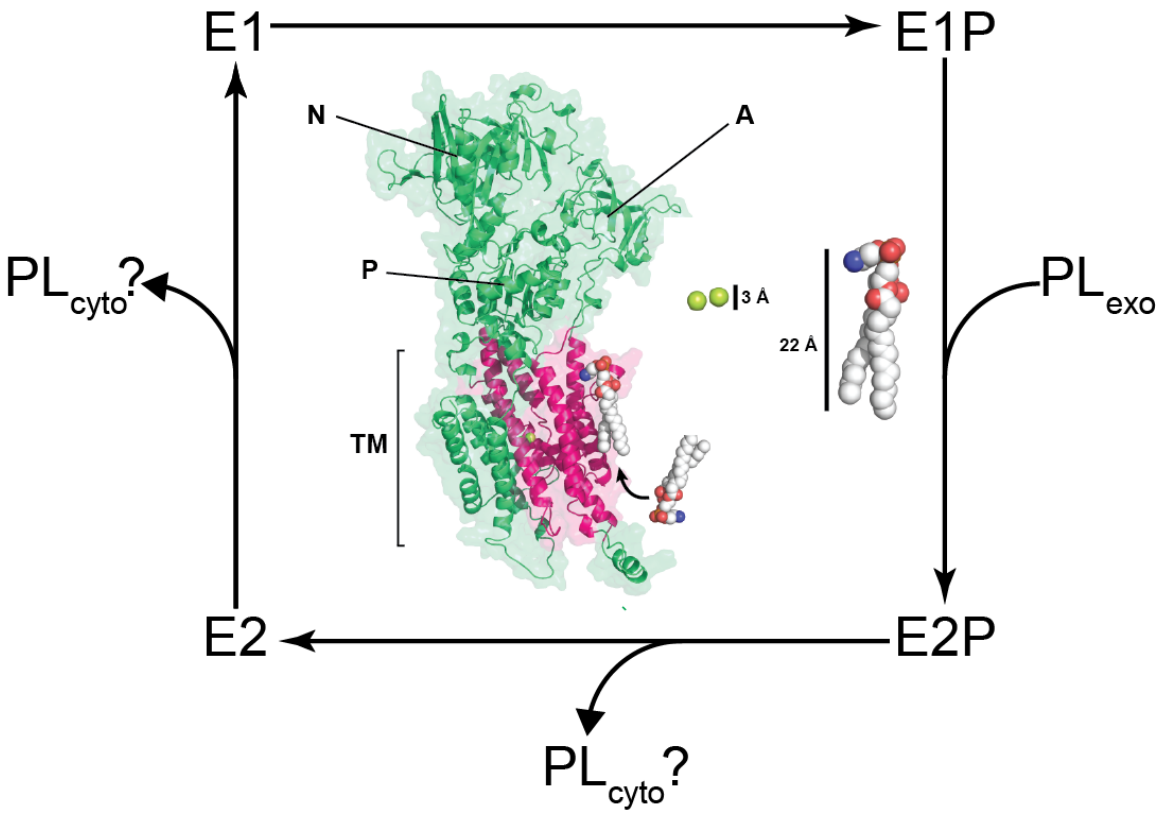

Figure 1-4. Proposed Post-Alber's cycle of P4-ATPase. Relative sizes of phospholipid and calcium ion were shown here.

recognition and transport? How is the specificity for particular phospholipids determined? A number of recent studies are making progress towards a solution to this giant substrate problem.

Mutational studies with ATP8A2 could be consistent with evidence for a canonical transport mechanism for the P4-ATPases (71,76). For example, E309 within M4 of SERCA1 plays important roles in ushering Ca^{++} ions from the cytosol into the 2 binding sites, and helping form one of the binding sites (site II) (78,80).

As all known phospholipid substrates for P4-ATPases have positively charged amine or choline groups within the headgroup, one might expect the negatively charged glutamate to be conserved in the P4-ATPases if the canonical binding site is used. However, nearly all P4-ATPases have a PISL sequence in M4 rather than the PEGL found in Ca^{++}, Na^+/K^+ and H^+/K^+-ATPases (71,81). While an isoleucine would not be expected to coordinate a charged headgroup, this residue is important for P4-ATPase function as a PISL→PMSL mutation in ATP8A2 causes cerebellar ataxia, mental retardation, disequilibrium syndrome (CAMRQ) in a Turkish family (51). ATP8A2-I364M displays a substantial loss of PS flippase activity without significant alteration of the apparent K_m for PE and PS. Similarly, an N359A mutation in ATP8A2, 4 amino acids N-terminal to the highly conserved proline (P – 4 position), substantially perturbs flippase activity and the apparent affinity for both PS and PE (81). The central proline breaks the M4 helix allowing backbone carbonyls at the P – 3 and P – 4 positions to participate in K^+ binding in the Na^+/K^+ ATPase (82). Thus, it is possible that the N359A mutation promoted helix formation at the P - 4 position and the loss of free backbone carbonyls to perturb transport by a canonical mechanism (71).

However, these ATP8A2 mutagenesis studies, along with homology modeling of ATP8A2 on SERCA1 and molecular dynamic simulations, led the authors to favor an alternative

noncanonical route and "hydrophobic gate" hypothesis for substrate transport (71,81). The idea is that substrate translocates along a groove in the M domain bordered by M2, M4 and M6, and is driven by water penetration along this protein-lipid interface. Evidence in favor of this model is that the N359 sidechain (P – 4 position in M4) important for substrate selection and transport projects into this cleft (71,81). In addition, a critical feature of the P + 1 isoleucine in the PISL motif appears to be the hydrophobicity of the residue. M4 undergoes bobbing and twisting movements during the Post-Albers cycle of the Ca^{++}-ATPase. Comparable movements of the isoleucine sidechain and neighboring hydrophobic residues in ATP8A2 may control water penetration within the groove to help chaperone the polar phospholipid headgroup though the membrane as it flips (71,76,81). An attractive feature of this model is that the cytosolic end of this groove in the Ca^{++} ATPase has a bound phospholipid molecule in the crystal that co-purified with the protein trapped in the E2 conformation. This groove closes up in the E1 conformation to presumably eject the phospholipid into the cytosolic leaflet (80). Whereas phospholipid would enter and exit this site in the Ca^{++}-ATPase from the cytosolic leaflet (no transbilayer transport), the P4-ATPases may have evolved the ability to load this same binding site from the extracellular leaflet to allow net transport across the membrane.

Evidence for a noncanonical mechanism of transport initially derived from studies of budding yeast P4-ATPases (70,83). The strategy was to map residues that conferred differences in substrate specificity between Drs2 and Dnf1. Surprisingly, most of the specificity-altering mutations mapped to M1, M2, M3, and M4, at positions well removed from positions involved in cation selection in the P2-ATPases . In addition, subtle point mutations at several positions were sufficient to allow PS transport by Dnf1 (65,70,83). For example, a Tyr to Phe substitution at the M4 P + 4 position in Dnf1 converted Dnf1 into a PS flippase. The reciprocal Phe to Tyr mutation in Drs2 disrupted PS transport by this flippase (70). Another surprising observation was that Dnf1

mutants could gain the ability to flip PS without altering its ability to flip PC and PE. Similarly, the Phe to Tyr mutation that reduced PS recognition by Drs2 did not seem to affect PE recognition (65,70,83). These gain-of-function and separation-of-function mutations are valuable because they do not noticeably perturb the catalytic cycle and are likely altering substrate recognition specifically.

It was also possible to identify mutations that influenced phospholipid headgroup recognition, backbone recognition, or both. PS-flipping Dnf1 mutants fell into two categories: those that maintained the Dnf1 preference for lysophospholipid (lyso-PS) and those that acquired the ability to flip diacyl-PS (65). Moreover, an M1 mutation (N220S) was identified in Dnf1 that allowed it to transport sphingomyelin, thus shedding light on how the glycerol backbone of PC is distinguished from the sphingosine backbone because both lipids have the same headgroup (84). In homology models, the substrate-defining residues cluster at two sites, one near the surface of the exofacial leaflet where substrate is selected and one near the cytosolic leaflet where substrate is delivered (65,70,83). The involvement of residues in M1, M2 and M3 for P4-ATPase substrate selection argues for a noncanonical mechanism because these membrane segments do not directly contribute to cation binding in the P2-ATPases (85).

The yeast P4-ATPases studies led to a "2-gate hypothesis" for substrate selection and transport: an entry gate formed from residues at the extracellular side of M1 - M4, and an exit gate on the cytosolic side of these membrane segments. These gates would act sequentially to select substrate as it flipped across the bilayer (15,65,70,83). The individual gates seem to filter substrate imperfectly because point mutations in the exit gate, for example, allow Dnf1 to transport PS even when the entry gate bore wild-type residues that normally restricted PS transport. Combining entry and exit mutations gave an additive affect on PS transport, supporting the idea for two distinct sites for substrate interaction. It was also suggested that phospholipid

headgroup would slide along a groove bounded by M1, M3 and M4 to as it traveled from entry to exit gate, while the fatty acyl chains would reorient in the lipid bilayer (48,65,70,83-85). The exit gate residues in Dnf1 overlap the site where the Ca^{++}-ATPase binds phospholipid. However, the involvement of residues in M1 and M3 suggests the orientation of the lipid may be different in the P4-ATPases if the exit gate defines a phospholipid-binding site as suspected (70,72,83).

Can we rationalize these different models for substrate transport by the P4-ATPases? Both noncanonical models provide a potential solution to the giant substrate problem because the entire phospholipid would not need to enter a deeply buried, occluded state. These transport models emphasize headgroup movement along rather linear paths on the M domain surface (analogous to the swiping of a credit card magnetic strip through a reader), but it is certainly possible that the lipid headgroup could penetrate more deeply between pairs of membrane segments (for example, between M1,2 and M3,4) (40,50,72). In this case, the distinction between the two proposed noncanonical transport routes becomes blurred and it remains possible that phospholipid substrate could also engage segments of the canonical transport pathway.

An important point is that these mechanistic studies are still in their early days and the models are likely to be refined as additional P4-ATPases and substrates are better characterized. Moreover, inferences are made based on homology models that are quite useful for developing hypotheses to test, but are a poor substitute for experimentally derived structural information. Given the observation that mutations are readily obtained that alter transport of one substrate without changing transport of a second substrate implies that there may be more than one solution to the Giant Substrate Problem (70,83).

What is the purpose of pumping PL across the membrane?

The establishment of membrane asymmetry is the most obvious consequence of P4-ATPase activity, but why do cells need asymmetric membranes? For single-celled eukaryotic organisms, the initial selective advantage of having P4-ATPases may have been the production of an inert and tightly sealed outer leaflet of the plasma membrane (15,72,86). A number of toxins can target specific lipids when they are exposed on the outer leaflet, and thus sequestering more reactive aminophospholipids on the inner leaflet while leaving phosphatidylcholine and sphingolipids in the outer leaflet (87,88) may protect cells from attack. The dynamic movement of PE to the inner leaflet plays an important role in cytokinesis (88,89) and the inner leaflet phospholipids are also intimately tied to signaling cascades. For example, PS in the inner leaflet influences the membrane association and activity of protein kinase C (90), K-Ras (91)and Cdc42 (92,93). The regulated exposure of PS in the outer leaflet occurs by activation of a scramblase, and this occurs during apoptosis and blood clotting reactions (68,94-96). P4-ATPases that flip lyso-phospholipid may do this for nutrient uptake from external sources, clearance of signaling lipids, or repair of damaged membranes (64,66,97).

Many P4-ATPases localize to Golgi and/or endosomal membranes, implying a role for membrane asymmetry in these organelles. As membrane flows through the secretory pathway, it may be necessary to generate asymmetry prior to arrival of the lipids at the plasma membrane. Consistently, inactivation of yeast Golgi flippases (e.g. Neo1 or Drs2) causes exposure of PS and PE on the outer leaflet of the plasma membrane (11,69,70). This loss of asymmetry also appears to impinge on the vacuole membrane as *neo1* mutants display a fragmented vacuole phenotype that is likely caused by loss of PE asymmetry (6). The flippases are part of a larger set of integrated membrane remodeling processes within the Golgi that provide the transition from an ER membrane composition to a plasma membrane-like composition and organization (98).

Another crucial function for the P4-ATPases is in vesicle-mediated protein trafficking (15,47,86). In yeast, *drs2* and *cdc50* mutants display a defect in protein trafficking between the *trans*-Golgi network and early endosomes (2,10,11,74,99,100). Similarly, depletion of ATP8A1 (Drs2 ortholog) causes a defect in protein trafficking through recycling endosomes of mammalian cells (49). Cells deficient for Neo1 display trafficking defects at the Golgi that are similar COPI mutants (3,6) and Neo1 is also linked to retromer function at late endosomes (6,101). Strains deficient for Dnf1, Dnf2 and Dnf3 (*dnf1,2,3*Δ*)* display a modest defect in endocytosis (64), and combining *dnf*Δ mutations with *drs2*Δ exacerbates Golgi trafficking defects (2,102). Drs2 catalyzed translocation of PS from the luminal leaflet to the cytosolic leaflet increases the curvature of the membrane and the negative charge of the cytosolic leaflet (48). These features of the membrane can facilitate the recruitment of effectors to the membrane that facilitate vesicle (or tubule) formation. For example, the ArfGAP Gcs1 is an effector of PS translocation by Drs2 and EHD1 (a protein potentially involved in tubule scission) is an effector of ATP8A1 (48,49). P4-ATPases are uniquely found in eukaryotic cells and it is possible they evolved to facilitate these trafficking functions within the endomembrane system.

Division of labor among P4-ATPases

Single gene mutations in human or mouse P4-ATPases cause profound pathologies, suggesting a lack of functional redundancy between members of this gene family. Differences in tissue-specific expression patterns may help segregate P4-ATPase gene function in metazoans, but this can not explain why single-celled eukaryotes maintain multiple P4-ATPase genes. A number of observations indicate that the yeast P4-ATPases have both overlapping and non-overlapping cellular functions. For example, *drs2*Δ cells are cold sensitive for growth and displays defects in protein trafficking in spite of the presence of four other P4-ATPases in these

cells (2,69). A *drs2*Δ *dnf1*Δ double mutant display defects in trafficking between Golgi and late endosomes that neither single mutant displays (2). Thus, Dnf1 can compensate for the loss of Drs2 in some pathways but not others. Conversely, *neo1*Δ single mutants are inviable and therefore Neo1 must exert an essential function that cannot normally be served by the other P4-ATPases (2,3). What determines this division of labor among the P4-ATPases?

Intrinsic factors that determine the division of labor among budding yeast P4-ATPases

Intrinsic factors that make each P4-ATPase functionally distinct are ultimately defined by the unique amino acid sequence of each protein, which will determine substrate specificity, subcellular localization, and means of regulation. The most important factor that determines the unique function of the yeast P4-ATPases appears to be their lipid substrate specificity. This claim is based on studies describing the cellular consequences of Drs2 and Dnf1 mutations that alter their substrate specificity (65,70,83). As described above, Drs2 has a unique function in supporting bidirectional protein transport between the TGN and early endosomes that cannot be supported by Dnf1 (48,86). Mutations in Drs2 that disrupt its ability to flip PS, without substantially altering PE recognition, also disrupt these trafficking pathways (48). Remarkably, gain of function Dnf1 mutants that acquire the ability to flip PS ($Dnf1^{PS+}$) will restore these trafficking pathways in *drs2*Δ cells (48). Importantly, these substrate-altering mutations in Drs2 and Dnf1 do not influence the interactions with their respective ß-subunits or have a measurable influence on their localization (70,83) (Figure 1-3).

Differences in P4-ATPase subcellular localization could help enforce a division of labor. The localization of all five yeast P4-ATPases overlap within the Golgi complex, but they differ in their trafficking patterns and steady-state distributions (2,6,69). Neo1 is broadly localized throughout the Golgi (6) and traffics to late endosomes where it is retrieved back to the Golgi by

retromer (6,101). Drs2 localizes primarily to the TGN, appears to traffic to an early endosome and back, but rarely visits the late endosomes or the plasma membrane (2,68,74,100,102). Dnf1 actively cycles between the Golgi, plasma membrane, and endosomes displaying a steady-state localization at all three locales (69,102). Dnf2 is 69% identical to Dnf1 and likely follows a similar trafficking itinerary. However, Dnf2 lacks NPFXD endocytosis signals found in Dnf1, and localizes primarily to the plasma membrane at steady-state (2,102-104). Dnf3 is weakly expressed and less well characterized, but it appears to localize primarily to the TGN (2). Together, the P4-ATPases can patrol most of the secretory and endocytic pathways, but interestingly are not localized appreciably to the ER or vacuole membrane. By expressing multiple P4-ATPases, the cells can simultaneously modulate membrane organization in multiple compartments in the cell.

Expression of multiple P4-ATPases also allows each pump to be independently regulated. Dnf1 and Dnf2 are regulated through their phosphorylation by Flippase Protein Kinases (Fpk1 and Fpk2), which are linked through a signaling network to TORC2 and the regulation of sphingolipid synthesis (105-108). The reason why lyso-PC/PE flippases are linked to sphingolipid metabolism is currently unclear, but it is suggestive of a homeostatic mechanism that controls membrane composition and organization. Drs2 is regulated by the signaling lipid

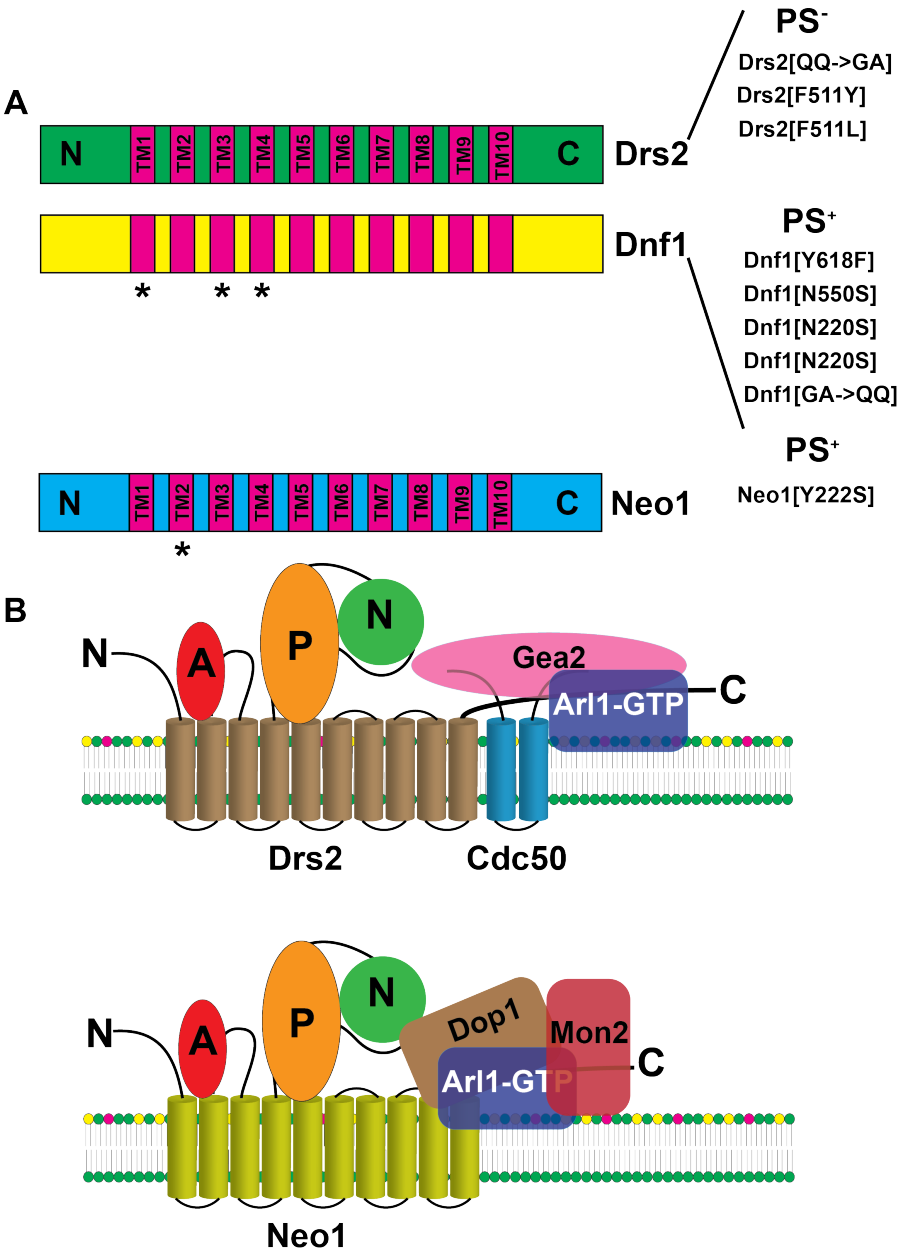

Figure 1-3. Intrinsic and extrinsic regulators of P4-ATPase activity in *S. cerevisiae.* (A) (A) Residues that alter the substrate preference were shown for Drs2, Dnf1 and Neo1. (B) Extrinsic regulators of P4-ATPases. β-subunits and autoregulatory C-terminal tail might regulate the P4-ATPase activities.

phosphatidylinositol-4-phosphate (PI4P) and by interactions with proteins involved in vesicular transport (62,109,110). The Arf-GEF Gea2 and Arf-like protein Arl1 bind to N- and C-terminal regulatory domains in Drs2 to activate flippase activity (101,110,111).

The Drs2 C-terminal regulatory domain also binds Rcy1, a protein required for recycling proteins through the endocytic pathway back to the Golgi, and this interaction may also stimulate Drs2 flippase activity (112). The influence of these interactions on ArfGEF, Arl1 and Rcy1 activities is not known. However, this network of regulatory interactions implies a crucial role for integrating PS translocation with the vesicle budding machinery. Neo1 forms a complex with Mon2 and Dop1 (9,101,113), proteins implicated in protein trafficking but with no known function. The consequences of these interactions are also unknown although it is possible that they regulate Neo1 activity.

Extrinsic factors that enforce the division of labor among yeast P4-ATPases

Other proteins that influence the segregation of duties for the P4-ATPases have been identified through extragenic suppressor screens (114,115). The first such example was the isolation of *osh4* (also called *kes1*) loss of function mutations as suppressors of *drs2*Δ cold-sensitive growth (115). Osh4 is a lipid transfer protein that exchanges ergosterol for PI4P at the TGN. The action of Osh4 is thought to increase ergosterol content of the TGN and/or exocytic vesicles budding from the TGN, while diminishing PI4P content (86,115,116). Osh4 is a potent inhibitor of Drs2, likely through its ability to remove PI4P from the TGN. Drs2's PS flippase activity also appears to antagonize Osh4 by presumably inhibiting exchange activity at the TGN (86). However, these regulatory interactions between Drs2 and Osh4 do not explain how deletion of *OSH4* can bypass the function of Drs2 in an *osh4*Δ *drs2*Δ strain (86,115). Importantly, the

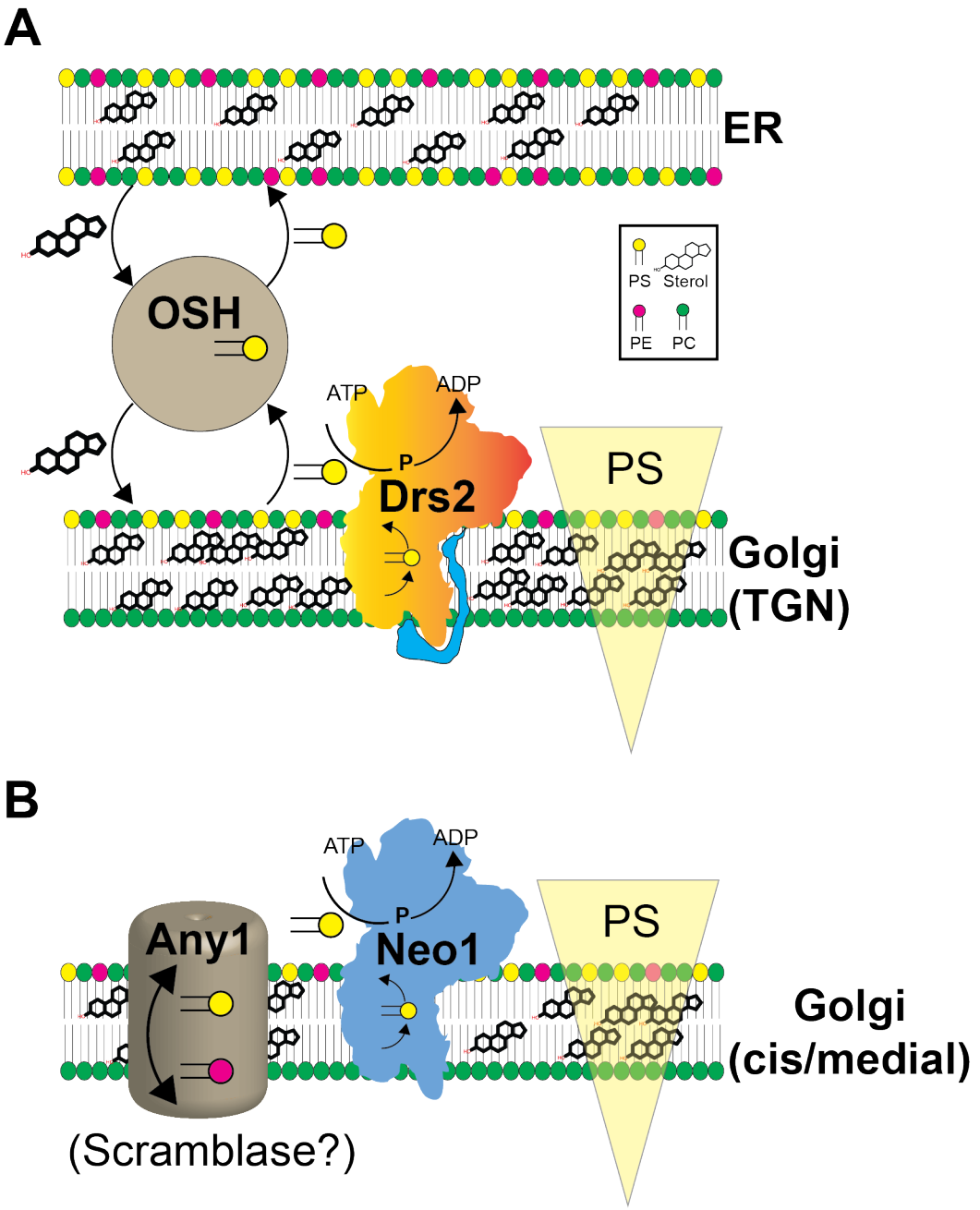

Figure 1-4. Negative extrinsic regulators of Golgi P4-ATPases Drs2 and Neo1. (A) Kes1 antagonizes Drs2 activity through depleting the activatory PI4P pools from the Golgi membranes. (B) Any1 counteracts Neo1 activity through its putative scramblase activity.

bypass suppression requires the activity of Dnf P4-ATPases (86,115). Thus, it appears that the altered Golgi membrane environment of the *osh4*Δ *drs2*Δ cells removes a barrier that normally segregates the functions of Drs2 and Dnf P4-ATPases (86,115). It is not clear if this reflects increased activity of the Dnf P4-ATPases, greater availability of endogenous Dnf substrates in the Golgi, or some other consequence of *osh4*Δ (Figure 1.4).

A more recently discovered extrinsic factor that segregates P4-ATPase function is the PQ loop protein Any1 (*A*ntagonist of *N*eo1 in *Y*east) (114,117). *NEO1* is normally an essential gene, but I found that deletion of *ANY1* bypasses the requirement for Neo1 and a *neo1*Δ *any1*Δ strain grows as well as wild-type yeast (114). Deletion of *ANY1* also partially suppresses *drs2*Δ cold-sensitive growth, but importantly a *drs2*Δ *neo1*Δ *any1*Δ triple mutant is inviable (114). Therefore, the ability of a *neo1*Δ *any1*Δ strain to grow absolutely relies on Drs2. These results imply that Any1 somehow forms a barrier that segregates the duties of Drs2 and Neo1 in the cell, and removal of Any1 allows Drs2 to carry out Neo1's functions (114). Any1 is an integral membrane protein predicted to have 8 membrane segments and has the PQ motif in the loop between M6 and M7 (114). The function of most PQ loop proteins is unknown, although some members of this family are transporters (118). Any1 is proposed to be a scramblase that disrupts the phospholipid gradients established by Neo1 and Drs2 in the Golgi. However, this proposed role for Any1 remains speculative at this time and it is possible that it is regulating membrane asymmetry and/or P4-ATPase function by a different mechanism (Figure 1.4).

Concluding remarks

The P4-ATPase family has a substantial impact on cell and organismal physiology. While this family is large and diverse, the essential and common biochemical function appears to be transport of phospholipid to the cytosolic leaflet of the plasma membrane, Golgi and endosomes.

An important functional distinction for individual members of this family is the specific phospholipid substrate that is transported. This conclusion is based on the ability to mutationally tune the substrate specificity of a few budding yeast P4-ATPase and test the consequences of these mutations on cellular functions. Other proteins, such as Osh4 and Any1 can also help segregate the duties of yeast P4-ATPases. However, factors most important for segregating the function of mammalian P4-ATPases are unknown at this time. A better understanding of how the division of labor is achieved for human P4-ATPases could provide novel therapeutic avenues for treating disease if one could pharmacologically coax a healthy member of the family to carry out the tasks of a defective member.

Neo1 Regulatory Network

Neo1 possess potential regulatory cytosolic domains that influence its localization and activity. Altering PS recognition and transport pathways defined in the Drs2/Dnf family of P4-ATPases are not vital for Neo1 activity. Although it requires the cytosolic domains for ATPase activity (5), directed mutagenesis studies only revealed a residue (Y222) in TM2 region associated with its activity (unpublished data). Both cytosolic tails of Neo1 regulate its activity, localization and protein-protein interactions. For instance, the N-terminal tail of Neo1 is required for its sorting to endosomes by Snx3, but N-terminal tail is not essential for viability (101). Neo1 C-terminal tail is essential for viability, but it does not seem to involve with its interactions with Dop1 and Mon2 (9). Unlike Neo1, Drs2 C-terminal tail is autoinhibitory in the absence of PI4P and its interaction partners (119). In the absence of C-terminal tail, the catalytic activity of Drs2 is significantly increased compared to the full length Drs2 (119). Intrinsic regulators of Neo1 also dictate its interaction with the extrinsic regulators such as Dop1 and Mon2.

Dop1 and Mon2 are two cytosolic proteins that bind Neo1 and may regulate Neo1 activity. Dop1 is an essential protein that is highly conserved evolutionarily in eukaryotes, although its cellular function is not clear. The Dop1 homolog, DopA, was first identified in the filamentous fungus *Aspergillus nidulans* as a member of Dopey protein family and has vital roles in cell morphology and establishment of essential multicellular structures (120). In *S. cerevisiae*, Dop1 a large protein containing leucine zipper domain along with other structural domains and it disrupts cell morphology upon overexpression (120).

In higher eukaryotes, Dop1 homologues participate in tissue patterning and morphogenesis during development. In *C. elegans*, loss of Pad-1 (Dop1 homologue) leads to embryonic lethality as well as improper gastrulation and morphogenesis during development (121). In humans, C21orf5 shares extensive homology with other Dopey family members such Dop1, Pad-1 and DopA. C21orf5 gene is located in the chromose 21 and expressed highly in the brain cortex associated with cognitive abilities (122). Based on mouse and clinical studies, C21orf5 might have defined roles in brain morphogenesis. In down syndrome (DS) patients, C21orf5 is overexpressed due to its location in the duplicated region of chromose 21 and its overexpression potentially leads to neurological disorders and loss of cognitive abilities in DS patients (122).

The physiological role of Dop1 is not yet clearly defined, but defects associated with *dop1* mutants suggest that there is a molecular link between Dop1 and Neo1 activities. Dop1 forms a complex with Mon2, which is distantly related to guanine nucleotide exchange factors (GEF) for activating Arf at Golgi membranes (123). Dop1 is mainly localized to Golgi membranes and its localization is dependent on the scaffolding protein Mon2. Loss of Dop1 activity not only affects endosome to Golgi transport, but it also perturbs the membrane organization of endoplasmic reticulum (ER) (123). $dop1^{ts}$ and *mon2*Δ mutants display defects in

the trafficking of v-SNARE Snc1 between endosomes and the TGN. Despite the roles of Dop1 and Mon2 in the endocytic trafficking, Mon2 and Dop1 have no influence on the AP-3 transport pathway (123).

Although *dop1*^{ts} phenocopies *mon2*Δ in terms of endosome to Golgi transport defects, *dop1*^{ts} additionally displays accumulation of enlarged structures in the endoplasmic reticulum (123). *dop1*^{ts} also exhibits an accumulation of multivesicular, elongated, tubular and ring-like structures similar to those in *neo1*^{ts} and *mon2*Δ mutants (9). This accumulation of abnormal structures suggests a role for Dop1 in vesicle budding or tubule formation in endosomes (9). Dop1 forms a dimer or multimer with Mon2 and Neo1 and this indicates that they form a complex and cooperate as a complex (9). The leucine zipper domains at the C-terminus of Dop1 are crucial for complex formation, whereas the internal region of Dop1 facilitates its association with membranes (9). *dop1*^{ts} displays a reduced level of Mon2 and Neo1 proteins; conversely *neo1*^{ts} and *mon2*Δ mutants exhibits a reduced level of Dop1. Although *dop1*^{ts} is synthetically lethal with *neo1*^{ts}, *dop1*^{ts} *mon2*Δ double mutants do not show any suppression or enhancement of growth defect (9). Despite the uncertainties in Dop1 function, recent studies with yeast Dop1 and Pad-1 in *C. elegans* suggest that Dop1 might be involved in retromer function as well as the formation of extracellular vesicles from endosomes (101,124).

Mon2 acts as another scaffolding protein that synergistically cooperates with Dop1 and Neo1 to execute lipid transport as well as regulatory functions for vesicular transport. *mon2*Δ mutant is both sensitive to brefeldin-A, a small hydrophobic molecule blocking transport between ER and Golgi; and monesin, a Na^+/K^+ ionophore blocking intracellular transport in both the *trans*-Golgi and post-Golgi compartments (125). Sensitivity of *mon2*Δ mutant to monesin and brefeldin A suggest that Mon2 has a vital role in intracellular transport (125). Mon2 was also discovered in a screen to identify mutants that display synthetic growth defects with *ypt51*Δ, a rab mutant

defective in membrane traffic where endocytic and vacuolar sorting pathways intersect (126). *mon2/ysl2*Δ cells are defective in endocytosis, vacuolar protein sorting, vacuole biogenesis and organization of the cytoskeleton (126).

Mon2/Ysl2 is a novel 186.8 kDa peripheral membrane protein that shares homology with the members of Sec7 family (9). *mon2*^{ts} mutants exhibit defects in ligand-induced degradation of Ste2 and alpha factor and undergo vacuole fragmentation at the non-permissive conditions (127). Mon2 also regulates sorting of hydrolyses to the yeast vacuole through the carboxypeptidase Y and alkaline phosphatase pathways (128). Mon2 is a peripheral membrane protein that requires in N- and C- termini regions for its association with Golgi/endosomal membranes, and the C-terminal region of Mon2 is essential for its activity (129). Mon2 might execute endosome to Golgi trafficking functions with Arl1 and cell polarity with Dop1 (129).

Mon2 interacts genetically and biochemically with Arf-like protein Arl1 and this interaction is consistent with a potential function as an Arf guanine nucleotide exchange factor (GEF) (123). In *neo1*^{ts} mutants, both stability and subcellular distribution of Mon2 are affected (113). Overexpression of *ARL1* or *NEO1* suppresses both lethality of *mon2*Δ at 37^{o}C as well as defects in the ligand induced Ste2 and alpha factor degradation (113). Unlike large Arf GEFs, Mon2 lacks the Sec7 domain that can potentially catalyze the nucleotide exchange on Arf1. On the contrary, Mon2 shares extensive homology with the noncatalytic parts of both the BIG and Golgi brefeldin A resistance factor subfamilies of Arf GEFs (123). Studies with mammalian Mon2 showed that its depletion does not affect the Golgi-localized or active GTP-bound Arl1 pools within the cell (130). *In vitro* studies performed with the recombinant Mon2 indicated that Mon2 is neither necessary nor sufficient for catalyzing nucleotide exchange of Arl1(130). Possibly, Mon2 acts as a negative regulator of Arl1 activity (131). These findings support the

notion that Mon2 regulates endosome to Golgi trafficking through its conserved non-catalytic domains by acting as a scaffolding protein for Neo1-Dop1-Arl1 regulatory interactions.

Mon2 appears to mediate its protein trafficking functions through direct protein-protein interactions. Mon2 forms an complex with the P4-ATPase Neo1 and oligomeric Dop1 (9). Mon2 is mainly localized to endocytic elements enriched in the FM4-64 dye (9,127) as well as late Golgi compartments enriched with Neo1 and Dop1 (114). Along with *dop1*^{ts} and *neo1*^{ts} mutants, *mon2*Δ mutant also displays a defective v-SNARE Snc1 trafficking between endosomes and the Golgi (31). Subcellular distribution of the Gga adaptors that are involved in vesicle budding at the tubular endosomal/trans Golgi network relies on numerous interactions between the scaffold Ysl2/Mon2, the small GTPase Arl1, and the flippase Neo1 (132). Deletion of *MON2* or *ARL1* causes mislocalization of Gga2 and Mon2 physically interacts with Gga proteins through the VHS domain (132). Recent studies also showed that Neo1-Mon2-Dop1 essential complex could regulate the retromer function in the endosomes (101).

Any1 (Antagonist Yeast Neo1) was recently identified as a Neo1 antagonist in our collaborative screen to decipher genome-wide suppressor interactions in *S. cerevisiae* (114). Any1 was also independently identified in an insertional mutagenesis screen to search for suppressors of *cdc50*Δ cold-sensitivity (117). Although we identified Any1 as a Neo1 antagonist, it also acts as antagonist for Mon2 and Dop1 proteins based on growth assays (114). Although we functionally categorized Any1 (Ymr010w) as a flippase antagonist, it bioinformatically segregated into a gene cluster involved in metabolic pathways (133). Any1 (Ymr010w) was also shown to be expressed as a long polycistronic mRNA that also includes in *ADI1* mRNA under stress conditions (134). There is no structural or biochemical data about the molecular function of Any1, but based on a conserved sequence motif Any1 belongs to the PQ-loop protein family.

In a search of KDEL cargo receptor homologues, a large family of proteins was identified as "PQ-loop" proteins. PQ-loop proteins are seven-transmembrane segment membrane proteins that contain a distinctive proline-glutamine (PQ) motif (135). One of the first members of this protein family, cystinosin was discovered to be mutated in patients with infantile nephropathic cystinosis, which is a lysosomal storage disorder caused by a defect in the cysteine transport across the lysosomal membrane (136) *CTNS* is the gene encoding for the protein cytinosin in humans (136). Cystinosin is a lysosomal seven transmembrane protein that transports cystine molecules out of the lysosome (137). The PQ motif was shown to be critical for the localization of cytinosin to lysosomes, but later studies proposed a more critical role in the substrate transport for PQ motif than as a lysosomal localization signal (138). Although there is not much sequence homology or conservation of structural motifs in the PQ-loop protein family, the PQ-motif and topological similarities suggest a common function for this large protein family (135). Interestingly, members of the PQ-loop protein family are present in all eukaryotes and prokaryotes. The link between prokaryotic and eukaryotic PQ-loop proteins might be evolutionarily conserved function of these proteins in metabolite transport (135).

Eukaryotic PQ-loop proteins have versatile functionality within the cells. For instance, cystinosins in humans are implicated in proteolysis-derived dimeric amino acid export from the lysosomes by an ion-coupling mechanism (137). In *C. elegans ctns-1* (*CTNS* homologous gene) mutants, an arginine/lysine transporter called "Laat-1" is required to elevate the accumulation of lysosomal cysteine levels in the presence of a cystinosis drug cysteamine (139). On the other hand, yeast PQ-loop proteins Ypq1, Ypq2, and Ypq3 are localized to the vacuoles and are involved in the vacuolar homeostasis by regulating cationic amino acid (CAA) transport. The human PQLC2 is closely related to Ypq1/Ypq2/Ypq3 and can revert the canavanine resistance of *ypq2*Δ to wild-type levels and facilitate the transport of cationic amino acids into the vacuole

(118). Both yeast (Ypq1/2/3) and human (PQLC2) basic amino acid transporters require the AP-3 pathway to localize to the yeast vacuoles or to lysosomes of human cells (140).

Structural studies done with the eukaryotic SWEET and prokaryotic semi-SWEET transporters proposes that the conserved PQ-loop motif serves as a molecular hinge facilitating the binder-clip like motion of triple helix bundles in Semi-SWEET transporters (141). Semi-SWEET transporters consist of a triple helix bundle (THB), while eukaryotic SWEET transporters consist of 2 THBs that are connected with a inversion linker helix (141,142). According to the structural studies, prokaryotic semi-SWEET transporters have symmetrical transport pathway through the homodimer of 2 THBs, on the other hand SWEET transporters asymmetrical transport pathway that facilitates transport of a wide range of substrates other than mono-/di-saccharides (141,142).

Although, PQ-loop proteins share a common functionality and evolutionarily conservation, Any1/Ymr010w seems to be functionally divergent from evolutionarily related basic amino-acid transporters Ypq1/2/3 in *S. cerevisiae*. Any1 is part of regulatory network acting on the essential Neo1/Mon2/Dop1 complex and Any1 enforces its antagonistic activity through altering lipid landscapes in the Golgi/endosomal system (114,117). Deciphering the complete regulatory network of Neo1 requires further proteomic and biochemical analyses of its interaction partners.

CHAPTER II

THE ESSENTIAL NEO1 FROM BUDDING YEAST PLAYS A ROLE IN ESTABLISHING AMINOPHOSPHOLIPID ASYMMETRY OF THE PLASMA MEMBRANE[1]

[1] This work is published: Takar M., Wu Y. , Graham T.R. "The Essential Neo1 Protein from Budding Yeast Plays a Role in Establishing Aminophospholipid Asymmetry of the Plasma Membrane. Journal of Biological Chemistry.291 (30): 15727-39. doi: 10.1074/jbc.M115.686253.

Abstract

Eukaryotic organisms typically express multiple type IV P-type ATPases (P4-ATPases), which establish plasma membrane asymmetry by flipping specific phospholipids from the exofacial to the cytosolic leaflet. *Saccharomyces cerevisiae,* for example, expresses five P4-ATPases including Neo1, Drs2, Dnf1, Dnf2 and Dnf3. Neo1 is thought to be a phospholipid flippase, although there is currently no experimental evidence that Neo1 catalyzes this activity or helps establish membrane asymmetry. Here we use temperature-conditional alleles (*neo1*^{ts}) to test if Neo1 deficiency leads to loss of plasma membrane asymmetry. Wild-type (WT) yeast normally restrict most of the phosphatidylserine (PS) and phosphatidylethanolamine (PE) to the inner, cytosolic leaflet of the plasma membrane. However, the *neo1-1*^{ts} and *neo1-2*^{ts} mutants display a loss of PS and PE asymmetry at permissive growth temperatures as measured by hypersensitivity to pore forming toxins that target PS (papuamide A) or PE (duramycin) exposed in the extracellular leaflet. When shifted to a semipermissive growth temperature, the *neo1-1*^{ts} mutant became extremely hypersensitive to duramycin while sensitivity to papuamide A was unchanged, indicating preferential exposure of PE. This loss of asymmetry occurs in spite of the presence of other flippases that flip PS and/or PE. Even when overexpressed, Drs2 and Dnf1 were unable to correct the loss of asymmetry caused by *neo1*^{ts}. However, modest overexpression of Neo1

weakly suppressed loss of membrane asymmetry caused by *drs2*Δ, with a more significant correction of PE asymmetry than PS. These results indicate that Neo1 plays an important role in establishing PS and PE plasma membrane asymmetry in budding yeast

Introduction

The plasma membrane is a complex amalgam of proteins, carbohydrates and lipids with an overall asymmetric distribution of these molecules between the two leaflets (15,42). For example, the aminophospholipids phosphatidylethanolamine (PE) and phosphatidylserine (PS) are mainly concentrated in the cytosolic leaflet, while phosphatidylcholine and sphingolipids are enriched in the extracellular leaflet (23,143,144). Phospholipid asymmetry is crucial for plasma membrane integrity and several cellular processes such as signal transduction (20), cell division (88,145) and vesicular transport (47,48,64). Controlled disruption of phospholipid asymmetry and exposure of PS in the extracellular leaflet stimulates blood coagulation and is required for the recognition and phagocytosis of apoptotic cells (44,96,146). Plasma membrane asymmetry is established by P4-ATPases, which pump specific phospholipid substrates (e.g. PS and PE) from the extracellular leaflet to the cytosolic leaflet.

P4-ATPases belong to the P-type ATPase superfamily, which has been phylogenetically divided into five subgroups (P1 - P5) (40,147). The well-characterized P1, P2 and P3-ATPases transport cations (e.g. the Ca^{++}-ATPase and Na^{+}/K^{+}-ATPase) or heavy metals (e.g. the Menkes disease copper transporter). In contrast, the P4-ATPases evolved the ability to transport bulky phospholipid molecules across biological membranes and the P5-ATPase substrate is still unknown (36,37,148). Although there are no crystal structures determined for the P4-ATPases, they share the same domain organization as ion-transporting P-type ATPases, for which multiple

crystal structures are available (16). The cytosolic actuator (A), nucleotide-binding (N) and phosphorylation (P) domains catalyze phosphate transfer from ATP to an Asp residue in the P domain and its subsequent dephosphorylation by the A domain. For P4-ATPases, unidirectional phospholipid translocation from the extracellular (or lumenal) leaflet to the cytosolic leaflet is associated with the dephosphorylation step (E2~P to E1 conformational transition) (71). The membrane domain is usually composed of 10 transmembrane segments, which form transport substrate binding sites and conduits through the membrane. Most P4-ATPases associate with a β–subunit consisting of a glycosylated ectodomain flanked by two transmembrane segments (74,149,150).

Eukaryotic organisms usually express multiple P4-ATPase genes. There are fourteen mammalian P4-ATPases that are associated with intellectual disability (51), neurodegeneration (52), liver disease (31,151), hearing loss (152), diabetes (153), immune deficiency (54,56), anemia (55) and reduced male fertility (154). Budding yeast express five members of this subgroup: Dnf1, Dnf2, Dnf3, Drs2 and Neo1. Neo1 is the only P4-ATPase essential for viability, although Drs2 and the Dnf proteins are collectively essential (2). The reason why a single-celled organism requires so many P4-ATPases is unclear. However, gene duplication and subsequent specialization for substrate specificity, subcellular localization, modes of regulation and binding partners may have contributed to the expansion.

The substrate preferences and transport mechanism is best understood for Drs2 and Dnf1, and least well understood for Neo1 (70). Dnf1 (and the nearly identical Dnf2) interacts with the Lem3 β-subunit, cycles between the plasma membrane, endosomes and TGN, and has a strong substrate preference for lyso-phosphatidylcholine (lyso-PC) and lyso-PE, phospholipids lacking one fatty acyl chain (2,65,66,74,102,149). Drs2 is a heterodimer with Cdc50, localizes to the TGN and early endosome, and primarily flips di-acylated phosphatidylserine (PS) and has a

weaker activity towards PE (35,36,65,70,74,83,155). Neo1 has no known β-subunit, localizes broadly throughout the Golgi and endosomes (3,113,156), and the substrate preference of this essential P4-ATPase has not yet been determined. The substrate transported by mammalian Neo1 orthologs ATP9A and ATP9B is also unknown. However, knockdown of the *C. elegans* Neo1 ortholog *TAT-5* causes exposure of PE in the outer leaflet of the plasma membrane, suggesting that PE may be the preferred substrate (7).

Exposure of aminophospholipids (PS and PE) on the cell surface can be detected using membrane impermeable cytotoxic peptides that bind to the headgroup and subsequently generate a pore in the membrane. Papuamide A (Pap A) is potent cytotoxic agent that binds specifically to PS, and duramycin binds specifically to PE with affinity in the nanomolar range (22,87,157). Wild-type (WT) yeast cells are relatively resistant to Pap A and duramycin because most of these aminophospholipids are restricted to the inner, cytosolic leaflet of the plasma membrane. In contrast, flippase mutants expose aminophospholipids in the extracellular leaflet and are hypersensitive to these cytotoxic agents. Here we use thermal inactivation of temperature conditional alleles of *NEO1* (*neo1-ts*) to explore the influence of Neo1 on plasma membrane phospholipid asymmetry, and the relationship between Neo1, Drs2 and Dnf1 for this function.

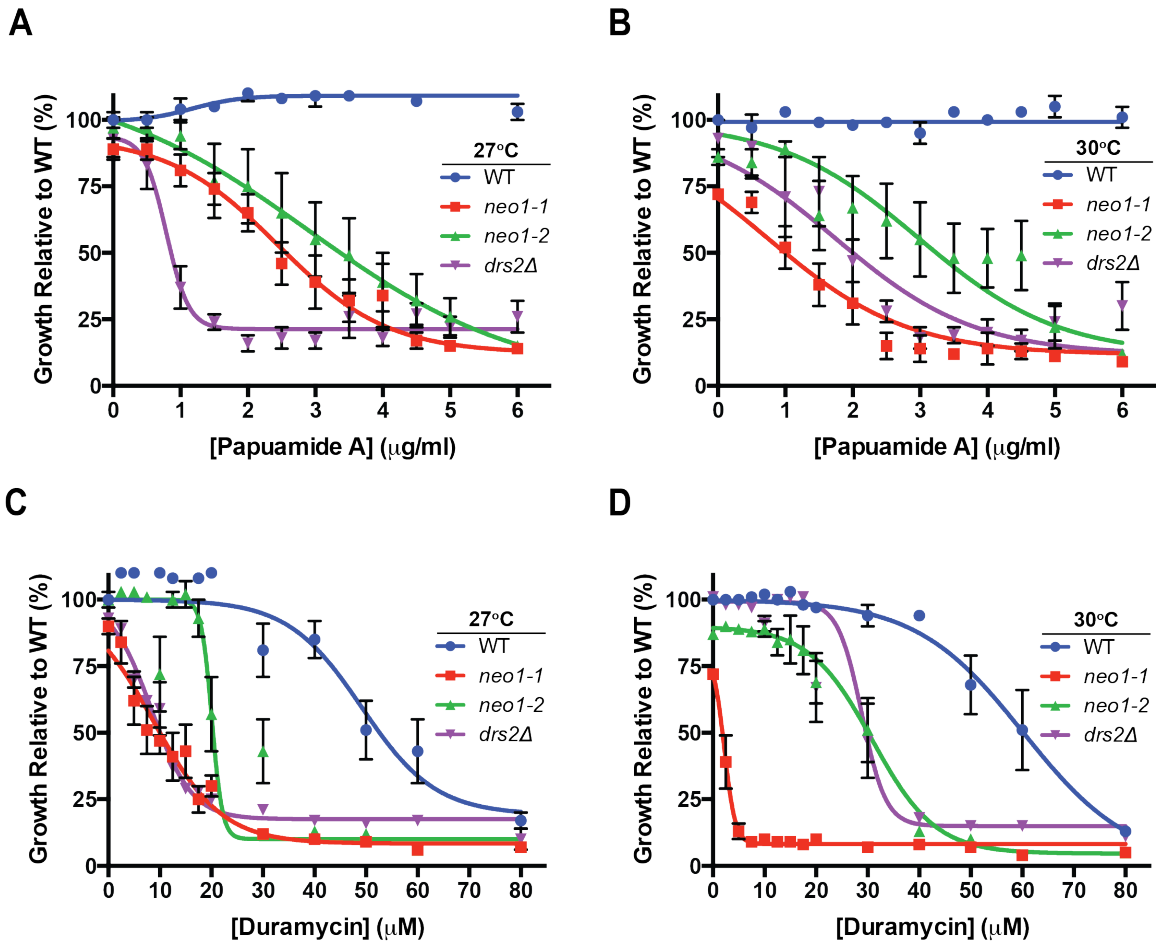

Figure 2-1. *neo1*^{ts} cells display a loss of membrane asymmetry. (A and B) WT (MTY219RR), *neo1-1* (MTY628-15B), *neo1-2* (MTY628-34A) and *drs2*Δ cells were incubated for 20 hours at the permissive growth temperature of 27°C (A) or the semi-permissive growth temperature of 30°C (B) with increasing concentrations of Papuamide A. (C and D) The same set of strains was assayed for duramycin sensitivity at 27°C (C) or 30°C (D). Growth relative to WT cells in the absence of drug was plotted (n≥5, error bars ±SEM). Sigmodial dose response curve fitting modality was applied, when the adjusted R^2 values are greater than 0.8, adjusted R^2 [0.8, 1]

Results

Inactivation of Neo1 causes a loss of membrane asymmetry

To test the influence of Neo1 on membrane asymmetry, we probed *neo1* mutants with pore-forming cytotoxic peptides that preferentially bind to PS or PE exposed on the outer leaflet of the plasma membrane. Cells become hypersensitive to Pap A when they lose PS asymmetry and become hypersensitive to duramycin when they lose PE asymmetry. Growth of *neo1*^{ts} (*neo1-1* and *neo1-2*) mutants over a range of toxin concentrations was compared to WT and *drs2*Δ, a flippase mutant that is known to display a loss of PS and PE asymmetry. Growth of each strain was plotted relative to WT cells incubated in the absence of toxin (Figure 2-1). These *neo1-1* and *neo1-2* alleles harbor a different set of mutations and the *neo1-1* mutant has a lower restrictive temperature, indicating that the Neo1-1 protein function is more strongly perturbed than Neo1-2 at a given temperature (e.g. 30˚C) (3).

At the *neo1*^{ts} permissive growth temperature of 27˚C, *neo1-1*, *neo1-2* and *drs2*Δ strains grew nearly as well as WT in the absence of Pap A or duramycin, but all three mutants were hypersensitive to both toxins relative to WT cells (Fig 2-1A and 2-1C). The *neo1-1*^{ts} and *neo1-2*^{ts} mutants showed a similar level of sensitivity to Pap A at 27˚C (IC_{50} of 2.5 – 3.5 µg/ml), whereas *drs2*Δ cells displayed the greatest Pap A sensitivity (IC_{50} of ~1.0 µg/ml (Figure 2-1A and Table 2-2).

Thus, *drs2*Δ had a greater loss of PS asymmetry at this temperature. In contrast, the *neo1-1* and *drs2*Δ mutants were equally sensitive to duramycin at 27˚C, while the weaker *neo1-2* mutant was less sensitive (IC50 of ~10 µM versus ~20 µM, Table 2-2). Even though the temperature conditional Neo1 mutants retained sufficient activity to support nearly WT growth at 27˚C (Figure 1, 0 toxin), they clearly displayed a loss of PS and PE asymmetry. Thus, the mutant Neo1 proteins must have reduced activity at 27˚C relative to WT Neo1.

At 30˚C, the growth defect of the stronger temperature-sensitive mutant, *neo1-1*, became detectable as the rate of growth was reduced to 75% relative to WT cells in the absence of toxins (Figure 2-1B and 2-1D). Sensitivity of *neo1-1* to Pap A was modestly enhanced at this semipermissive temperature, but sensitivity of *neo1-2* was unchanged relative to 27˚C (Figure 2-1A and 2-1B). The *drs2*Δ mutant actually became more resistant to Pap A and duramycin at 30˚C relative to 27˚C (Figure 2-1A and 2-1B), which likely reflects a greater ability of the remaining P4-ATPases to compensate for the loss of Drs2 at higher temperatures (3). Most striking was the extreme hypersensitivity of *neo1-1* to duramycin at 30˚C (IC50 of ~2 μM) (Figure 2-1D and Table 2-2). At this temperature, *neo1-2* and *drs2*Δ displayed a comparable hypersensitivity to duramycin. Importantly, a sufficient inactivation of *neo1-1* to just give a detectable growth defect, correlated with a substantial loss of PE asymmetry. These results suggest that the primary role of Neo1 is to establish PE asymmetry, but it also has a significant influence on PS asymmetry.

Exposure of PE and PS on *neo1*^{ts} cells is not a secondary effect of Drs2/Dnf mislocalization or loss of activity at the plasma membrane

Inactivation of Drs2 or the Dnf1/2 flippases also causes a loss of PS and PE asymmetry of the plasma membrane. Thus, it was possible that the expression or activity of these other P4-ATPases was perturbed in *neo1*^{ts} mutants, thereby causing the loss of membrane asymmetry. Initially, we tested whether loss of Neo1 activity can influence expression of Drs/Dnf proteins. To test this, we quantified the expression of Dnf1-HA, Dnf2-HA and Drs2 using Western blot analysis (Figure 2-2A). The HA tags were integrated into the chromosomal loci and so Dnf1-HA and Dnf2-HA were expressed from their endogenous promoters. WT* cells lack the HA tags while WT cells express both the tagged Dnf proteins and the WT Neo1 and Drs2. Equal amounts of total protein were loaded in each lane, which was confirmed by probing for Arf1 as a loading control. While there

appeared to be a partial reduction in the amount of Dnf1-HA and Drs2 in the *neo1-1* cells relative to WT cells, these differences were not statistically significant (Fig 2-2B, n=3).

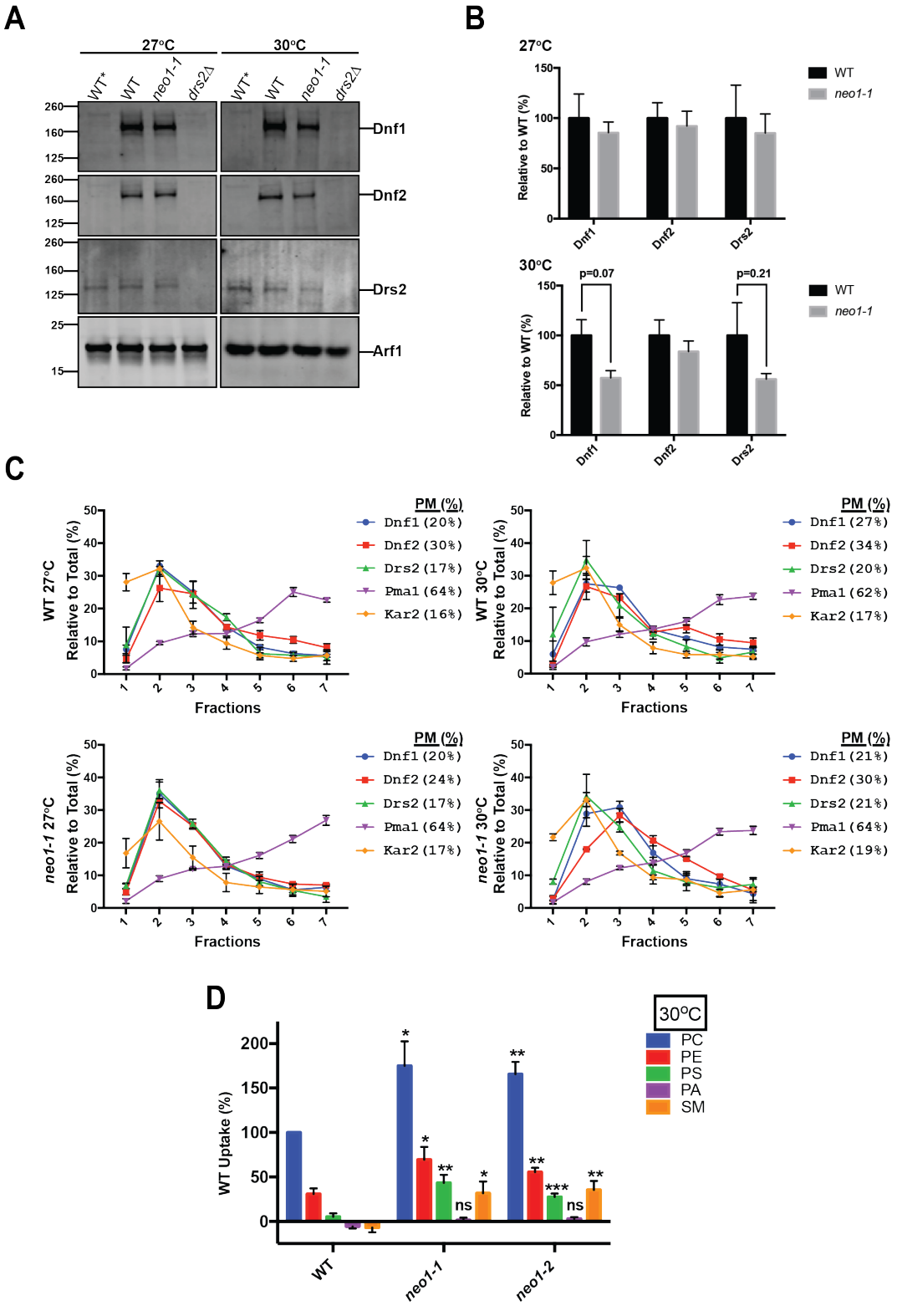
A
27°C
30°C
WT*
WT
neo1-1
drs2Δ
260
160
125
25
15
Dnf1
Dnf2
Drs2
Arf1
B
27°C
30°C
Relative to WT (%)
WT
neo1-1
p=0.07
p=0.21
Dnf1
Dnf2
Drs2
C
WT 27°C
WT 30°C
neo1-1 27°C
neo1-1 30°C
Relative to Total (%)
Fractions
PM (%)
Dnf1 (20%)
Dnf2 (30%)
Drs2 (17%)
Pma1 (64%)
Kar2 (16%)
Dnf1 (27%)
Dnf2 (34%)
Drs2 (20%)
Pma1 (62%)
Kar2 (17%)
Dnf1 (20%)
Dnf2 (24%)
Drs2 (17%)
Pma1 (64%)
Kar2 (17%)
Dnf1 (21%)
Dnf2 (30%)
Drs2 (21%)
Pma1 (64%)
Kar2 (19%)
D
WT Uptake (%)
30°C
PC
PE
PS
PA
SM
ns
WT
neo1-1
neo1-2

Figure 2-2. Inactivation of Neo1 does not lead to significant changes in the distribution or expression of Drs2/Dnf P4-ATPases, but does increase Dnf1 and Dnf2 plasma membrane flippase activity. (A) Western blot analysis of wild-type and *neo1^{ts}* cells expressing HA-tagged Dnf1 (MTYD1-219RRL and MTYD1-62815BL) and HA-tagged Dnf2 (MTYD2-219RRL and MTYD2-62815BL) at 27^{o}C and 30^{o}C. Equal amount of total protein (7.5mg) was loaded from each sample and probed with anti-HA, anti-Drs2 and anti-Arf1. WT* (untagged) and *drs2*Δ were used as specificity controls. Arf1 levels were used to demonstrate equal loading of the samples. These images are representative of at least three biological replicates. (B) Quantifications of Dnf1-HA, Dnf2-HA and Drs2 levels in wild-type and *neo1^{ts}* cells at 27^{o}C and 30^{o}C. Intensity values for *neo1^{ts}* cells were normalized to those values of wild-type cells at corresponding temperatures (n≥3, error bars ±SEM). (C) Subcellular fractionation was done with wild-type and *neo1^{ts}* cells expressing Dnf1-HA and Dnf2-HA (same strains as used for panel A). Kar2 and Pma1 were probed as ER and plasma membrane markers respectively. Dnf1-HA, Dnf2-HA, Drs2, Kar2 and Pma1 levels for each fraction was plotted as the percentage of total intensity for each protein in all 7 fractions (For example, Dnf1-HA in fraction 7 divided by the sum of Dnf1-HA in all 7 fractions). The percent in plasma membrane fractions (%PM) is the sum of the percentages in fractions 5, 6 and 7. (D) Inactivation of *neo1^{ts}* alleles leads to increased Dnf1/Dnf2 activities at the plasma membrane. Lipid uptake assays were performed with WT (MTY219RR), *neo1-1* (MTY628-15B) and *neo1-2* (MTY628-34A) cells grown at 30^{o}C using fluorescent-labeled (NBD) phospholipids. Lipid uptake activities were plotted as percentage of NBD-PC uptake for wild-type cells. (* $p<0.05$, ** $p<0.01$, *** $p<0.001$, Student's t-test, n≥9; error bars ±SEM)

We also tested if the loss of PS and PE plasma membrane asymmetry in *neo1*^{ts} cells could be explained by loss of Dnf1-HA and/or Dnf2-HA from the plasma membrane using subcellular fractionation. Dnf1 and Dnf2 are localized to Golgi, endosomes and the plasma membrane, whereas Drs2 is normally localized to the TGN (2,155). However, loss of Drs2 activity does cause a substantial increase in its transport to the plasma membrane (100). WT and *neo1-1* cells were grown at 27˚C and half of the culture was shifted to 30˚C for 1 hr prior to lysis and fractionation in a sucrose gradient (Fig 2-2C). This fractionation method does not separate ER, Golgi and endosomes from each other, but it does separate these organelles from the plasma membrane reasonably well (158)

To assess the success of subcellular fractionation, we probed each fraction for Kar2 as an ER marker and Pma1 as a plasma membrane marker. We defined Pma1-enriched and Kar2-depleted fractions as plasma membrane fractions (fractions 5, 6 and 7; %PM). In plasma membrane-enriched fractions, Pma1 did not significantly change upon temperature shift in wild-type (64.1± 1.5% and 62.5±1.9% respectively) and *neo1*^{ts} cells (64.1±1.6% and 64.0±2.0% respectively) at 27^{o}C and 30^{o}C. In wild-type cells, there is a slight, but significant (Student t-test; p=0.032) increase in the percentage of plasma membrane-enriched Dnf1 upon temperature shift from 20±1.90% to 26.6±0.80%, while the percentage of plasma membrane enriched Dnf2 (30.3±3.1% and 34.2±2.0% respectively) did not change significantly (Figure 2-3C). In *neo1*^{ts} cells, the percentage of plasma membrane-enriched Dnf1 remain unchanged upon temperature shift (20.8±5.2% and 20.8±0.6% respectively), while the percentage of Dnf2 in plasma membrane-enriched fractions increased non-significantly (Student t-test; p=0.13) from 23.8±1.3% to 30.2±3.1%. Upon temperature shift, we did not observe any significant increase in the percentage of Drs2 in the plasma membrane-enriched fractions in either wild-type (17.2±1.8%

and 19.7±3.7% respectively) or *neo1*^{ts} cells (17.0±1.3% and 21.3±5.0%), implying Drs2 retained activity in *neo1*^{ts} cells. In summary, neither the total amount nor the distribution of Drs2/Dnf family flippases between the plasma membrane and internal organelles changed significantly upon inactivation of *neo1*^{ts}. Based on these results, exposure of PE and PS on *neo1*^{ts} cells cannot be accounted for by a decrease in the expression or loss of plasma membrane localization for the Drs2/Dnf family flippases.

However, loss of PE and PS asymmetry in *neo1*^{ts} cells might be due to reduced activities of Dnf1 and Dnf2 at the plasma membrane. To test this, we measured plasma membrane flippase activity, catalyzed primarily by Dnf1 and Dnf2, in WT and *neo1*^{ts} cells using NBD-labeled PC, PE, PS, phosphatidic acid (PA) and sphingomyelin (SM). A *dnf1,2*Δ stain was also assayed and the low level of fluorescent lipid uptake was subtracted as background. Rather than a loss of activity, we found significantly enhanced activity for all substrates except NBD-PA (Figure 2-2D). The ability of *neo1*^{ts} cells to exclude NBD-PA argues against an increase in nonspecific flip-flop. These strains also excluded propidium iodide, which was used to eliminate dead cells from this flow cytometry based analysis. We conclude that Dnf1 and Dnf2 are present and active at the plasma membrane of *neo1*^{ts} mutants. Although Drs2 cannot be directly measured using this lipid uptake activity assay, it is unlikely that Drs2 activity is substantially perturbed in *neo1*^{ts} cells because even partial loss of Drs2 activity in the *neo1*^{ts} background is lethal (3).

Exposure of PE on neo1ts cells is not a secondary effect of perturbing COPI function

Inactivation of Neo1 causes protein trafficking defects in the early secretory pathway and the COPI cargo protein GFP-Rer1 is mislocalized from the *cis*-Golgi to the vacuole lumen (3). It is possible that the loss of plasma membrane asymmetry in *neo1*^{ts} mutants is a secondary

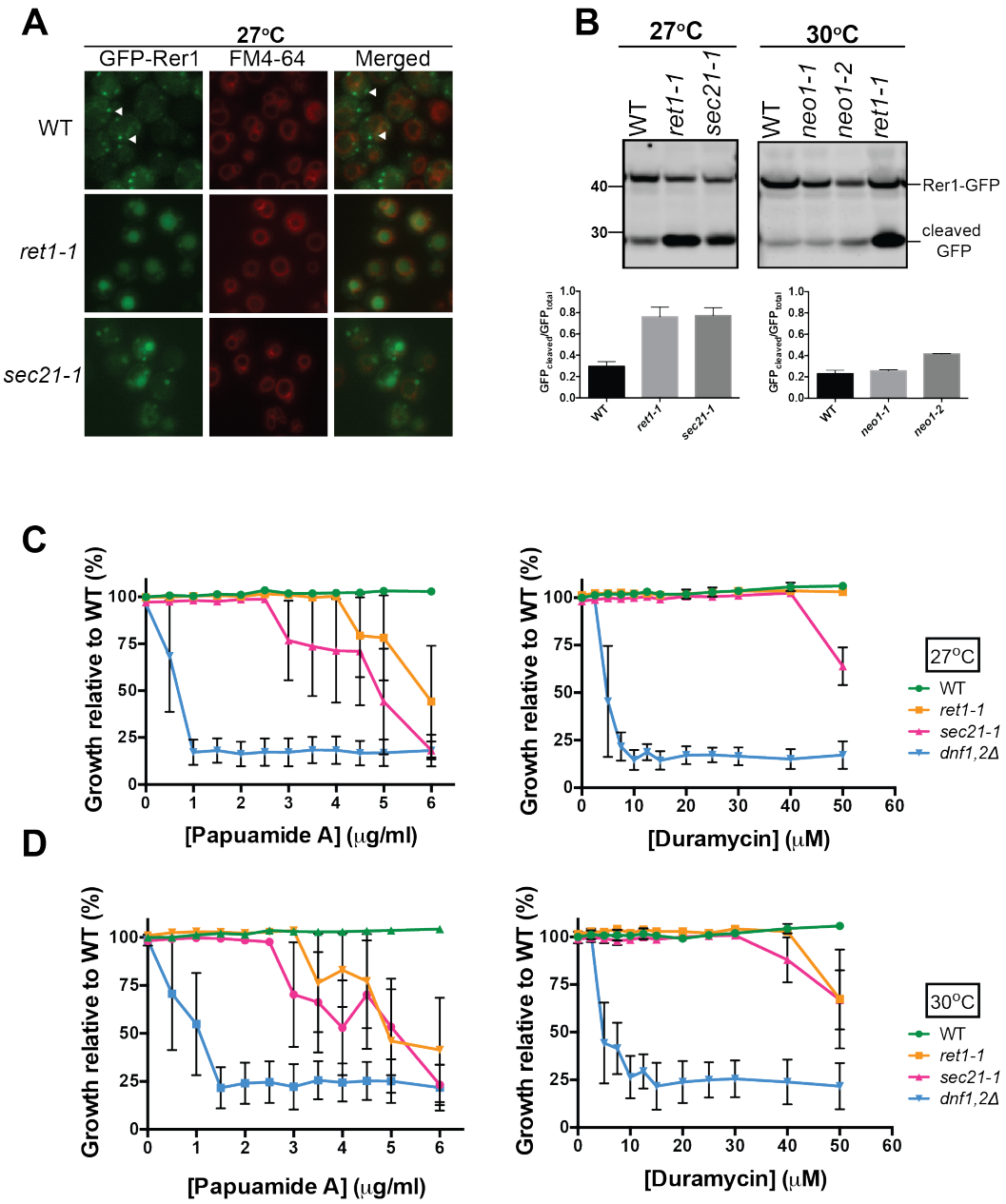

Figure 2-3. *neo1*^{ts} mutants display a dramatic loss of membrane asymmetry at growth temperatures that do not disrupt protein trafficking. (A) Rer1-GFP trafficking in wild type cells (SEY6210) and *copI*^{ts} alleles (*ret1-1* and *sec21-1*) at 27°C. FM4-64 staining was done with wild-type and *copI*^{ts} alleles expressing *pURA3-GFP-RER1*. White arrows indicate the punctate localization for GFP-tagged Rer1. (B) Quantitative analysis of Rer1-GFP localization by Western blot analysis for wild type, *copI*^{ts} and *neo1*^{ts} cells grown at 27°C. Ratios of GFP cleaved versus total GFP were determined for wild type, *copI*^{ts} and *neo1*^{ts} cells; n≥2. (C) Duramycin and Papuamide A sensitivity assays was performed with wild type and *copI*^{ts} cells at 27°C and (D) at 30°C. Growth relative to wild type cells (SEY6210) was plotted; n≥3. Sigmodial dose response curve fitting modality yielded adjusted R^2 values smaller than 0.8. Data points were connected to generate the graphs.

consequence of perturbing COPI-dependent trafficking pathways. To test this, we examined plasma membrane organization in COPI mutants (*ret1-1* and *sec21-1*) at a temperature where the strains grow well, but show a strong defect in GFP-Rer1 localization. At 27˚C, most of GFP-Rer1 localized to Golgi punctae in WT cells, but was mislocalized to the vacuole, marked by FM4-64, in *ret1-1* and *sec21-1* (Fig 3A). Vacuoles are fragmented in *neo1*^{ts} cells making the mislocalization of GFP-Rer1 difficult to detect by microscopy (3), and so Western blots were used to quantify the amount of GFP-Rer1 mislocalized to the vacuole (159).

Upon arrival in the vacuole, the GFP-Rer1 fusion protein is cleaved by vacuolar proteases to release GFP. In WT cells, ~30% of GFP-Rer1 is cleaved at steady-state, providing a population average of the amount of the fusion protein in the vacuole. Consistent with the imaging result, about 75% of GFP-Rer1 is cleaved in the COPI mutants indicating mislocalization to the vacuole (Figure 2-3B). At 30˚C, where *neo1-1* displayed substantial sensitivity to duramycin (Figure 2-1D) GFP-Rer1 was not mislocalized to the vacuole as indicated by the small percentage (22%) of GFP-Rer1 that was cleaved (Figure 3B).

The COPI mutants were modestly sensitive to papuamide A and almost completely resistant to duramycin at 27˚C, and became slightly more sensitive to the toxins at 30˚C (Figure 3C and 3D). These results indicate that loss of COPI function does cause a partial loss of PS asymmetry and a relatively minor exposure of PE in the outer leaflet of the plasma membrane. In contrast, *neo1*^{ts} mutants display a dramatic loss of membrane asymmetry at growth temperatures that do not disrupt protein trafficking. Thus, loss of membrane asymmetry in *neo1*^{ts} cells cannot be explained by a loss of COPI function.

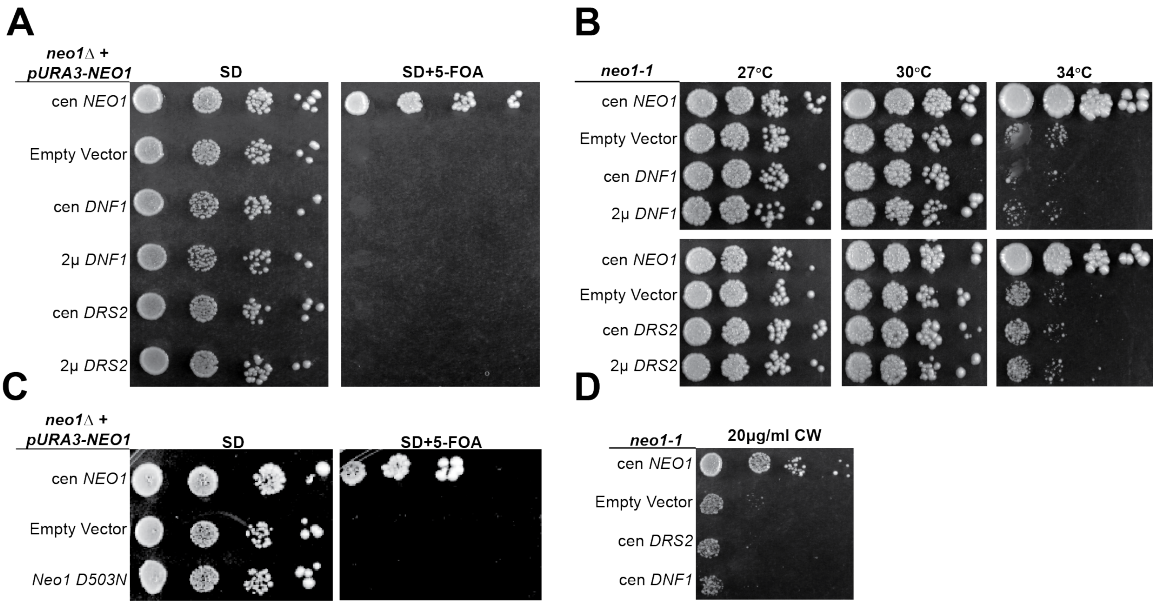

Figure 2-4. *NEO1* exerts an essential function that cannot be provided by *DNF1* or *DRS2* (A) Overexpression of *DNF1* or *DRS2* with their co-chaperones failed to suppress *neo1*Δ lethality. *neo1*Δ + pRS416-*NEO1* (YWY10) expressing single copy (cen) *NEO1* (pRS313-*NEO1*), empty vector (pRS313), single copy or multi-copy (2μ) *DNF1* or *DRS2* (pRS313-*DNF1*, pRS423-*DNF1*, pRS315-*DRS2* or pRS425-*DRS2*) and their co-chaperones (pRS425-*LEM3* or pRS423-*CDC50*, respectively) were spotted onto minimal media plates (SD) and the pRS416-*NEO1* plasmid was counter selected on 5-fluorotic acid (5-FOA). (B) A *neo1*^{ts} mutant (MTY628-15B) was transformed with the same set of plasmids and assayed for growth at the indicated temperatures. (C) *neo1*Δ + pRS416-*NEO1* (YWY10) expressing single copy *NEO1* (pRS313-*NEO1*), empty vector (pRS313) or single copy catalytically-dead *neo1-D503N* (pRS313-*neo1-D503N*) were spotted onto minimal media plates (SD) and the pRS416-*NEO1* plasmid was counter selected on 5-FOA. (D) *neo1-1* hypersensitivity to calcofluor while (CW) at 30^{o}C was not suppressed by overexpression of *DRS2* or *DNF1*. Images are representative of 3 independent experiments.

Relationship between P4-ATPases that potentially flip PE

The loss of PE and PS asymmetry in *neo1* mutants suggested that Neo1 shares a substrate preference with Drs2 and Dnf1, and that translocation of PE across membranes could be Neo1's essential function. Neo1 is broadly distributed throughout the Golgi and has an overlapping localization with Drs2 and Dnf1 in the late Golgi and endosomal system (2,113,156). Disruption of *NEO1* in a haploid strain is lethal, indicating that the other P4-ATPases cannot compensate for loss of *NEO1* at endogenous levels of expression. However, we hypothesized that overexpression of Drs2 or Dnf1, which are both capable of flipping NBD-phosphatidylethanolamine (NBD-PE), might compensate for loss of Neo1. To test this, we performed a plasmid shuffle assay to replace *NEO1* with low copy (cen) or multi-copy (2μ) plasmids expressing *DNF1* with its β-subunit *LEM3*, or *DRS2* with its β-subunit *CDC50*. *neo1*Δ strains covered by *NEO1* on an *URA3*-marked plasmid and harboring *DNF1* or *DRS2* plasmids were serially diluted on 5-FOA plates to select for colonies having lost the *URA3*-marked *NEO1* plasmid (Figure 2-4A). A control strain harboring a second copy of WT *NEO1* on a *LEU2* plasmid formed colonies on 5-FOA and all of the strains grew well on minimal medium (SD) lacking 5-FOA, as expected. In contrast, no colonies grew on 5-FOA from the *neo1*Δ cells expressing additional copies of *DNF1* or *DRS2*. Thus, overexpression of *DNF1* or *DRS2* with their co-chaperones was unable to suppress *neo1*Δ lethality.

To provide a more sensitive assay for suppression, we next transformed the *neo1-1*^{ts} mutant with the same set of plasmids harboring *DRS2* or *DNF1* and their β-subunits. The *neo1-1* cells carrying an empty vector grew well at the permissive temperatures of 27˚C and 30˚C, but grew very slowly at the semi-permissive temperature of 34˚C relative to the *neo1-1* strain complemented with WT *NEO1*. Overexpression of neither *DNF1* nor *DRS2* was able to suppress the growth defect of *neo1-1* at 34^{o}C (Figure 2-4B). Lack of suppression by *DRS2* or *DNF1* raised

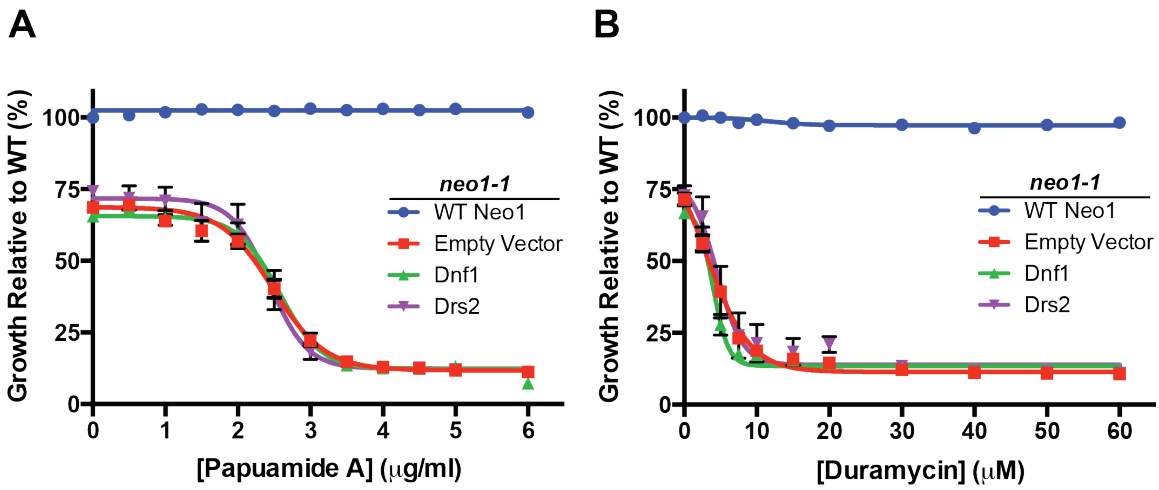

Figure 2-5. Moderate overexpression of *DNF1* or *DRS2* failed to suppress loss of membrane asymmetry in *neo1-1* cells. Papuamide A (Pap A) (A) and duramycin (B) sensitivity of *neo1-1* cells expressing single copy *NEO1*, *DNF1*, *DRS2* or empty vector at 30°C; n≥4. Sigmodial dose response curve fitting modality was applied, when the adjusted R^2 values were greater than 0.8, adjusted R^2 [0.8, 1]. (C) Inactivation of *neo1*^{ts} alleles leads to increased Dnf1/Dnf2 activities at the plasma membrane. Lipid uptake assays were performed with WT (MTY219RR), *neo1-1* (MTY628-15B) and *neo1-2* (MTY628-34A) cells grown at 30°C using fluorescent-labeled (NBD) phospholipids. Lipid uptake activities were plotted as percentage of NBD-PC uptake for wild-type cells. (* $p<0.05$, ** $p<0.01$, *** $p<0.001$, Student's t-test, n≥9; error bars ±SEM)

the concern that Neo1 might have an essential function that is independent of its presumed catalytic activity. However, mutation of the aspartic acid predicted to be phosphorylated during the catalytic cycle inactivated Neo1 based on its inability to complement the *neo1*Δ strain (Figure 4C, *neo1-D503N*).

The *neo1-1* mutant has previously been shown to also display a defect in Golgi glycosylation events, potentially caused by hyperacidification of this organelle (3,4). This underglycosylation of cell wall components causes hypersensitivity to the chitin-binding compound calcofluor white (CW) (3). To determine if overexpression of the other flippases would suppress the glycosylation defects, we tested if *DRS2* or *DNF1* overexpression could suppress *neo1-1* CW hypersensitivity. We found that *DRS2* and *DNF1* overexpression both failed to suppress this phenotype (Figure 2-4D).

We next tested if overexpression of Drs2 or Dnf1 could correct the loss of plasma membrane asymmetry caused by inactivating *neo1-1*. For example, if Neo1 failed to translocate PE to the cytosolic leaflet of early Golgi membranes, Drs2 and/or Dnf1 could potentially flip this substrate as membrane flowed through the TGN or upon arrival at the plasma membrane. However, when assayed at 30˚C, additional copies of Drs2 or Dnf1 failed to suppress the Pap A or duramycin sensitivity of *neo1-1*. As expected, WT *NEO1* fully complemented this phenotype and restored PS and PE asymmetry (Figure 2-5A, B).

To further address the relationship between P4-ATPases with potentially overlapping substrates, we tested if *NEO1* could suppress growth and membrane asymmetry defects caused by loss of the Drs2/Dnf group of P4-ATPases. A plasmid shuffle assay was used to show that overexpression of *NEO1* from low copy or multi-copy vectors failed to suppress the lethality of the *drs2*Δ *dnf1,2,3*Δ quadruple mutant (Figure 2-6A). Surprisingly, we found that Neo1 overexpression from a low copy plasmid, but not the multi-copy plasmid, weakly suppressed the

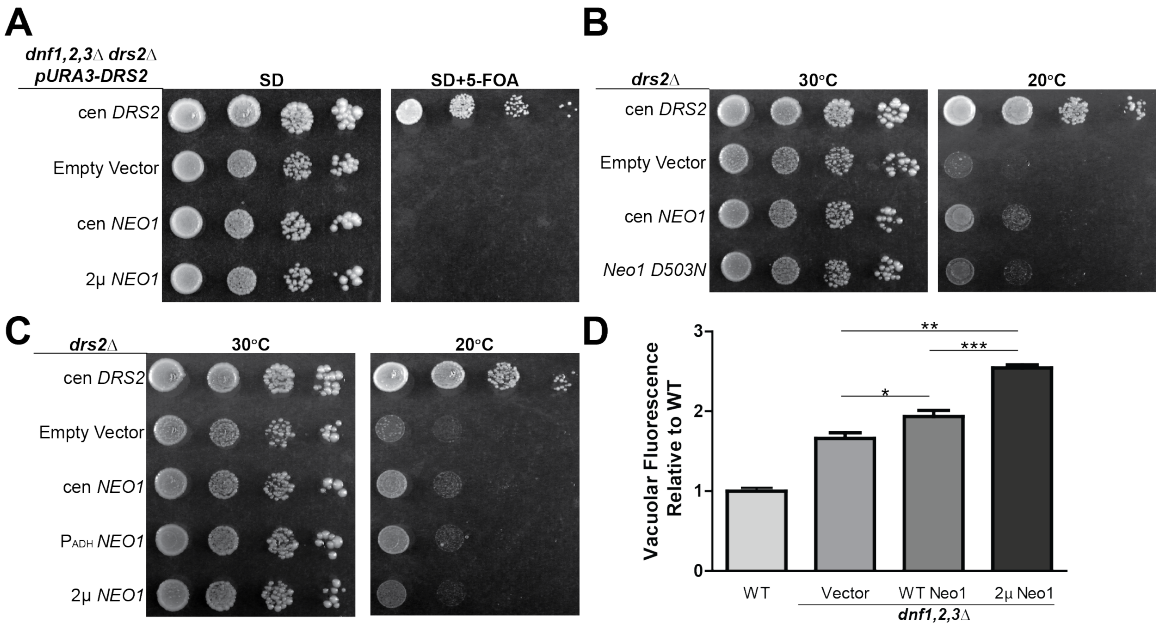

Figure 2-6. *NEO1* overexpression weakly suppresses *drs2*Δ, but not *dnf1,2,3*Δ. (A) Overexpression of *NEO1* failed to suppress *dnf1,2,3Δ drs2Δ* synthetic lethality. *dnf1,2,3*Δ *drs2*Δ pRS416-*DNF1* (ZHY704) strains expressing single copy (cen) *DRS2* (pRS313-*DRS2*), empty vector (pRS313), single copy or multi-copy (2μ) *NEO1* (pRS313-*NEO1* or pRS423-*NEO1,* respectively) were spotted onto minimal media plates (SD) and pRS416-*DRS2* was counter selected on 5-FOA. (B) Overexpression of *NEO1* can partially suppress *drs2Δ* cold sensitivity. *drs2Δ* strains (ZHY615M2D) expressing single copy *DRS2* (pRS313-*DRS2*), empty vector (pRS313), or constructs driving increasing *NEO1* expression (pRS313-*NEO1,* pRS413-P_{ADH}-*NEO1* and pRS423-*NEO1* respectively) were spotted onto SD plates and incubated at indicated temperatures. (C) Catalytically-dead *neo1-D503N* failed to suppress *drs2*Δ cold sensitivity. (D) Overexpression of *NEO1* exacerbated the hyperacidification of vacuoles in *dnf1,2,3Δ* cells (PFY3273A). Wild-type cells and *dnf1,2,3*Δ cells transformed with empty vector (pRS313), single copy *NEO1* (pRS313-*NEO1*) or multi-copy *NEO1* (pRS423-*NEO1*) were stained with quinacrine and vacuolar fluorescence was quantified using flow cytometry relative to WT cells (BY4741)(* $p<0.01$, ** $p<0.001$, ***$p<0.0001$, Student's t-test, n=4). Images of colony growth are representative of 3 independent experiments.

cold-sensitive growth defect of *drs2*Δ at 20˚C. *NEO1* overexpressed from a low copy plasmid, but using the moderate strength ADH promoter (P_{ADH}-*NEO1*) also weakly suppressed *drs2*Δ (Fig 2-6B). To further probe this weak suppression, we compared WT *NEO1* with *neo1-D503N* and found that only WT *NEO1* could suppress *drs2*Δ (Fig 2-6C).

The *dnf1,2,3*Δ triple mutant does not exhibit a growth defect but it does display hyperacidic vacuoles, a phenotype also displayed by *neo1*^{ts} mutants (4). Therefore, we tested if *NEO1* overexpression could suppress this *dnf1,2,3*Δ phenotype. To assay the relative degree of vacuolar acidification, we stained cells with quinacrine and measured their fluorescence by flow cytometry. Quinacrine accumulation in cells is driven by the pH gradient across the vacuolar membrane and so the fluorescence intensity is proportional to vacuole acidity. As previously observed, *dnf1,2,3*Δ cells accumulated more quinacrine in the vacuole than WT cells (Fig 6D, vector). Surprisingly, instead of suppressing, *NEO1* overexpression exacerbated the vacuole hyperacidification phenotype (Fig 2-6D, WT and 2μ *NEO1*). The reason for these negative effects of 2μ *NEO1* are unclear, but these data show that moderate overexpression of *NEO1* fails to compensate for loss of the Dnf P4-ATPases.

We also examined the influence of *NEO1* overexpression on plasma membrane asymmetry defects exhibited by *drs2*Δ and *dnf1,2*Δ strains. *NEO1* overexpression had no influence on the Pap A or duramycin sensitivity of *dnf1,2*Δ cells (Fig 2-7A, B). However, we observed a small, but statistically significant increase in Pap A and duramycin resistance for *drs2*Δ cells overexpressing *NEO1* from a low copy plasmid relative to the empty vector control (Fig 2-7C, D). The increase in duramycin resistance was more pronounced than the increase is Pap A resistance, again implying that Neo1 has a greater influence on PE than PS asymmetry.

Discussion

Membrane asymmetry is a highly conserved feature of the eukaryotic cell plasma membrane and the P4-ATPases play a crucial role in establishing the differences in phospholipid composition between inner and outer leaflets of the bilayer. Biochemical and genetic data strongly support the proposed flippase activity of several P4-ATPases and demonstrate important differences in substrate preferences for these pumps (35-37,64,70). However, there is a paucity of data for the Neo1/ATP9/TAT-5 branch of the P4-ATPase phylogenetic group with regard to substrate specificity, influence on membrane asymmetry and functional relationship with other P4-ATPases in the cell.

Here we show that *neo1*^{ts} mutants display a loss of plasma membrane asymmetry and aberrantly expose PS and PE in the outer leaflet of the plasma membrane at permissive growth temperatures. Partial thermal inactivation of Neo1^{ts} to produce a mild growth defect led to a substantial increase in PE exposure without significantly increasing exposure of PS relative to cells grown at permissive temperature. This correlation between diminished growth and enhanced exposure of PE suggests that PE translocation by Neo1 could be its essential function. Alternatively, Neo1 could flip PS and PE equally well, but the anionic PS could be preferentially retained in the cytosolic leaflet by interactions with the cytoskeleton or membrane proteins.

Neo1 localizes to cis, medial and TGN cisternae of the Golgi in addition to late endosomal compartments (3,113,156). The failure to flip PE and PS from the lumenal leaflet to the cytosolic leaflet of the Golgi could allow exposure of these aminophospholipids in the extracellular leaflet of the plasma membrane as membrane flows by vesicular transport from the Golgi to the plasma membrane. However, the *neo1*^{ts} mutants express four other P4-ATPases with the ability to flip PE and/or PS that localize downstream of Neo1 to the TGN, early endosomes

and plasma membrane. It is unclear why these P4-ATPases cannot compensate for the Neo1 deficiency and correct the membrane asymmetry defect.

We considered the possibility that loss of asymmetry in *neo1*^{ts} mutants was a secondary effect of disrupting the function of these other P4-ATPases. However, we could find no evidence that inactivation of Neo1 indirectly perturbed the levels, localization or activity of Dnf1, Dnf2 or Drs2. We further tested if there was an inadequate amount of Drs2 and Dnf1 in *neo1*^{ts} cells by overexpressing these proteins from multicopy plasmids, but there was a striking lack of suppression of either the growth defect or the loss of plasma membrane asymmetry in *neo1*^{ts} cells. In contrast, we could detect a mild suppression of *drs2*Δ growth and membrane asymmetry defects by modest overexpression of Neo1. We observed a more substantial correction of PE exposure relative to PS, again suggesting a preference of Neo1 in establishing PE asymmetry. However, the overriding conclusion is that there is very little functional overlap between Neo1 and the Drs2/Dnf group of P4-ATPases.

One possible reason for the lack of functional overlap is that Neo1 flips a different molecular species of PE and PS than does Drs2 or Dnf1. Pap A and duramycin recognize only the headgroups of the lipids and do not appear to distinguish between forms differing in their acyl chain composition. Therefore, we do not know the precise molecular composition of the aminophospholipids exposed in the outer leaflet of *neo1*^{ts} and *drs2*Δ mutants. The flippases, in

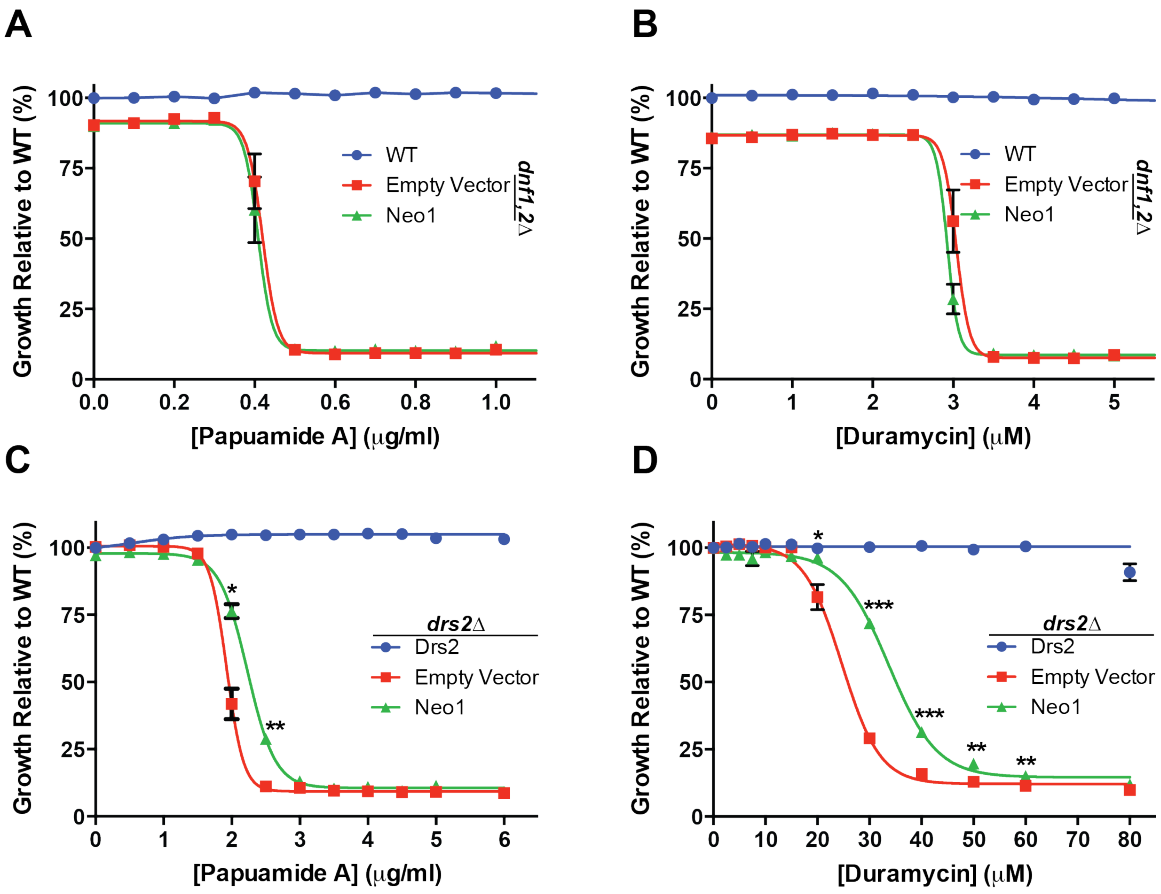

Figure 2-7. Moderate overexpression of *NEO1* can partially suppress loss of PE and PS asymmetry in *drs2*Δ cells, but not in *dnf1,2*Δ cells. (A and B) Sensitivity of WT (BY4741) and *dnf1,2*Δ cells (PFY3275F) expressing empty vector (pRS313) or single copy *NEO1* (pRS313-*NEO1*) to Pap A (A) and duramycin (B) at 30^0C. (C and D) Sensitivity of *drs2*Δ cells expressing single copy-*DRS2* (pRS313-*DRS2*), empty vector (pRS313) or single copy *NEO1* (pRS313-*NEO1*) to (C) Papuamide A or (D) duramycin at 30^0C. Growth relative to WT cells in the absence of drug was plotted (* $p<0.01$; ** $p<0.001$, *** $p<0.0001$ Student's t-test; $n\geq5$). Images are representative of 4 independent experiments. Sigmodial dose response curve fitting modality was applied, when the adjusted R^2 values were greater than 0.8, adjusted R^2 [0.8, 1].

contrast, can distinguish phospholipids by both their headgroup and acyl chain occupancy. For example, we have isolated gain of function mutations in Dnf1 that greatly increase its ability to transport NBD-PS across the plasma membrane and these mutants fall into two classes (65,70,83). The first class of Dnf1 mutants will transport lyso-PS (lacking one acyl chain), but not diacyl-PS, and will not replace the function of Drs2 *in vivo*. The second mutant class transports lyso-PS and diacyl-PS and these Dnf1 mutants will replace the function of Drs2 *in vivo* (65). Similarly, the ability of Neo1 to weakly replace Drs2 function *in vivo,* but not the function of Dnf1, suggests that Neo1 can flip dually acylated phospholipid. Perhaps there is a significant difference in the preference of Drs2 and Neo1 for phospholipids with different acyl chain lengths or degree of saturation. For example, if Neo1 preferentially flips PE with unsaturated fatty acids while Drs2 prefers fully saturated PE we would expect a lack of functional overlap.

What is the function of Neo1 and how does this protein influence membrane asymmetry? The loss of membrane asymmetry in *neo1*^{ts} mutants supports the idea that Neo1 is a phospholipid flippase, but is insufficient evidence to prove this point. For example, general defects in membrane biogenesis in *neo1* cells could lead to plasma membrane instability and transient ruptures that expose aminophospholipids in the outer leaflet. However, a nonspecific membrane defect would presumably expose PS and PE equivalently and we observe conditions where PE is preferentially exposed in *neo1*^{ts} cells relative to PS, or preferentially restored to the inner leaflet when Neo1 is overexpressed in *drs2*Δ cells. Our data also suggest that there is not a general increase in non-specific lipid flip-flop across the *neo1-ts* membrane and the Dnf1 and Dnf2 flippases are active at the plasma membrane.

It was also possible that the loss of membrane asymmetry reflected a secondary consequence of disrupting Neo1 function in protein trafficking or the regulation of organellar pH

(3,4). Prior work has shown *neo1*^{ts} mutants mislocalize the COPI cargo Rer1 from Golgi membrane to the vacuole and hyperacidify Golgi and vacuole compartments (3). However, these phenotypes were observed at the nonpermissive temperature of 37˚C and no significant defect was observed at permissive growth temperatures. In contrast, *neo1*^{ts} mutants display a loss of asymmetry even at permissive growth temperatures. Moreover, COPI mutants that display a strong defect in Rer1-GFP localization display only a partial loss of PS asymmetry (relative to *neo1* or *drs2*Δ cells) and a negligible loss of PE asymmetry. Together, these data argue that loss of membrane asymmetry is not secondary consequence of disrupting protein trafficking or organelle acidification in *neo1*^{ts} cells.

These observations suggest that the primary function of Neo1 is phospholipid translocation with a preference for PE. However, definitive evidence for this biochemical activity requires reconstitution of purified Neo1 into proteoliposomes and detection of a flippase activity. Attempts to reconstitute Neo1 have not yet been successful, but the results reported here will help guide the choice of substrates to test in these assays.

Materials and Methods

Reagents

5-fluoroootic acid (5-FOA) was purchased from Zymo Research. Papuamide A was purchased from the University of British Columbia Depository. Duramycin, quinacrine dihydrochloride and calcofluor white were purchased from Sigma Aldrich. FM4-64 was purchased from Life Technologies. Mono-clonal anti-GFP (clone 1C9A5) and anti-HA antibodies (clone 12CA5) were purchased from Vanderbilt Antibody and Protein Resource. Anti-Arf1 antibody was generated at Graham laboratory (100). Anti-Pma1 and Anti-Kar2 were gifts from Amy Chang (University of

Michigan) and Jeff Brodksy (University of Pittsburgh), respectively. IRDye® 800CW goat anti-rabbit IgG (H+L) and 680RD goat anti-mouse IgG (H+L) secondary antibodies were purchased from Li-COR Biosciences.

Strains and plasmid construction

Strains and plasmids used in this study are listed in Table 1. Yeast strains were grown and transformed using standard media and transformation techniques (160-162) For growth tests on solid media, 0.1 OD_{600} cells were spotted with 10-fold serial dilutions onto synthetic media or synthetic media containing 5-FOA. A *NEO1* genomic DNA fragment with 518 bp upstream and 126 bp downstream of the *NEO1* open reading frame (ORF) was amplified from yeast genomic DNA using primers containing BamHI and XhoI restriction sites and cloned into *pRS416*, *pRS313* and *pRS423* to generate *pRS416-NEO1*, *pRS313-NEO1* and *pRS423-NEO1*. *pRS313-Neo1 D503N* and *pRS416-Neo1 D503N* plasmids were generated by gene splicing overlap extension PCR using Neo1_D503N_For (5'-CGTATTGAATACCTTCTAAGCAATAAAACAGGGACGCTTA-3') and Neo1_D503N_Rev (5'-TAAGCGTCCCTGTTTTATTGCTTAGAAGGTATTCAATACG-3') (163).

The plasmid *pRS416-NEO1* was transformed into BY4743 *neo1*Δ and the resulting cells were sporulated. After random sporulation, spore YWY10 (MATa *his3 leu2 met15 ura3 lys2 neo1Δ pRS416-NEO1*) was selected on SD plates with G418 but lacking uracil. A plasmid shuffling strategy was used to replace the plasmid *pRS416-NEO1* in YWY10 with plasmids containing *neo1*^{ts} alleles. *pRS413-neo1-1* and *pRS413-neo1-2* were transformed into YWY10 and the resulting cells were selected with 5-FOA to exclude cells containing *pRS416-NEO1*. The resulting strains transformed with *pRS413-neo1-1* and *pRS413-neo1-2* were MTY628-15B and MTY628-34A, respectively.

Sensitivity Assays

For Pap A and duramycin treatments, 0.1 OD_{600} of midlog phase cells were seeded in 96-well plates with or without drug. Plates were incubated at 27°C or 30°C for 20h and concentration of cells were measured in OD_{600}/ml with a Multimode Plate Reader Synergy HT (Bio-Tek). Relative growth was compared to vehicle-treated WT cells in the assay. For data presentation, the sigmodial curve fitting modality from Graphad Prism6 was used when adjusted R^2 values were greater than 0.8 for all experimental groups. When curve fitting produced an R^2 value <0.8, data points were simply connected without curve fitting to generate the toxin sensitivity graphs.

Quinacrine staining

For quinacrine staining, cells were grown to mid-logarithmic phase in enriched media at 30°C. Cells were resuspended in YPD medium containing 100 mM HEPES, pH 7.6, 200 μM quinacrine with 25 μg/ml propidium iodide and stained for 8 min at 30°C. Stained cells were washed three times with 100 mM HEPES, pH 7.6 and the average vacuolar fluorescence intensity of 10,000 live cells was measured using the FITC channel of a fluorescence activated cell sorter (4).

Lipid uptake assay

Lipid uptake assays were performed with with approximately one OD_{600} of wild type and *neo1*^{ts} mutant cells grown at 30°C to mid-logarithmic phase and using 1-palmitoyl-2{6-[(7-nitro-2-1,3-benzoxadiazol-4-yl)amino]hexanoyl)-sn-glycero-3-phospholipids (NBD-PLs) for 30 min as described previously (70). The amount of NBD-PL taken up by *dnf1,2*Δ cells was measured and subtracted as background from the NBD-PL taken up by WT and *neo1*^{ts} cells. Lipid uptake activities were plotted as the percentage of NBD-PC lipid uptake activity for wild type cells.

Fluorescence microscopy

Cells were washed three times prior to imaging with PBS containing 2% glucose. Images were acquired on a Zeiss Axioplanscope using a 63x Plan-ApoChromat oil DIC objective. An FITC or Cy3 filter was used for visualizing GFP or FM4-64 respectively.

Vacuolar staining

Cells were grown at the indicated temperatures to mid-logaritmic phase and stained using 32 μM of FM4-64 in enriched medium (YPD) for 20 min in the dark. The cells were chased in YPD lacking FM4-64 for 3 hours, then washed twice with PBS containing 2% glucose prior to imaging.

Western blot analysis

Cells were grown to mid-logarithmic phase at indicated temperatures. 0.1 OD_{600} equivalent of cell lysate was subjected to SDS-gel electrophoresis. Western blot analysis was performed using anti-GFP antibody (1:2000) (86) to distinguish between cleaved GFP (26 kD) and intact GFP-tagged Rer1 (40 kD). For quantitation, membranes were scanned at 800 nm using the Odyssey Infrared Imaging System; median GFP intensities were quantified using Odyssey software (LI-COR Biosciences). Ratios of $GFP_{cleaved}$ versus GFP_{total} were plotted.

Subcellular fractionation

Cell lysates were analyzed by subcellular fractionation as previously described (86). Seven fractions in total were collected from the top of the sucrose gradient. Each fraction was immunoblotted against Kar2 (ER marker) (anti-Kar2, 1:2000, (164)) and Pma1 (plasma membrane marker) (anti-Pma1, 1:5000, (165)) to assess the success of the fractionation. In addition, Dnf1, Dnf2 and Drs2 levels were quantified in each fraction by immunoblotting against an HA tag (Dnf1-HA and Dnf2-HA) (anti-HA antibody, 1:1000, Vanderbilt Antibody and Protein

Resource) and Drs2 (anti-Drs2, 1:500, (155)). The HA tags were integrated into the chromosomal DNF1 and DNF2 loci so the tagged proteins would be expressed at endogenous levels. Protein levels in each fraction were quantified as the percentage of total amount of that protein in the 7 fractions. Subcellular fractionation was performed three independent times. Protein concentrations of total cell lysates collected for subcellular fractionations were measured using a bicinchoninic acid assay (BCA) according to the manufacturers instructions. 7.5 mg of total cell lysates from each experimental group was subjected to SDS-gel electrophoresis. Western blot analysis was performed to measure the levels of endogenously HA-tagged Dnf1, Dnf2 and native Drs2 levels in wild-type and *neo1*^{ts} cells both at permissive and non-permissive temperatures. Immunoblots were also probed with anti-Arf1 serum (100). Levels of Dnf1, Dnf2 and Drs2 proteins were quantified in *neo1*^{ts} cells relative to the levels of these proteins in wild-type cells. Three independent transformants from each experimental group was used for western blot analysis.

Acknowledgements

We also thank Jeff Brodsky for anti-Kar2 and Amy Chang for anti-Pma1 antibodies. Flow Cytometry experiments were performed in the VUMC Flow Cytometry Shared Resource. We would like to thank Hannah M. Hankins for reviewing an earlier version of the manuscript. The VUMC Flow Cytometry Shared Resource is supported by the Vanderbilt Ingram Cancer Center (P30 CA68485) and the Vanderbilt Digestive Disease Research Center (DK058404). This research was supported by NIH grant GM107978 awarded to Todd R. Graham.

Table 1-1. Approximate IC_{50} values for strains treated with cytotoxic peptides at the indicated temperatures

IC_{50}-Papuamide A (µg/ml)		
	27°C	**30°C**
WT	> 6	> 6
neo1-1	2.5- 3.5	2.5- 3.5
neo1-2	2.5- 3.5	2.5- 3.5
*drs2*Δ	~1.0	2.5- 3.5
IC_{50}-Duramycin (µM)		
	27°C	**30°C**
WT	40- 50	50- 60
neo1-1	~10	~2
neo1-2	~20	30- 40
*drs2*Δ	~20	30- 40

CHAPTER III

NEO1-ANY1-DRS2 AXIS IS REQUIRED FOR VIABILITY AND PLASMA MEMBRANE ASYMMETRY

Abstract

Membrane asymmetry is a key organizational feature of the plasma membrane and is primarily defined by the near absence of phosphatidylserine (PS) and phospatidylethanolamine (PE) in the outer leaflet and their enrichment in the cytosolic leaflet. Type IV P-type ATPases (P4-ATPases) are phospholipid flippases that establish membrane asymmetry by translocating specific phospholipids from the exofacial leaflet to the cytosolic leaflet. There are five P4-ATPases in *Saccharomyces cerevisiae*: Drs2, Neo1, Dnf1, Dnf2 and Dnf3. Inactivation of Neo1 is normally lethal, suggesting Neo1 mediates an essential function that cannot be exerted by the other four P4-ATPases. However, disruption of *ANY1 (A*ntagonist of *N*eo1 in *Y*east*),* allows growth of *neo1*Δ and reveals a functional redundancy between the Golgi-localized Neo1 and Drs2. Here we show that Drs2 PS flippase activity is required to support viability of *neo1*Δ *any1*Δ cells. In addition, a Dnf1 variant with enhanced ability to flip PS can replace the function of Drs2 and Neo1 in *any1*Δ cells. *any1*Δ can also suppress *drs2*Δ growth defects but not the loss of membrane asymmetry. However, we identified a gain-of-function mutation in Neo1 (Neo1[Y222S]) that partially replaces Drs2 functions, including establishment of PS and PE asymmetry. Surprisingly, Neo1[Y222S] requires Any1 to restore membrane asymmetry. These results indicate a critical role for PS flippase activity in Golgi membranes to sustain viability and that Any1 plays a more complex role in Golgi membrane remodeling than previously assumed.

Introduction

In eukaryotes, phospholipid asymmetry is an essential property of the plasma membrane bilayer. For instance, phosphatidylcholine (PC) and sphingolipids (Sph) are enriched in the exofacial leaflet, and aminophospholipids such as phosphatidylserine (PS) and phosphatidylethanolamine (PE) are confined to the cytofacial leaflet (23,143,144). Membrane asymmetry is regulated through transbilayer movement of amphipathic phospholipids by the concerted activities of three types of transporters: floppases, flippases and scramblases (166). Floppases belong to the ABC transporter family and translocate phospholipid substrates to the exofacial leaflet of membranes (167). Flippases in the P4-ATPase family transport primarily aminophospholipids to the cytofacial leaflet of membranes in an ATP-dependent manner, although some members transport either PC or lyso-PC. Membrane asymmetry is thought to be produced from the net effect of relatively slow and nonspecific outward transport of phospholipid by ABC transporters, coupled with a rapid inward transport of aminophospholipids. Scramblases in the TMEM16f and Xkr8 protein families are phospholipid channels that open in response to a Ca^{++} influx (TMEM16F) or caspase cleavage (Xkr8) to dissipate the phospholipid gradient (44). These scramblases play important roles in blood clotting and removal of apoptotic cell corpses, respectively. In mammals, loss of P4-ATPase activity is associated with liver disease (151), diabetes (58), hearing loss (152), increased risk of myocardial infarction, neurodegeneration (52), and intellectual disability (51).

Membrane remodeling events within the Golgi complex play an important role in establishing plasma membrane asymmetry. Sphingolipid and glycosphingolipids are synthesized in the luminal (exofacial) leaflet of the Golgi and are exported by vesicular transport to the exofacial leaflet of the plasma membrane (20,98). Aminophospholipids are flipped by P4-ATPases from the luminal leaflet of the Golgi to the cytosolic leaflet, and subsequently move to

the cytosolic leaflet of the plasma membrane by either vesicular or nonvesicular routes. These events are also coupled to loading of sterol in late compartments of the Golgi complex to transition the bilayer from an ER-like composition and organization at the *cis*-face to a plasma membrane-like composition and organization at the *trans*-face (86,115). P4-ATPases also localize to the plasma membrane and endosomal compartments to ensure asymmetry is maintained as membrane fluxes through the endocytic pathway and recycles back to the plasma membrane (15).

While differences in subcellular localization may confer unique functions, it remains unclear why a single-celled organism like *Saccharomyces cerevisiae* expresses 5 different P4-ATPase. Dnf1, Dnf2, Dnf3 and Drs2 form an essential group with both overlapping and non-overlapping functions. For example, cells harboring *drs2*Δ grow well at 30˚C but fail to grow at 20˚C or below because the Dnf P4-ATPases can partially compensate for loss of Drs2 at higher temperatures but not the lower temperatures. Even at permissive growth temperatures, *drs2*Δ cells display protein trafficking defects between Golgi and endosomal membranes. Drs2 localizes to the *trans*-Golgi network (TGN), but Neo1, Dnf1 and Dnf3 also localize significantly to the TGN and yet fail to support these trafficking pathways in the absence of Drs2. Similarly, *neo1*Δ cells cannot grow at any temperature suggesting this essential P4-ATPase has a unique function that none of the other P4-ATPases can perform. (1,2). Consistently, Drs2 and Neo1 regulate different vesicular transport pathways: early endocytic / late secretory and early secretory pathways, respectively (2,3,5,48).

The phospholipid substrate specificity of budding yeast P4-ATPases appears to be the major determinant of their specific roles in the cell. Drs2 and its mammalian orthologs (ATP8A1 and ATP8A2) are primarily PS flippases, although they are also capable of flipping PE. Consistently, *drs2*Δ cells display a loss of plasma membrane PS and PE asymmetry. The favored substrates of Dnf1 and Dnf2 are lysoPC and lysoPE, phospholipids lacking one of the two fatty

acyl chains, and these P4-ATPases may function in nutrient scavenging and membrane repair. We previously mapped residues that conferred substrate specificity differences between Dnf1 and Drs2, and identified mutations that alter their specificity. Separation-of-function mutations in Drs2 were isolated that abrogates PS recognition without measurably perturbing PE recognition ($Drs2^{PS-}$). Conversely, gain-of-function mutations were isolated in Dnf1 that allow it to flip diacyl-PS without perturbing recognition of its normal substrates ($Dnf1^{PS+}$). Remarkably, *drs2*Δ cells expressing $Drs2^{PS-}$ display trafficking defects, but normal trafficking and growth at low temperature is restored in *drs2*Δ cells expressing $Dnf1^{PS+}$ (but not Dnf1). These observations imply that Drs2 is the primary PS flippase in the cell and the other P4-ATPases lack sufficient PS flippase activity to compensate for loss of Drs2.

However, both Drs2 and Neo1 (orthologs of mammalian ATP9A and ATP9B) are involved in regulating PS/PE plasma membrane asymmetry, and these P4-ATPases become functionally redundant when *ANY1* is deleted (5,6). Inactivation of $Neo1^{ts}$ more substantially perturbs PE asymmetry, but these cells also aberrantly expose PS. By contrast, inactivation of the *C. elegans* Neo1 ortholog, *Tat-5*, causes exposure of PE but without loss of PS asymmetry (7). The possibility that Neo1 and Drs2 have similar substrate preferences is supported by the observation that the PQ-loop membrane protein Any1 enforces separate functions for Drs2 and Neo1 in the Golgi/endosomal membranes (114,117). In the absence of Any1, PS and PE membrane asymmetry is restored in $neo1^{ts}$ ($neo1^{ts}$ *any1*Δ) to wild-type levels. Moreover, Drs2 is able to bypass the essential requirement for Neo1 as *neo1*Δ *any1*Δ viability depends on a wild-type copy of *DRS2* (114). Any1 was proposed to function as a "scramblase" in the Golgi, acting to dissipate the PS/PE gradients formed by Drs2 and Neo1 to segregate their functions (114). However, the mechanism by which Any1 antagonizes Neo1 has not been determined.

In this study, we provide evidence that the essential role of Drs2 and Neo1 in Golgi membranes lacking Any1 is to flip PS. We also identify a mutation in Neo1 (Y222S) that partially suppresses the cold-sensitive growth defect of *drs2*Δ and substantially corrects the membrane asymmetry defects in these cells. Y222 is conserved in Neo1/Atp9a/Atp9b/Tat-5 and this residue may help restrict PS transport in the wild-type proteins. Alternatively, Y222S may abrogate the ability of Any1 to antagonize Neo1 function. We find that Neo1 and Any1 co-immunoprecipitate although Y222S does not appear to disrupt this interaction. Thus, this study supports the proposed PE/PS flippase activity of Neo1 reported earlier and define a protein interaction network facilitating membrane remodeling events in the secretory pathway.

Materials and Methods

Reagents

Papuamide A was purchased from the University of British Columbia Depository. Duramycin, quanicrine dihydrochloride, calcofluor white, neomycin sulfate, monoclonal FLAG antibody and EzView FLAG beads were purchased from Sigma Aldrich. 5-fluoroorotic acid (5-FOA) was purchased from US Biologicals. Monoclonal GFP antibody (clone 1C9A5) was purchased from Vanderbilt Protein and antibody core and polyclonal GFP antibody was purchased from Torrey Pines Biolabs. Anti-Arf1, anti-Mnn1 and anti-Drs2 antibodies were generated at Graham Laboratory (100). IRDye® 800CW goat anti-rabbit IgG (H+L) and 680RD goat anti-mouse IgG (H+L) secondary antibodies were purchased from LiCOR Biosciences.

Strains and Plasmid Construction

Strains and plasmids used were listed in the Supplementary Table 1. Yeast strains were grown and transformed using standard media and transformation techniques (161,162,168).

Growth and plasmid shuffling assays, 0.1 OD_{600} of cells were spotted onto synthetic media or synthetic media containing 5-FOA and other toxic agents. Yeast knock-out and knock-in strains were generated as instructed previously (169). For co-IP experiments, *9XGLY-5XFLAG::HPHMX6* cassette was amplified from *pFA6a-G9-5FLAG-HPHMX6* and integrated in the carboxyl terminus of *ANY1* gene (BY4742). *pRS313-NEO1-9XGLY-5XFLAG* was generated by Gibson assembly mediated insertion of *9XGLY-5XFLAG* tag into *pRS313-*P_{NEO1}*-NEO1* vector. *pRS313-NEO1-9XGLY-5XFLAG* was transformed into *YWY10* and shuffled as a replacement of *pRS416-*P_{NEO1}*-NEO1*. Dnf1[Neo1] chimeras and Neo1 mutants were generated using 3-fragment and 2-fragment Gibson assembly according to the manufacturer's instructions.

Toxin Sensitivity assays

For toxin sensitivity assays, 0.1 OD_{600} of mid-log cells were distributed to each well of 96 well-plate with or without the toxin. Plates were incubated at 30^{o}C for 20 hours. Concentrations of the cells were measured in OD_{600}/ml with a Multimode Plate Reader Synergy HT (Biotek). Sigmodial curve fitting modality from Graphpad Prism7 was used to fit the data point from all samples, when R^2 values are equal or greater than 0.8 for all samples.

Lipid uptake assays

Lipid uptake assays were performed with approximately one OD_{600} of mid-log phase *dnf1,2*Δ (PFY3275F) cells expressing wild-type Dnf1, empty vector and Dnf1 mutants and using 1-palmitoyl-2{6-[(7-nitro-2-1,3-benzoxadiazol4yl)amino]hexanoyl)-sn-glycero-3-phospholipids (NBD-PLs) for 30 min as described previously (65,70,83). At least, three independent transformants were assayed for each experiment. Lipid uptake activities were plotted as the percentage of NBD-PC lipid activity of wild-type Dnf1.

Fluorescence microscopy

Strains expressing fluorescent fusion proteins were grown to mid-log phase in synthetic media. Images were acquired using a DeltaVision Elite system (GE Healthcare) and ImageJ was used to process the images. For quantifying colocalization, Mander's correlation coeffient was employed. Multiple images (at least 100 cells) were analyzed for calculating the Mander's correlation coeffient.

Immunoprecipitation and Western blot analysis

Mid-log phase cells were lysed and subjected to Western blot analysis as described previously (5). For expression analysis, polyclonal anti-GFP (1:2000) and monoclonal FLAG (1:5000) antibodies were used. Total protein concentrations were assessed by Bio-RAD stain-free gel system. The preparation of crude and Golgi-enriched membranes was performed as described previously (11). Golgi-enriched membrane fractions were solubilized with lysis buffer (10mM Tris-HCl pH7.5, 150mM NaCl, 2mM EDTA) supplemented with 1% CHAPS. Protein concentrations of Golgi-enriched membranes were quantified using a using a bicinchoninic acid assay (BCA). Immunoprecipitions of FLAG-tagged bait were performed from equal amount of total input using 50 µl of EzView FLAG beads for 2 hours at 4^{o}C. To assess the immunoprecipitations (IP), 1% of total input and 10% total elute were loaded onto SDS-PAGE gel and immunoblotted for GFP-tagged and FLAG-tagged bait protein levels. IP(s) were quantified as a percentage of input.

Results

PS flippase activity is required in *any1* deficient Golgi membranes

Neo1 and Drs2 have non-redundant functions in the Golgi complex despite their similar effects on plasma membrane asymmetry (5). However, removal of Any1 makes Neo1 and Drs2 redundant, but it was not clear whether a PS or PE flippase activity, or both activities were required to support viability in a *neo1*Δ *any1*Δ *drs2*Δ strain. To test this, we expressed wild-type (WT) Neo1, WT Drs2, Drs2^{PS-} (Drs2[QQ→GA]), WT Dnf1 and Dnf1^{PS+} (Dnf1[N550S]) in *neo1*Δ *drs2*Δ *any1*Δ cells expressing WT *NEO1* on *URA3*-marked plasmid. We counter-selected *pURA3-NEO1* on 5-FOA plates that maintained selection for the *HIS3*-marked plasmids bearing the P4-ATPases variants to be tested, and incubated the plates at 30^{o}C (Figure 3-1A). As previously reported, wild type Neo1 or Drs2 was sufficient to complement the *neo1*Δ *drs2*Δ *any1*Δ synthetic lethality and support growth, but the empty vector and extra copy of WT Dnf1 failed to suppress this synthetic lethality. Importantly, Drs2^{PS-} failed to complement the growth defect, but Dnf1^{PS+} fully suppressed the *neo1*Δ *drs2*Δ *any1*Δ synthetic lethality (Figure 3-1A). Thus, bypass of *neo1*Δ in cells lacking Any1 requires a PS flippase activity that can be provided by either Drs2 or Dnf1.

The cold-sensitive (CS) growth defect of *drs2*Δ can be fully suppressed by deletion of *KES1/OSH4*, encoding an ergosterol/phosphatidylinositol-4-phosphate exchange protein involved in Golgi membrane remodeling. Therefore, we tested if the synthetic lethality between *neo1*Δ and *drs2* alleles could be suppressed by *kes1*Δ. The same plasmid shuffling strategy was used to express WT Neo1, WT Drs2, Drs2^{PS-} and empty vector control in *neo1*Δ *any1*Δ *drs2*Δ and *neo1*Δ *any1*Δ *drs2*Δ *kes1*Δ cells (Figure 1B). In this experiment, *kes1*Δ failed to suppress the *neo1*Δ *any1*Δ *drs2* synthetic lethality (empty vector and Drs2[QQ→GA]), and only WT Neo1 or Drs2 were able to support growth of *neo1*Δ *drs2*Δ *any1*Δ *kes1*Δ cells (Figure 3-1B).

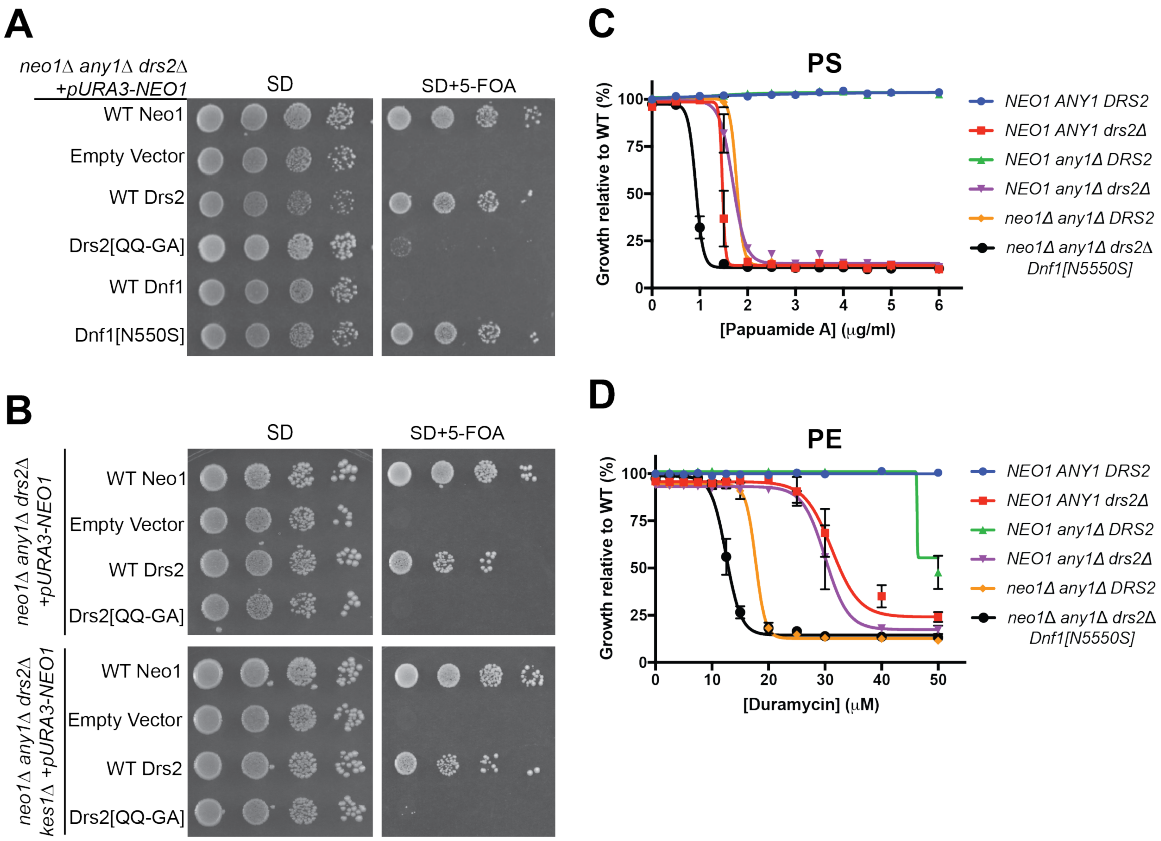

Figure 3-1. PS-flip in the Golgi membranes is required for viability. (A) PS-flipping Neo1, Drs2 and Dnf1[N550S] mutant can suppress the synthetic lethality of *neo1*Δ*drs2*Δ*any1*Δ mutant. *neo1*Δ*drs2*Δ*any1*Δ + pRS416-*NEO1* (MTY10-615M2DS) expressing single copy (cen) *NEO1* (pRS313-*NEO1*), empty vector (pRS313), *cen DRS2* (pRS313-*DRS2)*, *cen Drs2[QQ→GA]* (pRS313-*Drs2[QQ→GA])*, *cen DNF1* (pRS313-DNF1) and *cen Dnf1[N550S]* (pRS313-Dnf1[N550S]) respectively were spotted onto minimal media plates (SD) and the pRS416-*NEO1* plasmid was counter selected on 5-fluorotic acid (5-FOA). (B) Loss of Kes1 failed to suppress the synthetic lethality of *neo1*Δ*drs2*Δ*any1*Δ mutant. *neo1*Δ*drs2*Δ*any1*Δ*kes1*Δ + pRS416-*NEO1* (MTY10-615M2DS) expressing single copy (cen) *NEO1* (pRS313-*NEO1*), empty vector (pRS313), *cen DRS2* (pRS313-*DRS2)* and *cen Drs2[QQ→GA]* (pRS313-*Drs2[QQ→GA* respectively were spotted onto minimal media plates (SD) and the pRS416-*NEO1* plasmid was counter selected on 5-fluorotic acid (5-FOA). (C) None of the suppressors of *neo1*Δ*drs2*Δ*any1*Δ synthetic lethality can restore PS or (D) PS asymmetry to wild-type levels. Growth relative to WT cells in the absence of drug was plotted (n≥4, error bars ±SEM).

We previously found that *neo1*^{ts} mutants expose both PS and PE in the exofacial leaflet at semipermissive growth temperatures. Loss of asymmetry can be probed by hypersensitivity to pore-forming toxins that specifically target PS (papuamide A, PapA) or PE (duramycin) exposed on the exofacial leaflet of the plasma membrane. Loss of *neo1*^{ts} plasma membrane asymmetry is completely suppressed in *neo1*^{ts} *any1*Δ cells (114). Here we examined membrane asymmetry in strains carrying *neo1*Δ*, any1*Δ and *drs2*Δ null alleles. Wild-type and *any1*Δ cells were resistant to both PS-binding (PapA) and PE-binding (Duramycin) toxins, although any1Δ cells were partially sensitive to duramycin at the highest concentration tested (Figure 3-1C and 3-1D). The *neo1*Δ *drs2*Δ *any1*Δ cells expressing either Neo1, Drs2 or Dnf1^{PS+} were hypersensitive to PapA, and showed a similar level of sensitivity with Dnf1[N550S] displaying a slightly lower capacity to establish PS asymmetry relative to Drs2 or Neo1 (Figure 1C). Thus, none of these P4-ATPases could prevent PS exposure in the plasma membrane outer leaflet on their own. A comparison of *NEO1 ANY1 drs2*Δ to *NEO1 any1*Δ *drs2*Δ appeared to show *any1*Δ weakly suppressed drs2Δ, but these data were not significantly different (Figure 3-1C). Note that we cannot analyze the *neo1*Δ *ANY1 DRS2* strain because it is inviable. Dnf1[N550S], Drs2 and Neo1 conferred increasing resistance to duramycin with Neo1 restoring PE asymmetry to a significantly greater extent than Drs2 or Dnf1[N550S] in *neo1*Δ *drs2*Δ *any1*Δ cells. Again, none of the P4-ATPases were able to restore PE asymmetry to wild-type levels on their own, and *any1*Δ did not suppress PE exposure caused by *drs2*Δ. (Figure 3-1D). These findings indicate that Drs2, Neo1 and Dnf1^{PS+} have a near equivalent ability to support growth of neo1Δ any1Δ drs2Δ cells, and a comparable ability to establish PS asymmetry, whereas Neo1 has a more substantial impact on PE asymmetry than Drs2 or Dnf1^{PS+}.

To further explore these genetic relationships, we tested whether *any1*Δ could suppress growth phenotypes in strains deficient for several different P4-ATPases. Even though *any1*Δ did

not measurably suppress membrane asymmetry defects of *drs2*Δ, it was able to partially suppress the cs growth defect of *drs2*Δ (Figure 3-2A). Hypomorphic *neo1-1* and *neo1-2* alleles are synthetically lethal with *drs2*Δ (Figure 3-2A and (3)), but *any1*Δ effectively suppressed this synthetic lethality. The more stringent *neo1-1* allele still displayed a temperature sensitive (ts) growth phenotype in the *neo1-1 any1*Δ *drs2*Δ background while *neo1-2* was suppressed across the full growth temperature range (Figure 3-2A). However, *any1*Δ could not suppress the lethality caused by *drs2*Δ *dnf1,2,3*Δ (Figure 3-2B). Dnf1 and Dnf2 form heterodimers with Lem3 and *lem3*Δ cells grow well but are deficient for both Dnf1 and Dnf2 activities. Here we show that *lem3*Δ is synthetically lethal with *neo1-1* and *neo1-2* (Figure 3-1C top), but the growth defects of *neo1*^{ts} *lem3*Δ and *neo1*Δ *lem3*Δ are substantially, but not completely, suppressed by *any1*Δ (Figure 3-2C, bottom).

To test the influence of Any1 on the loss of membrane asymmetry caused by Drs2 and Dnf deficiency, we performed pore-forming toxin sensitivity assays with wild-type, *drs2*Δ*, drs2*Δ *any1*Δ*, dnf1*Δ*dnf2*Δ*, dnf1*Δ*dnf2*Δ *any1*Δ and *any1*Δ cells. *drs2*Δ and *drs2*Δ *any1*Δ were equally sensitive to PapA and equally sensitive to duramycin (Figure 3-2D, E). We further examined membrane asymmetry in wild-type, *dnf1*Δ*dnf2*Δ and *dnf1*Δ*dnf2*Δ *any1*Δ cells. Again, no significant difference in sensitivity to the toxins was observed with or without Any1 (Figure 2F and G). In summary, *any1*Δ suppresses growth and membrane asymmetry defects caused by hypomorphic *neo1* alleles and bypasses the essential function of Neo1 in a Drs2-dependent manner. *any1*Δ modestly suppresses the cs growth defect of *drs2*Δ, but does not enhance the ability of remaining P4-ATPases to restore PS/PE asymmetry. Similarly, *any1*Δ does not enhance the ability of remaining P4-ATPases to restore membrane asymmetry defects caused by *dnf1,2*Δ.

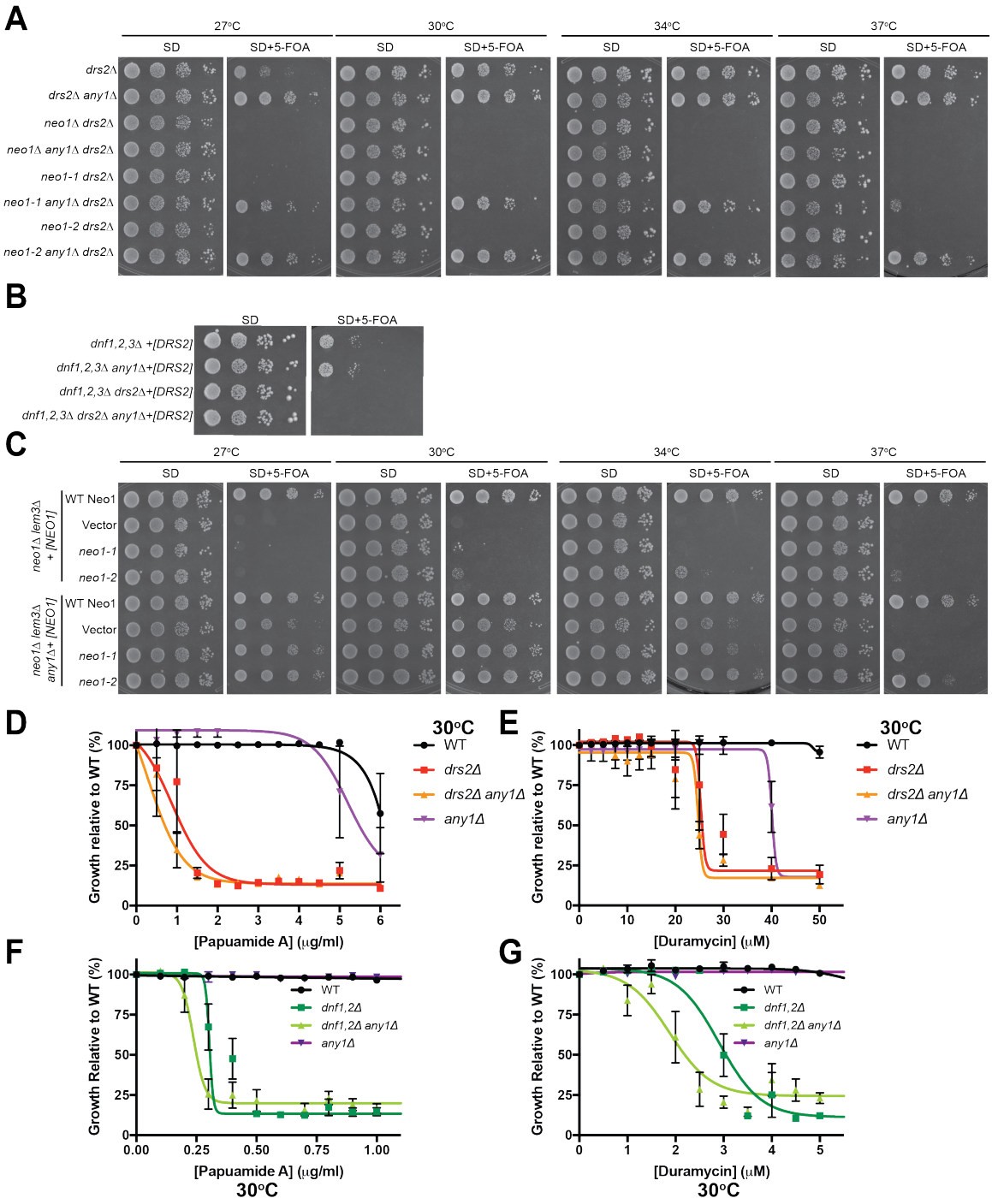

Figure 3-2. Any1 is in strong genetic interaction with Neo1, but not other P4-ATPases. (A) Both *neo1-1*^{ts} and *neo1-2*^{ts} mutants can support viability in the absence of Drs2 and Any1 at all temperatures tested except for 37°C. (B) Loss of Any1 failed to suppress the synthetic lethality of *dnf1,2,3*Δ*drs2*Δ mutant. (C) Loss of Any1 can suppress the synthetic lethality of *neo1*Δ*lem3*Δ or

neo1^{ts} *lem3*Δ mutant at all temperatures tested except for 37^{o}C. Loss of Any1 failed to suppress the PS (D,F) and PE (E,G) asymmetry defects in *drs2*Δ or *dnf1,2*Δ mutants respectively.

Overexpression of Any1 is toxic to P4-ATPase mutants.

We also tested if overexpression of Any1 would perturb growth of cells and/or alter membrane organization, as would be expected if it inhibits Neo1 and/or is a scramblase. *ANY1* was placed under transcriptional control of the GAL promoter (P_{GAL}), which is repressed by glucose and strongly induced by galactose. This P_{GAL}-*ANY1* construct was expressed in WT, and *neo1-2 any1*Δ strains and growth was examined over a range of temperatures on galactose or glucose media (Figure 3-3A). Any1 overexpression caused a very mild growth defect in WT cells relative to the empty vector control. In contrast, *neo1-2* was very sensitive to Any1 overexpression and failed to grow at any temperature on the galactose plates. The robust growth of *neo1-2 any1*Δ on the glucose plates and galactose plates with empty vector at high temperatures shows the strong suppression conferred by the absence of Any1. Deletion of *ANY1* also suppresses growth defects caused by mutations in Neo1-interacting proteins Dop1 and Mon2. *dop1-1* is temperature sensitive for growth, but the *dop1-1 any1*Δ double mutant (empty vector) grows well at 37˚C ((114)and Fig 3-3A). Similarly, *mon2*Δ mutants grow slowly, but this phenotype is suppressed in *mon2*Δ *any1*Δ strains (114). Like *neo1-2*, growth of *dop1-1* and *mon2*Δ is severely inhibited by Any1 overexpression (Figure 3-3A). We also found that growth of *drs2*Δ and *dnf1, 2*Δ strains is inhibited by Any1 overexpression (Figure 3B), but not as potently as with *neo1*, *dop1* and *mon2* mutants. Thus, cells deficient for Neo1/Dop1/Mon2 function are most sensitive to changes in Any1 levels within the cell.

If Any1 was functioning as a scramblase, we might expect that overexpression would cause a loss of membrane asymmetry. However, WT and *drs2*Δ showed no difference in PapB sensitivity between cells harboring P_{GAL}-*ANY1* and empty vector grown on galactose (Figure 3-

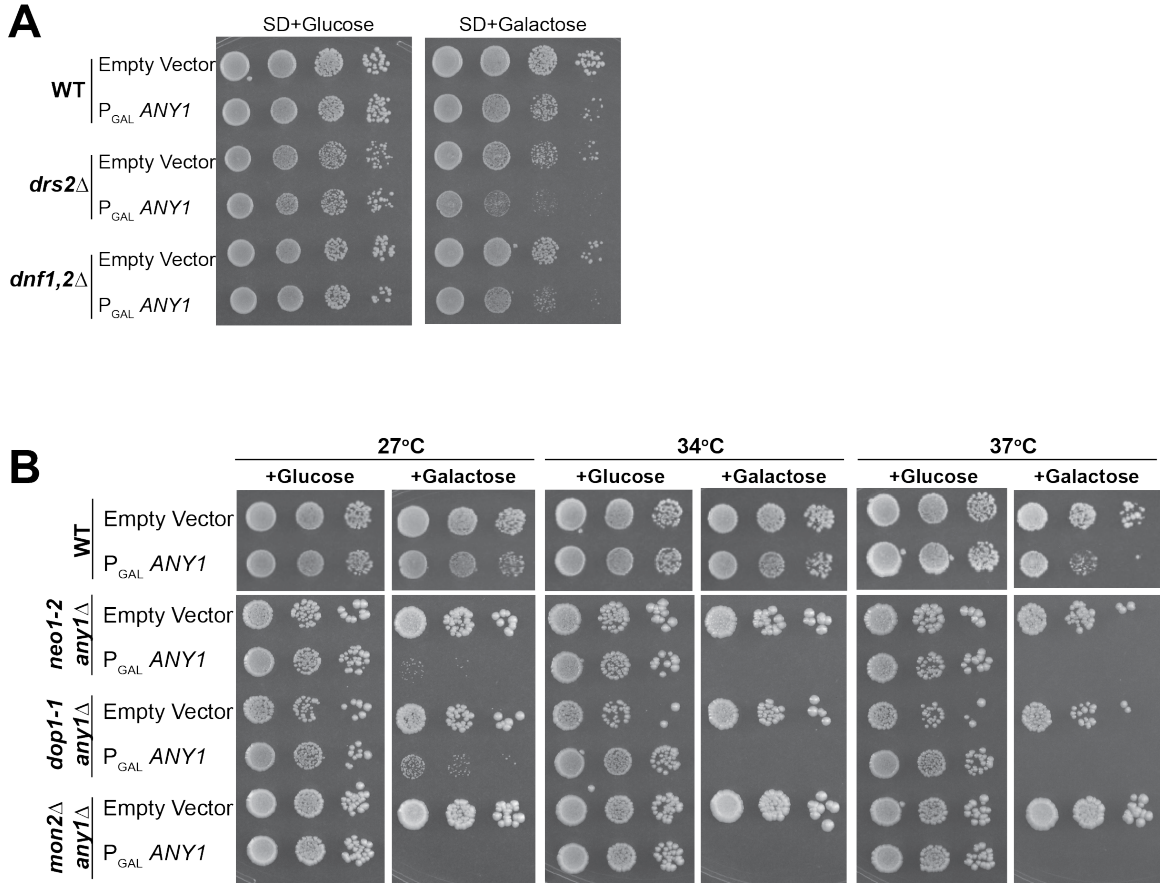

Figure 3-3. Overexpression of *ANY1* partially inhibits the growth of *drs2*Δ and *dnf1,2*Δ mutants, but it is detrimental to *neo1*^{ts}, *dop1*^{ts} and *mon2*Δ mutants. (A) Overexpression of *ANY1* partially inhibits the growths of *drs2*Δ and *dnf1,2*Δ mutants, but not wild-type cells. Wild-type, *drs2*Δ and *dnf1,2*Δ expressing *pRS416 (empty vector) or pRS416-*P_{GAL1}*-ANY1* were spotted onto the minimal media plates containing glucose or galactose at 30°C. (B) Overexpression of *ANY1* completely suppresses the growths of *neo1*^{ts}, *dop1*^{ts} and *mon2*Δ mutants. Growth assays were performed with wild-type, *neo1*^{ts}, *dop1*^{ts} and *mon2*Δ mutants expressing *pRS416 (empty vector) or pRS416-*P_{GAL1}*-ANY1* at 27°C, 34°C and 37°C. These images are representative of multiple growth assays.

3C,D). WT cells harboring P_{GAL}-*ANY1* displayed a small increase in sensitivity to duramycin, although not much difference was observed for *drs2*Δ cells with or without *ANY1* overexpression (Figure 3-3E,F). These experiments suggest that if Any1 is a scramblase or phospholipid transporter of some type, it may be specific for PE.

Neo1[Y222S] is a dominant gain of function mutation that suppresses *drs2*Δ defects

The functional overlap between Drs2 and Neo1 in *any1*Δ implies that Neo1 and Drs2 have a similar repertoire of phospholipid substrates (114,117). Functional complementation/suppression of *neo1*Δ *drs2*Δ *any1*Δ by Neo1, Drs2 or Dnf1$^{PS+,}$ and lack of complementation by Drs2^{PS-} further implies that di-acylated PS flippase activity is the critical common activity between Neo1 and Drs2 required for viability. We attempted to map residues contributing to PS transport in Neo1 using a targeted site directed mutagenesis strategy. We

Table 2-1. Survey of Neo1 mutants for growth

Neo1 mutant(s)	*neo1*Δ lethality	*neo1*Δ *drs2*Δ lethality	*drs2*Δ cold-sensitivity
Neo1[N199A]	Yes	Yes	No
Neo1[Q209G]	Yes	Yes	No
Neo1[A210Q]	Yes	Yes	No
Neo1[A210F]	Yes	Yes	No
Neo1[P212Q]	Yes	Yes	No
Neo1[Y222S]	Yes	Yes	Yes (partial-full)
Neo1[F228V]	Yes	Yes	No
Neo1[E237D]	Yes	Yes	No
Neo1[Y222S, F228V]	Yes	Yes	No
Neo1[Y222S, E237D]	Yes	Yes	No
Neo1[Y222S, F228V, EE237D]	Yes	**No**	Not applicable
Neo1[N412S]	Yes	Yes	No
Neo1[R460A]	Yes	Yes	No
Neo1[R460F]	Yes	Yes	No
Neo1[R460Y]	Yes	Yes	No
Neo1[R460Q]	Yes	Yes	No
Neo1[D503N]	No	No	No

targeted residues that are conserved in Neo1/Atp9a/Atp9b/Tat-5 and where the position is implicated in PS recognition in Drs2 or Dnf1^{PS+} variants (Figure 4A). We mutated these Neo1 residues to the corresponding Dnf1 residues and examined these *neo1* alleles for complementation of *neo1*Δ and *neo1*Δ*drs2*Δ (Table 3-1). Surprisingly, all of the single mutants complemented both strains as well as WT *NEO1*. An ATPase-dead *neo1-D503N* allele served as a control for a loss of function allele and failed to support viability as expected. An example of the complementation data for mutations in transmembrane segment 2 (TM2) is shown in Figure 3-4B-D. Neo1[Y222S], Neo1[F228V] and Neo1[E237D] mutants were expressed in *neo1*Δ*drs2*Δ cells and tested for growth at a range of temperatures (23^{o}C, 30^{o}C and 37^{o}C) (Figure 3-4D). Interestingly, Neo1[Y222S] not only complemented *neo1*Δ *drs2*Δ (Figure 3-4C, D), but it was also able to suppress the *cs* growth defect at 23^{o}C caused by *drs2*Δ. No other Neo1 mutant tested was able to suppress this cs growth defect (Figure 3-3D and Table 3-1). To examine the influence of Neo1[Y222S] on membrane asymmetry, we performed PapA and duramycin toxin sensitivity assays along with other Neo1[TM2] mutants in the *neo1*Δ *drs2*Δ background. Only Neo1[Y222S] was able to significantly suppress the PE and PS asymmetry defects in *neo1*Δ*drs2*Δ cells as the sole copy of Neo1 (Figure 3-4E, F).

We transformed wild-type Neo1, Neo1[Y222S] and Neo1[Y222A] mutants into *drs2*Δ *NEO1* cells to test whether the mutation is dominant or recessive, and if the loss of tyrosine or presence of serine at Y222 was responsible for the gain-of-function phenotype. An extra copy of WT Neo1 weakly suppressed *drs2*Δ cs growth as well as the PapA and duramycin sensitivity (Figure 3-5A-C). Neo1[Y222S] and Neo1[Y222A] suppressed *drs2*Δ cold-sensitivity at 20^{o}C and 23^{o}C to a greater extent than Neo1, but not as completely as Drs2 (Figure 5A). Thus, loss of the tyrosine at Y222 is critical for suppression of *drs2*Δ. Neo1[Y222S] weakly suppressed PS exposure in *drs2*Δ cells (Figure 5B), but restored PE asymmetry in *drs2*Δ cells to near WT levels.

There was no statistical difference in the suppression of PS exposure between wild-type Neo1 and Neo1[Y222S] when expressed in cells containing endogenous Neo1. Thus, Neo1[Y222S] appeared to be dominant with respect to duramycin sensitivity, but recessive with respect to PapB sensitivity (compare Figure 3-4E,F to Figure 3-5B,C), although the reason for this difference is unclear.

To test the influence of the reciprocal substitutions in TM2 of Dnf1, we mutated S243 to tyrosine, threonine or alanine (Figure 6A). Dnf1[S243A], Dnf1[S243Y] and Dnf1[S243T] were tested for their ability to complement *dnf1,2,3*Δ*drs2*Δ and support viability of this strain. Dnf1[S243Y] failed to complement *dnf1,2,3*Δ*drs2*Δ (Figure 3-6B). By contrast, Dnf1[S243A] and Dnf1[S243T] complemented *dnf1,2,3*Δ*drs2*Δ nearly as well as wild-type Dnf1 (Figure 3-6B). We tested the NBD-PL uptake activities of Dnf1[S243] mutants in a *dnf1*Δ *dnf2*Δ background. Surprisingly, Dnf1[S243Y] was active on the plasma membrane and displayed a significant increase ($p<0.01$) in the NBD-PC and NBD-PS transport activities and no change in NBD-PE transport relative to WT Dnf1 (Figure 3-6C). NBD-phospholipid transport activities of Dnf1[S243T] and Dnf1[S243A] were similar to that of wild-type Dnf1 (Figure 3-6C). These unexpected results indicate that the S243Y substitution attenuates the ability of Dnf1 to provide the essential function of this group of P4-ATPases, while retaining activity at the plasma membrane and actually enhancing the ability of Dnf1 to transport NBD-PS. Similarly, the presence of tyrosine at position 222 in Neo1 (the WT residue) attenuates its ability to substitute for Drs2 *in vivo* when Any1 is present, while Neo1[Y222S] can partially substitute for Drs2 (Figure 3-4D-F).

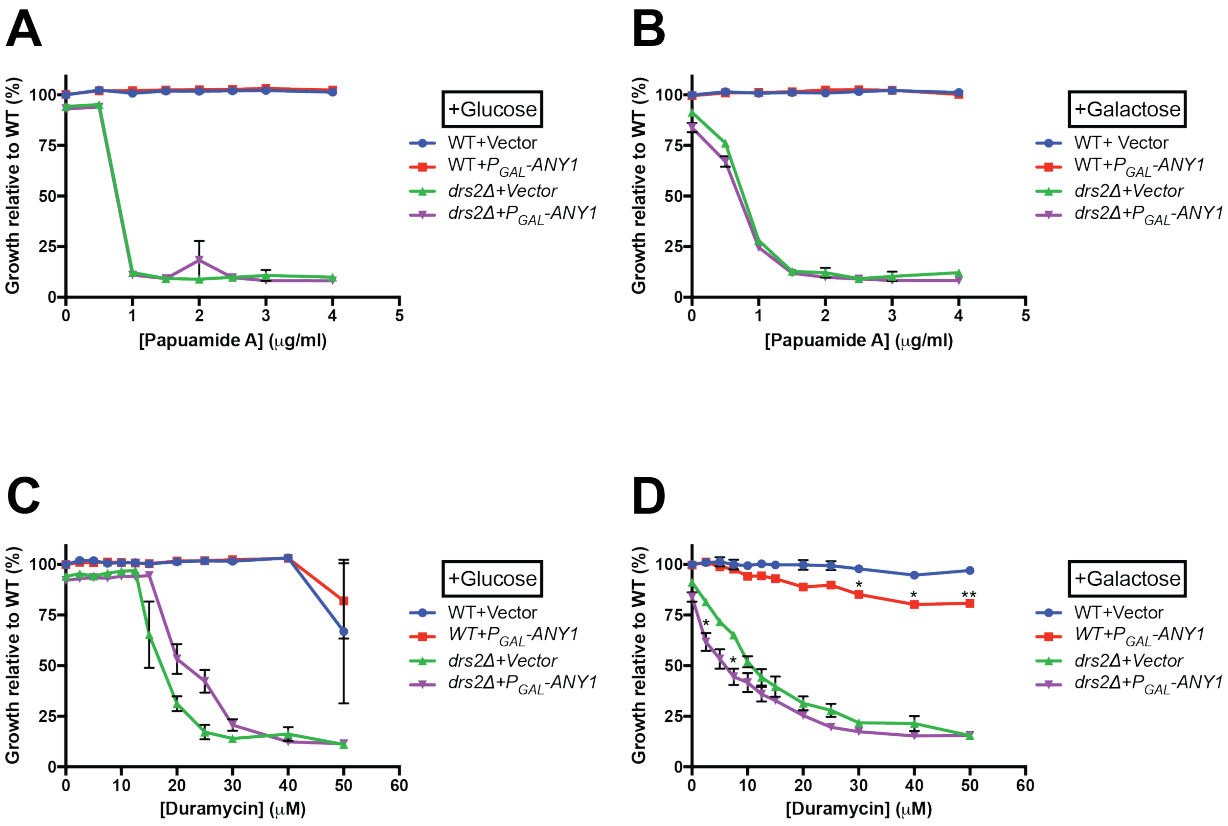

Figure 3-4. Overexpression of *ANY1* induces partial loss of PE asymmetry, but not loss of PS asymmetry in wild-type and *drs2*Δ cells. (A,B) Overexpression of *ANY1* does not induce loss of PS asymmetry in WT and *drs2*Δ cells. (C,D) Overexpression of *ANY1* induces partial but significant loss of PE asymmetry in WT and *drs2*Δ cells. Wild-type and *drs2*Δ cells expressing empty vector (*pRS416)* or *pRS416-*P_{GAL1}*-ANY1* were grown to mid-log phase in the minimal media containing glucose. 0.2 OD_{600} of cells were shifted to the minimal medium containing galactose or glucose (control) in the presence of pore-forming toxins Papuamide A or duramycin. Growth relative to the vehicle control was plotted. Student t-test was performed for each concentration tested between wild-type and *drs2*Δ cells ($n \geq 2$)

The gain of function phenotype of Neo1[Y222S] is dependent on Any1

We next tested whether Neo1[Y222S] suppression of *drs2*Δ was influenced by Any1. Neo1[Y222S] and Neo1[Y222A] fully supported growth of *neo1*Δ*drs2*Δ and *neo1*Δ*drs2*Δ*any1*Δ equivalently to Neo1 (Figure 3-7A,B). Growth of *neo1*Δ*drs*Δ and *neo1*Δ*drs2*Δ*any1*Δ strains expressing Neo1, Neo1[Y222S], Neo1[Y222A] or Drs2 were tested over a wide range of temperatures to examine suppression of *drs2*Δ cs growth. As shown before, Neo1[Y222S] and Neo1[Y222A] mutants partially suppressed the *drs2*Δ cold-sensitivity of *neo1*Δ*drs2*Δ at low temperatures (17˚C, 20˚C and 23˚C) (Figure 7C). For *neo1*Δ*any1*Δ*drs2*Δ, WT Neo1 supported viability and *any1*Δ suppressed the cs growth defects caused by *drs2*Δ and so these cells grew well at all temperatures. No influence of Neo1[Y222S] or Neo1[Y222A] on growth relative to Neo1 could be observed in this background (Figure 3-7C). To investigate the influence of Neo1[Y222S] and *any1*Δ on membrane asymmetry, we performed PapA and duramycin sensitivity assays in the *neo1*Δ*drs2*Δ*any1*Δ background along with wild-type cells. Surprisingly, Neo1[Y222S] failed to suppress PS (Figure 3-7D) and PE (Figure 3-7E) exposure when Any1 was absent. There was no significant difference between cells expressing wild-type Neo1 or Neo1[Y222S] in the sensitivities to these toxins. Thus, Neo1[Y222S] requires the presence of Any1 to suppress PS/PE asymmetry defects caused by *drs2*Δ (compare Figure 3-7D,E to Figure 3-4 E,F).

Changes in localization of Neo1[Y222S] relative to Neo1 might contribute to the gain-of-function phenotype. Neo1 localizes broadly throughout the Golgi and endosomes while Drs2 localizes primarily to the TGN. To test if the Y222S mutation shifts Neo1 localization to the TGN, we examined localization of GFP-tagged Neo1 and Neo1[Y222S] relative to mCherry-Tlg1 (TGN/early endosome), *Sec7-mKate2* (TGN), *Aur1-mKate2* (*medial*-Golgi), and *COPI-mKate2* (*cis*-Golgi) (Figure 3-9A and 3-9B). We quantified the extent of co-localization of GFP-tagged

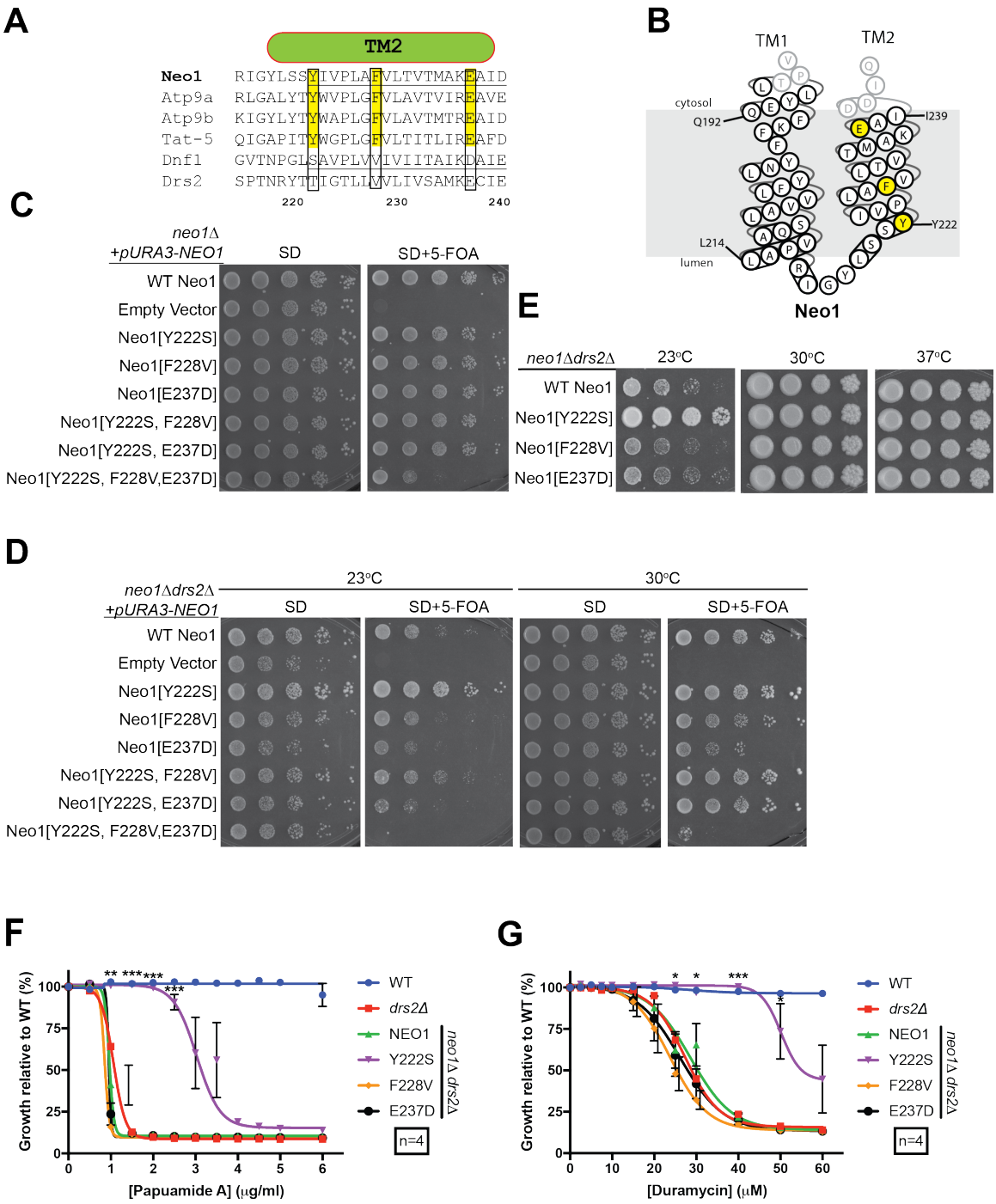

Figure 3-5. Neo1[Y222S] is a gain-of-function mutant that can suppress both growth and membrane asymmetry defects of *drs2*Δ mutant. (A) Sequence alignment of transmembrane (TM2) segments from Neo1, Atp9a, Atp9b, Tat-5, Dnf1 and Drs2. Residues conserved in Neo1/Atp9a/Atp9b/Tat-5 were highlighted in yellow. (B) Snake plot of TM2 region of Neo1. Conserved residues were highlighted in yellow. (C) All of Neo1[TM2] mutants can complement the essential function of Neo1 in *neo1*Δ mutant cells. (D) All of Neo1[TM2] mutants except for the triple mutant can suppresses the *neo1*Δ*drs2*Δ synthetic lethality, but only Neo1[Y222S] mutant can suppress (E) *drs2*Δ cold-sensitive growth defect at 23°C. (F) Neo1[Y222S] can suppress the loss of PE or PS asymmetry in *neo1*Δ*drs2*Δ cells as a sole copy. Growth relative to the vehicle control was plotted. Student t-test was performed for each concentration tested between wild-type and *drs2*Δ cells (n≥4).

and RFP-tagged proteins using Mander's correlation coefficient. While there was no substantial difference in the localization of GFP-Neo1[Y222S] relative to GFP-Neo1, the Mander's coefficients showed a small but statistically significant change in the distribution of Neo1[Y222S] towards later compartments of the Golgi marked by Sec7 and Tlg1 (Figure 3-9A-C). Altered localization of Neo1[Y222S] to late Golgi compartments where Drs2 normally resides might be a factor contributing to the gain-of-function phenotype, but whether this small difference is biologically significant seems unlikely.

Interaction between Neo1 and Any1

Genetic interactions and pore-forming toxin sensitivity assays suggest that Any1 specifically antagonizes the Neo1/Dop1/Mon2 complex. To test for an interaction between Any1 and Neo1, we performed immunoprecipitations of Neo1-5XFLAG from Golgi/endosomal enriched fractions containing Any1-GFP (74). As a positive control, we performed IPs from Dop1-TAP expressing Neo1-5XFLAG. Previously reported Dop1-Neo1 interaction was barely more than the background level (Figure 3-9A). On the contrary, Neo1-Any1 interaction can be clearly detected with the IP from Golgi-enriched fractions (Figure 3-9B). We also probed the Golgi-enriched fractions from Any1-GFP cells with other Golgi-related markers such as Mnn1, Arf1 and Drs2 (Figure 3-9B). Although there is a slight enrichment of Drs2 in Any1-GFP cells expressing Neo1-5XFLAG, Arf1 and Mnn1 are enriched in both untagged control and Neo1-5XFLAG (Figure 3-9A and 3-7B).

Discussion

Regulation of membrane asymmetry requires a complex network of membrane remodeling machineries. Type IV P-type ATPases are membrane-remodelers that generate a steep

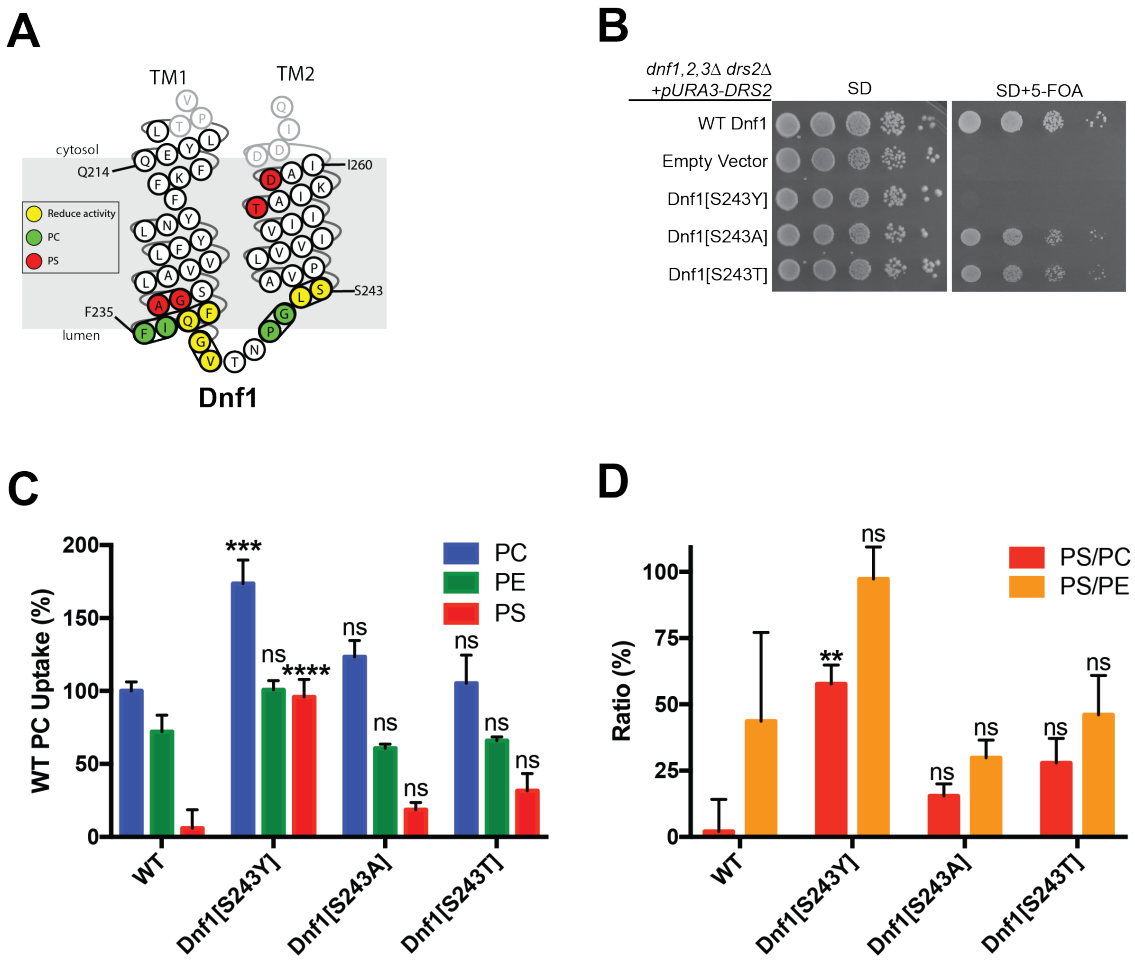

Figure 3-6. Reciprocal Dnf1[S243Y] mutant failed to complement the Dnf1 function, but it gained an ability to transport PS. (A) Snake plot of Dnf1 TM2 region. Previously identified residues influencing PC, PS and overall activity were highlighted. (B) Only Dnf1[S243Y] mutant failed to suppress the *dnf1,2,3*Δ*drs2*Δ synthetic lethality, but Dnf1[S234A] and Dnf1[S243T] mutants can suppress the synthetic lethality. (C) Dnf1[S243Y] mutant has a significant increase in NBD-PC and NBD-PS transport relative to wild-type Dnf1, Dnf1[S243A] and Dnf1[S243T]. Lipid uptake assays were performed with *dnf1,2*Δ cells expressing wild-type Dnf1, Dnf1[S243Y], Dnf1[S243A] and Dnf1[S243T] on a single copy plasmid grown at 30^{o}C using fluorescent-labeled (NBD) phospholipids. Lipid uptake activities were plotted as percentage of NBD-PC uptake for wild-type cells. (D) PC is the main substrate for Dnf[S243Y] mutant as wild-type Dnf1, but it has significant increase in its PS preference over PC. Lipid uptake activities of each experimental sample were expressed as PS/PC and PS/PE ratios.

gradient of specific glycerophospholipids in biological membranes. Prior studies showed that the Golgi P4-ATPases Neo1 and Drs2 execute non-redundant biological functions despite their apparently similar substrate preferences and localizations, and the PQ-loop protein Any1 somehow enforces these separate functions (5). In this study, we find that PS flippase activity is essential to support viability of *neo1*Δ*drs2*Δ*any1*Δ cells. Even a Dnf1^{PS+} variant (Dnf1[N550S]) is capable of providing the PS flippase activity required for viability in this background, while WT Dnf1 or a Drs2^{PS-} variant cannot. While none of the flippases can fully restore PS or PE asymmetry in *neo1*Δ*drs2*Δ*any1*Δ mutant cells, Drs2 and Neo1 establish an equivalent degree of PS asymmetry. These observations strongly suggest that Neo1 can also flip PS and so we targeted conserved residues in the membrane domain hypothesized to facilitate PS recognition. Surprisingly, none of the mutations disrupt Neo1 function. Instead, one mutation, Neo1[Y222S], is a gain-of-function suppressor of *drs2*Δ defects in growth and membrane asymmetry and this gain-of-function phenotype is masked by loss of Any1. Moreover, Neo1 and Any1 physically interact, but the Y222S does not appear to alter this interaction. We suggest the Y222S mutation alters substrate specificity of Neo1 or perhaps the consequence of the Any1-Neo1 interaction.

Our data argue that PS flip by a P4-ATPase in the Golgi/endosomal system of budding yeast is essential for growth, and yet strains lacking the sole PS synthase (*cho1*Δ) are viable. How do we explain this apparent discrepancy? We favor the idea that PS in the lumenal leaflet antagonizes vesicle budding from Golgi membranes, while the translocation of this negatively charged phospholipid and its concentration in the cytosolic leaflet promotes vesicle budding. Failure to flip PS will increase luminal leaflet PS and reduce cytosolic leaflet PS, with both effects likely contributing to the strong trafficking defect observed in *drs2* and *neo1* mutants. The *cho1*Δ mutant would obviously lack the luminal leaflet PS, thus relieving negative effects, and compensatory changes in the lipidome to this perturbation might provide sufficient anionic

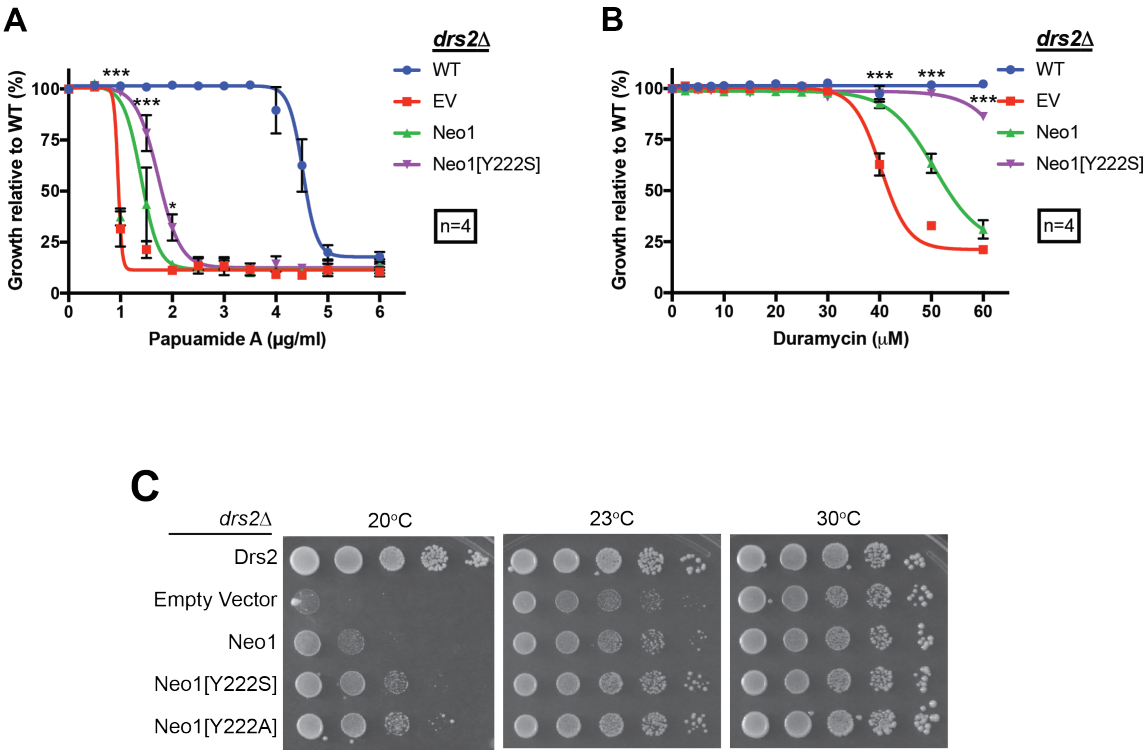

Figure 3-7. Neo1[Y222S] is a dominant gain-of-function mutant that can partially suppress both growth and membrane asymmetry defects of *drs2*Δ mutant cells in the presence of wild-type Neo1. (A) Neo1[Y222S] mutant can suppress the PS and (B) PE asymmetry defects of *drs2*Δ mutant cells as an extra single copy of Neo1. *drs2*Δ cells expressing *cen* empty vector, *cen DRS2*, *cen NEO1* and *cen Neo1[Y222S]* were tested for Papuamide A and duramycin sensitivity. Growth relative to the vehicle control was plotted for each sample. Student t-tests were performed between the empty vector and Neo1[Y222S] at each concentration of the toxins, n≥4, (* $p<0.05$, ** $p<0.01$, *** $p<0.001$, error bars ±SEM). (C) Neo1[Y222S] mutant can partially suppress *drs2*Δ cold-sensitive growth defect . Cold-sensitivity assays were performed at 20°C, 23°C and 30°C with at least three independent transformants.

phospholipid in the cytosolic leaflet to support vesicular transport, which appears normal in this mutant. In addition, transport of other phospholipid substrates by Drs2 and Neo1 may increase significantly in *cho1*Δ cells in the absence of competition by PS, providing another compensatory mechanism to support vesicular transport.

We have previously shown a requirement for PS flip to support protein trafficking in the Golgi/endosomal system using the same $Drs2^{PS-}$ and $Dnf1^{PS+}$ variants described here (48). PS flip increases the positive curvature (bending into the cytosol) and negative charge needed to recruit the ArfGAP Gcs1 via its ArfGAP lipid packing sensor (ALPS) motif onto Golgi/endosomal membranes from the cytosol (48). In mammalian cells, PS flip by ATP8A1 or ATP8A2 facilitates recruitment of EHD1, a membrane fission factor, to the cytosolic leaflet of recycling endosomes (49). Thus, concentration of PS in the cytosolic leaflet has positive roles in vesicle budding. A negative role for PS in the luminal leaflet is supported by the observation that endocytic recycling defects in the *C. elegans tat-1* mutant (ortholog of Drs2/ATP8A1/ATP8A2) are suppressed by depletion of PS synthase (170). In budding yeast, *drs2*Δ *cho1*Δ cells grow very poorly and transport defects are not suppressed (35), suggesting loss of PS in the luminal leaflet is insufficient to overcome the deficit in the cytosolic leaflet in this case.

Loss of Any1 has been shown previously to suppress deficiencies in Neo1 and Drs2/Dnf P4-ATPases (114,117). Tanaka and co-workers found that *any1*Δ (also called *cfs1*Δ) suppressed *drs2*Δ and *cdc50*Δ cold sensitive growth, and the synthetic lethality of *lem3*Δ*cdc50*Δ*crf1*Δ, a strain deficient for the b-subunits needed for the activity of Dnf1-Lem3, Dnf2-Lem3, Dnf3-Crf1 and Drs2-Cdc50 heterodimers (117). On the contrary, we found loss of Any1 failed to suppress the *dnf1,2,3*Δ*drs2*Δ synthetic lethality, a mutant that should be equivalent to *lem3*Δ*cdc50*Δ*crf1*Δ. This raises the possibility that *lem3*Δ*cdc50*Δ*crf1*Δ cells retain some residual activity of P4-ATPase a-subunits to allow suppression by *any1*Δ*/cfs1*Δ. However, it is also possible that some

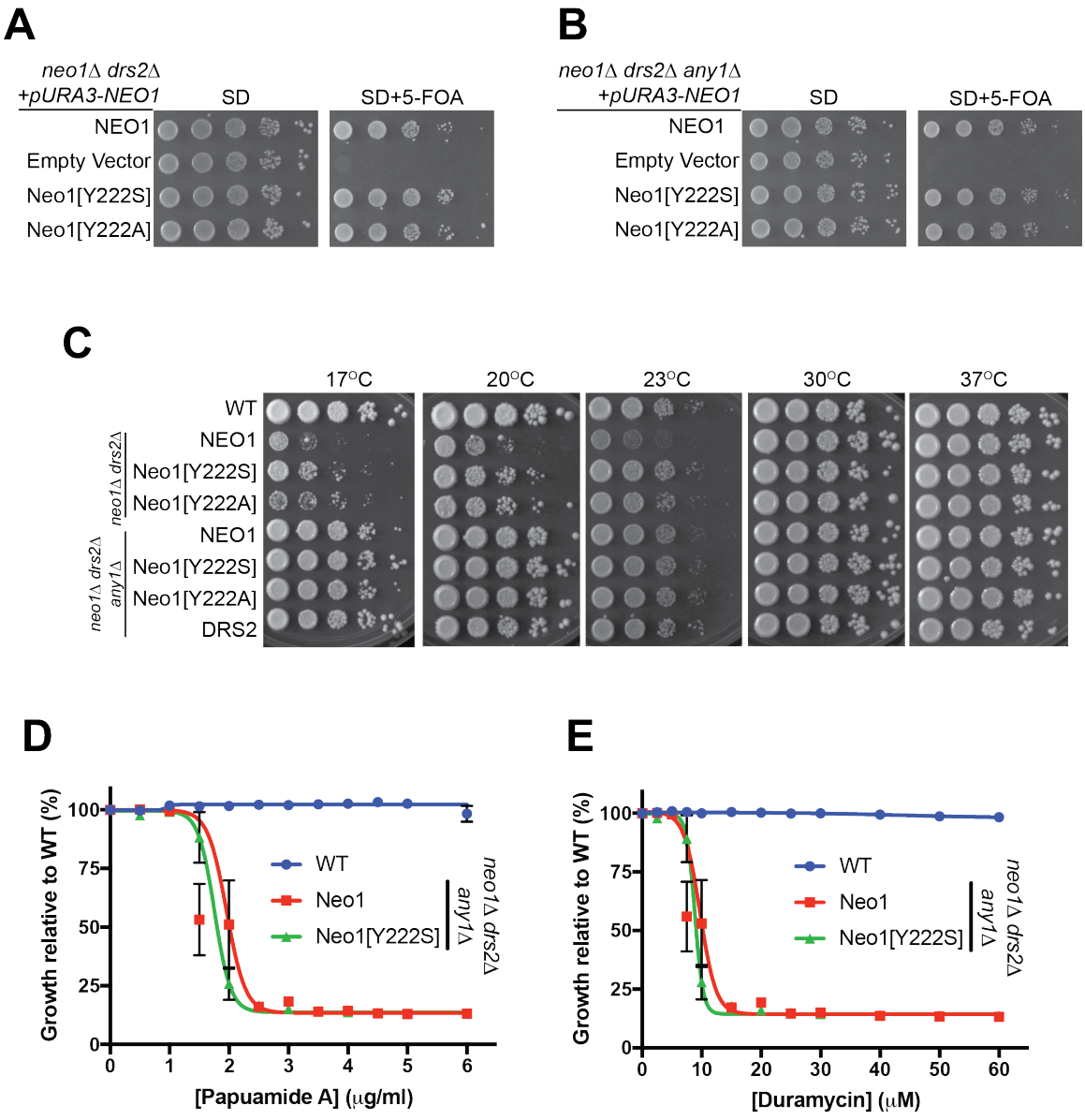

Figure 3-8. Loss of Any1 abolishes the gain-of-function phenotype of Neo1[Y222S]. (A) Neo1[Y222S] and Neo1[Y222A] mutants can suppress the *neo1*Δ*drs2*Δ and (B) *neo1*Δ*drs2*Δ*any1*Δ synthetic lethality. (C) Suppression of *drs2*Δ cold-sensitive growth defect by Neo1[Y222S] is dependent on Any1. (D) Neo1[Y222S] GOF mutant cannot suppress the PS and (E) PE asymmetry defects in *neo1*Δ*drs2*Δ*any1*Δ mutant cells.

minor difference in strain background was responsible for the different results, particularly considering that *lem3*Δ*cdc50*Δ*crf1*Δ*any1*Δ cells grew very slowly (117). We also find that *neo1* alleles are synthetically lethal with *lem3*Δ, but *neo1*Δ *any1*Δ *lem3*Δ cells grow similarly to wild-type and must rely on Drs2 for growth. In total, these genetic interactions argue that Any1 segregates the functions of multiple P4-ATPases and eliminating Any1 allows Drs2, in particular, to carry out the essential function of the P4-ATPase group.

Deletion of *KES1* or *ANY1* similarly suppresses growth and trafficking defects of *drs2*Δ/*cdc50*Δ mutants (86,115), raising the possibility that Any1 and Kes1 are performing comparable tasks. *kes1*Δ mutants display a substantial increase in the anionic phosphatidylinositol-4-phosphate in the cytosolic leaflet, which is likely the reason *kes1*Δ suppresses *drs2* and *sec14*. *any1*Δ does not suppress *sec14* and *kes1* does not suppress *neo1 (117)*, arguing that the mechanism for suppressing P4-ATPase deficiency is distinct for *any1*Δ and *kes1*Δ.

The biochemical function of Any1 remains enigmatic, although the current study provides some insight into potential roles for this protein in membrane organization. PQ-loop proteins share this simple PQ motif in a cytosolic loop and a similar membrane topology with 7 or 8 TM segments. Beyond this, the PQ loop proteins share little sequence homology. The best characterized PQ loop proteins include the KDEL receptor, the sweet and semisweet sugar transporters in plants, and basic amino acid transporters in lysosomes/vacuoles (refs). The potential transporter activity of Any1 and its ability to antagonize Neo1 function led to the proposal that Any1 is a scramblase that disrupts the phospholipid gradient formed by Neo1. However, it is also possible that Any1 antagonizes Neo1 through protein interactions. Consistent with this latter possibility, we find that Any1 and Neo1 interact based on a

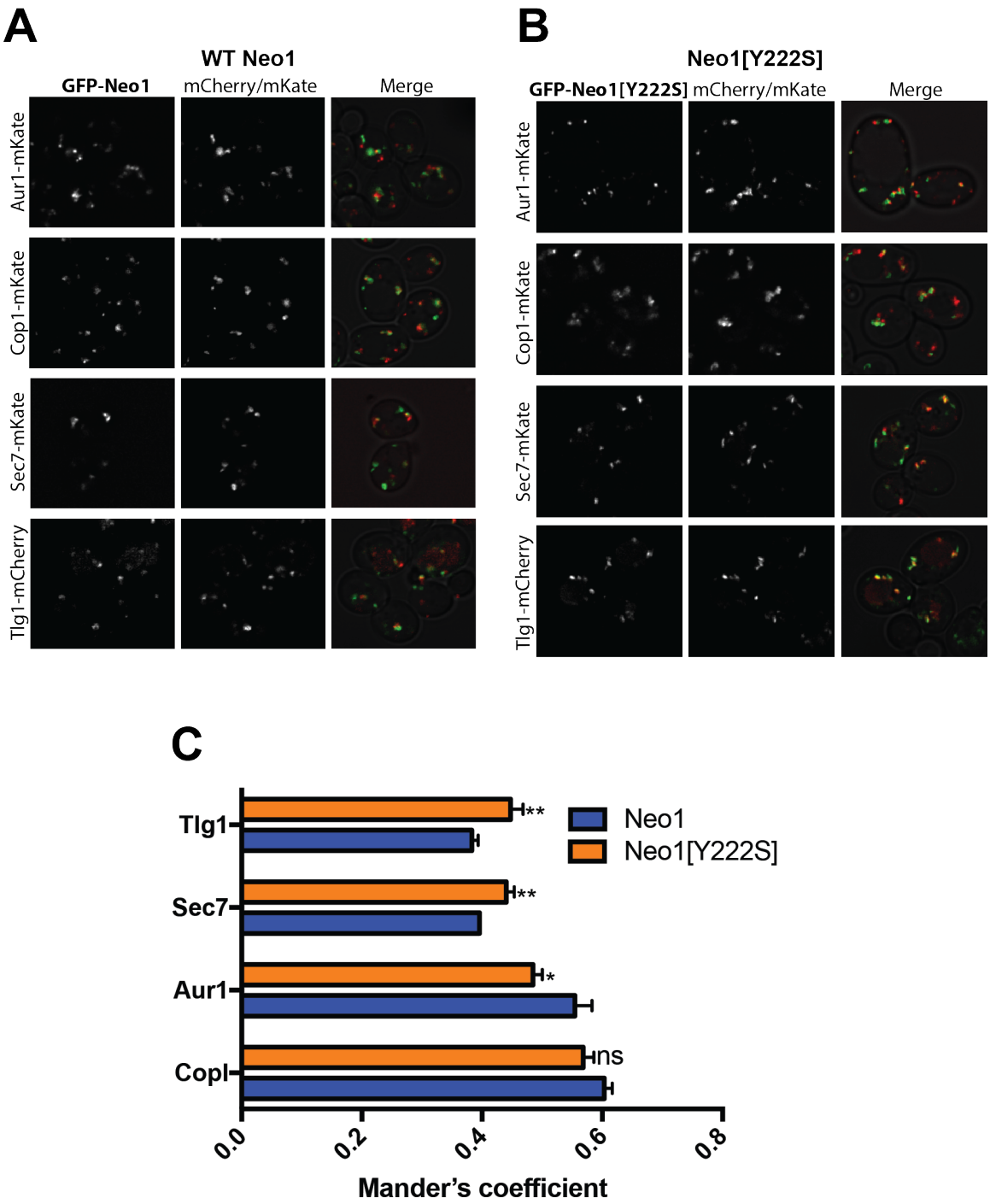

Figure 3-9. Neo1[Y222S] mutant is significantly more enriched in Drs2-positive compartments than wild-type Neo1. (A) Colocalization of wild-type GFP-tagged Neo1 with Cop1-mKate (*cis-Golgi*), Aur1-mKate (*med-Golgi*), Sec7-mKate (*TGN)* and mCherry-Tlg1 (endosome). (B) Colocalization of GFP-tagged Neo1[Y222S] with Cop1-mKate (*cis-Golgi*), Aur1-mKate (*med-Golgi*), Sec7-mKate (*TGN)* and mCherry-Tlg1 (endosome). (C) Manderson's coefficient analyses were done for GFP-Neo1/Neo1[Y222S] with Golgi/endosomal markers. At least 100 cells (imaged on different days) were used to calculate the Manderson's coefficient. (* $p<0.05$, ** $p<0.01$, *** $p<0.001$, error bars ±SEM)

coimmunoprecipitation assay. In addition, the influence of *any1*Δ on membrane asymmetry are most profound when assayed with hypomorphic *neo1*^{ts} alleles, which could be explained by removal of a protein interaction that negatively regulates Neo1 flippase activity. Overexpression of Any1 is particularly toxic to *neo1*^{ts} mutants and only slightly increases PE exposure in the outer leaflet of WT cells, a result more consistent with inhibition of Neo1 activity by Any1. If Any1 can scramble phospholipid as a monomer or homo-oligomer, we might expect to see a bigger impact on membrane organization when highly expressed from the strong *GAL* promoter. If Any1 is a scramblase, it may be part of a hetero-oligomeric complex and/or is tightly regulated such that the majority of Any1 expressed from the Gal promoter is inactive.

An additional clue to the function of Any1 comes from the observation that Any1 is required to observe gain-of-function phenotypes for Neo1-Y222S. This Neo1 Y222S mutation allows it to partially replace Drs2 functions required for growth at low temperature and in establishing PS/PE asymmetry. Neo1-Y222S suppresses exposure of PS and PE on the cell surface much better than Neo1 when expressed in *neo1*Δ *drs2*Δ cells, but fails to do so when expressed in *neo1*Δ *any1*Δ *drs2*Δ cells. This result again links Any1 to the function of Neo1, but in this case Any1 seems to facilitate the ability of Neo1-Y222S to compensate for the loss of Drs2

rather than simply being an inhibitor of Neo1. One interesting possibility is that Any1 somehow increases the availability of some substrate in the luminal leaflet of the Golgi, allowing Neo1-Y222S increased access to substrate for translocation but perhaps inhibiting Drs2 activity. The Y222S mutation does not appear to disrupt the interaction between Neo1 and Any1, but it may alter the effect of this interaction on either Neo1 or Any1 activity. Neo1 engages in a complex network of interactions, which includes Any1, Mon2 and Dop1. A more comprehensive

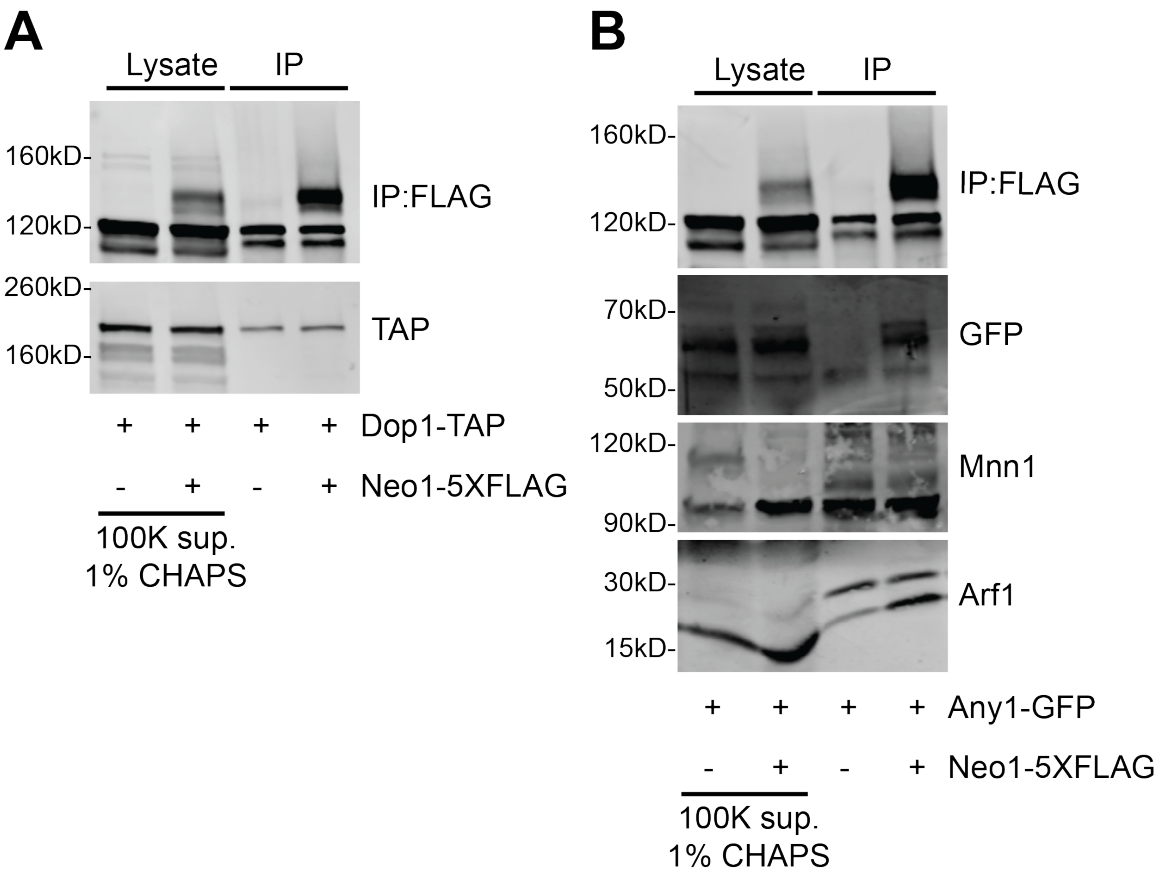

Figure 3-10. Any1 physically interacts with Neo1 in the Golgi-enriched membranes. (A) Dop1 does not interact with Neo1 in the Golgi-enriched membraes. (B) Any1 interacts with Neo1 in the Golgi-enriched membranes. *ANY1::GFP::HIS3MX6 or DOP1::TAP::HIS3MX6* cells expressing the empty vector, *pRS313-NEO1-5XFLAG* and *pRS313-Neo1[Y222S]-5XFLAG* were lysed and subjected to high-speed centrifugation (100,000Xg) in the presence of detergent. Immunoprecipitations were performed using these Golgi-enriched fractions. Input represents 1.25% of total lysate used for each reaction. Immunoprecipitations were also probed for Arf1 and Drs2 to assess the intactness of the Golgi membranes.

examination of all Neo1 interactions is needed to fully assess the impact of the Y222S gain-of-function mutation.

Neo1-Y222S came out of a study where we targeted several residues in the first 4 TM segments of Neo1 that are conserved in metazoan orthologs and in positions previously implicated in PS recognition by Drs2 or Dnf1^{PS+} variants. We were hoping to produce Neo1 variants specifically defective in PS recognition. Surprisingly, none of these point mutations noticeably disrupted the ability of Neo1 to support growth of a *neo1*Δ or *neo1*Δ *drs2*Δ strain. Rather than perturbing PS recognition, Neo1-Y222S appears to have an enhanced ability to restrict PS and PE to the inner leaflet of the plasma membrane. We assume the other mutations are not substantially perturbing substrate recognition, but more work is required to determine if any of the point mutations cause subtle changes in membrane organization that do not perturb growth rates. The supply of the natural product papuamide is limited and we were unable to more thoroughly explore the influence of these point mutations on PS asymmetry. We have found that *neo1*Δ*drs2*Δ and *neo1*Δ cells expressing a Neo1[Y222S, F228V, E237D] triple mutant displays a severe growth defect. It is possible that this triple mutant perturbs PS recognition although the poor growth made this mutant difficult to characterize. It is also possible that the essential function of Neo1 is distinct from its influence on membrane asymmetry.

In summary, we identified Any1 as a key regulator that enforces separate functions for Drs2 and Neo1 in Golgi membranes. When Any1 is deletion, the essential Golgi function can be provided by either Neo1 or variants of Drs2 or Dnf1 that are able to flip PS. This result emphasizes the importance of PS translocation for Golgi function and suggests Neo1 can flip PS. In addition, we discovered a novel Neo1 variant (Neo1-Y222S) that is able to compensate for the loss of Drs2 in the presence of Any1. We also provide evidence that Neo1 and Any1 form a complex in cells. However, further work is needed to determine if this interaction directly inhibits

Neo1 activity, if Any1 acts upstream of Neo1 to limit substrate availability (for both Neo1 and Drs2), or downstream of Neo1 to dissipate phospholipid gradients in the membrane.

CHAPTER IV

CONCLUSIONS AND FUTURE DIRECTIONS

The Essential Neo1 protein from Budding Yeast Plays a Role in Establishing Aminophospholipid Asymmetry of the Plasma Membrane

Biological membranes are an amalgam of complex biomolecules such as proteins, carbohydrates and lipids. A striking feature of biological membranes is phospholipid asymmetry. Regulation of phospholipid asymmetry is crucial for various biological processes such apoptosis, blood clotting and vesicular transport. Phospholipid asymmetry is established and maintained by the concerted activities of three main lipid transporters: flippases, floppases and scramblases. Of these phospholipid transporters, flippases are the major contributor to the establishment and maintenance of membrane asymmetry due to their substrate specificity and higher rate of transport. Flippases are type IV P-type ATPases (P4-ATPase) belonging to the superfamily of P type ATPases. P4-ATPases form a well-conserved clade of phospholipid transporters in eukaryotes. Deficiencies of P4-ATPases in humans cause a wide range of disorders such as neurodegeneration and metabolic disorders. By deciphering the biological functions of P4-ATPases, we will be able to understand the molecular basis of numerous metabolic conditions. It is an easier task to characterize the P4-ATPases functionally in a simpler model organism with the least functional redundancy. In this regard, we study the roles of P4-ATPases in *S. cerevisiae* (budding yeast).

Prior to my thesis work, substrate recognition and transport pathways were defined in Drs2/Dnf family of P4-ATPases through studies of chimeric P4-ATPases and directed evolution strategies (65,70,83). PS transport in Drs2/Dnf P4-ATPases was shown to be mediated through

two gates, consisting of residues in the TM1-4 region (70,83). The flippase activity of Golgi P4-ATPase Drs2 was defined using in vitro reconstitution and Drs2 was identified as a main PS flippase within the cell (36). In addition, Drs2 was shown to have auto-regulatory domain in the C-terminal tail and interactions of this domain with Gea2, Arl1 and PI4P regulate the Drs2 activity (109). On the contrary, Neo1 was not yet defined as phospholipid flippase and it was a big enigma how Neo1 regulates COPI-retrograde trafficking through its presumed flippase activity.

One aim of this thesis research was to define better the essential P4-ATPase Neo1 and determine if it is a phospholipid flippase. Our initial task was to test for the lipid transport activity of Neo1 biochemically. In this regard, Neo1 was purified from the yeast and incorporated into a model membrane bilayer with defined lipid composition. Our numerous attempts to reconstitute Neo1 flippase activity in vitro failed. There are several potential main reasons for our failure to detect Neo1 activity after purification and reconstitution into proteoliposomes:

Neo1 weakly interacts with several proteins and may require these interactions for activity.

It is possible that Neo1 transports a novel substrate that was not tested.

The relative inefficient reconstitution (<1 Neo1 molecule/liposome) and low intrinsic activity may have prevented detection of translocase activity.

Neo1 may require post-translational modification for activity and the purified protein may lack these activating modifications.

Despite the unsuccessful attempts to reconstitute flippase activity, we were able to detect a specific ATPase activity for Neo1 (0.04 μmol Pi/min/mg Neo1) that is 10 percent of the reported Drs2 basal ATPase activity (0.4 μmol Pi/min/mg Drs2) (36). In addition, we were able to detect 2-fold stimulation of Neo1 ATPase activity in the presence of yeast total lipid mixture. Overall,

we failed to get any definitive results about the flippase activity of Neo1 in vitro. Further optimizations are required to biochemically assay any flippase activity catalyzed by Neo1.

P4-ATPases influence the plasma membrane asymmetry independent of their subcellular localizations. For instance, abolishing the Drs2 activity in the Golgi membranes causes a loss of plasma membrane asymmetry. Membrane asymmetry in a *drs2*Δ mutant cannot be restored by plasma membrane P4-ATPases Dnf1/2, which preferentially flip lyso-phospholipids (65). To address the influence of essential Golgi P4-ATPase Neo1 on membrane asymmetry, we tested the sensitivity of hypomorphic *neo1*^{ts} alleles to the pore-forming cytotoxic peptides (11). Hypomorphic alleles displayed loss of PE and PS asymmetry at semi-restrictive temperatures where these alleles did not show any COPI trafficking defects (5). More interestingly, a more restrictive neo1ts mutant became very hypersensitive to PE-binding toxin duramycin relative to drs2Δ, suggesting that Neo1 has a primary role in establishing PE asymmetry. Addressing the influence of Neo1 on membrane asymmetry provided us clues about the potential substrates (PS+PE) transported by this P4-ATPase.

P4-ATPases can regulate the plasma membrane asymmetry through their flippase activities or by influencing the activity of other P4-ATPases. In the literature, there is no evidence that Golgi P4-ATPase Drs2 can regulate the activities of PM P4-ATPases Dnf1 and Dnf2. However, it was still a plausible explanation that loss of Neo1 activity also caused loss of the Dnf1/2 activities at the plasma membrane. Interestingly, partial inactivation of neo1ts mutants led to a significant increase in the NBD-PC and NBD-PE uptake activities of Dnf1/2. In conjunction, there was a significant increase in the NBD-PS uptake activities of Dnf1/2. Our results contradicts with the notion that inactivation of Neo1 indirectly disrupts the activity of Dnf1/2. These findings support the idea that loss of Neo1 activity directly influences membrane asymmetry.

Proper localization of P4-ATPases is crucial for their flippase and biological activities. Mislocalization of P4-ATPase can cause a loss of membrane asymmetry in the endomembrane compartments and eventually cause the loss of plasma membrane asymmetry. Inactivation of neo1ts mutants might also indirectly alter the subcellular localization of Drs2/Dnf P4-ATPases. Since Drs2/Dnf family of P4-ATPases are indistinguishable from the background when fluorescently tagged, we performed a subcellular fractionation in neo1ts mutants where Drs2/ Dnf P4-ATPases are C-terminally tagged in their genomic loci. Subcellular fractionations at permissive and semi-permissive temperatures revealed that there is no significant difference in the distribution of Drs2/Dnf P4-ATPases in neo1ts mutants relative to wild-type cells. In terms of plasma membrane enrichment, Dnf1 and Dnf2 were enriched at the plasma membrane fractions to the same extent in wild-type and neo1ts mutants. Increased PS uptake in neo1ts mutant might suggest that Drs2 was mislocalized to the plasma membrane. No significant change in Drs2 localization was observed, but it is challenging to distinguish slight changes in the distribution of Drs2/Dnf P4-ATPases by subcellular fractionation. These localization studies also supports the notion that loss of Neo1 activity in neo1ts mutants directly influence PE and PS asymmetry.

Vesicular and non-vesicular transport routes have a great impact on the phospholipid distribution within the cell. For instance, disruption of COPII-mediated transport can halt the transport of ER synthesized P4-ATPases and can indirectly cause the plasma membrane asymmetry via the entrapment of P4-ATPases in the symmetric ER membranes. One other aspect of trafficking is that availability of the phosphoinositides to the Golgi P4-ATPases, especially Drs2. It has been previously shown that PI4P species are required for the activation of Drs2 activity through its carboxyl tail (62,109). Although it is known that C-terminal tail of Neo1 is required for its essential function, there is no evidence about the influence of PIP(s) on Neo1 activity. On the other hand, Neo1 has been tightly linked to the COPI-retrograde transport and it

displays genetic interaction with various COPI mutants (3). Loss of Neo1 can alter the plasma membrane asymmetry through affecting COPI function. Clearly, COPI mutants displayed defective COPI-trafficking compared to wild-type cells, even at the permissive temperature for growth. On the other hand, they did not display any membrane asymmetry defects, whereas neo1ts mutants displayed severe membrane asymmetry defects even the permissive growth temperature. These results indicate that loss of trafficking is not the direct cause of loss of membrane asymmetry in neo1ts mutants.

In order to determine the influence of Neo1 inactivation on the lipid biosynthetic pathways, we performed lipidomic analyses of neo1ts mutants upon inactivation at the elevated temperatures. Although P4-ATPases can mainly change the lipid distribution in both leaflets, the accessibility of precursor lipid substrates can alter the lipid biosynthesis machinery. For instance, biosynthesis of complex sphingolipid inositolphosphoceramide (IPC) requires the presence of both ceramide and PI in the luminal leaflet of the Golgi. Some high throughput studies have suggested a link between Neo1 and IPC synthesis. Possibly, as P4-ATPases build-up aminophospholipids at the cytosolic side of the Golgi membranes, PI might leak to the lumenal side to facilitate the IPC production in the lumen. Interestingly, acute inactivation of Neo1 neither led to the accumulation of ceramide or reduction in the IPC levels relative to wild-type cells. Among different GPL species, lyso-PE was increased significantly as compared to the wild-type cells upon the inactivation of neo1ts mutants. This observation suggests Neo1 might prefer lyso-PE as a substrate. Sterol levels were also unaffected in neo1ts mutants at semi-permissive temperatures. Prolonged inactivation of Neo1 can have more drastic effect on the lipid biosynthesis machinery, but this treatment might disrupt cellular integrity due to the essential nature of Neo1. The essential function of Neo1 might be facilitating the lipid biosynthesis machinery rather than regulating vesicular transport.

It is still a big enigma why yeast P4-ATPases are functionally non-redundant, especially the Golgi P4-ATPases. Our study did not completely solve this enigma yet and the essential role of Neo1 has not yet been discovered. In order to find out the essential role of Neo1, we need to further characterize Neo1 and its substrate preferences biochemically. Our study shows supportive evidence that Neo1 regulates both PE and PS asymmetry through its flippase activity. In addition, it highly suggests that Neo1 is a major PE flippase with some activity towards PS. Understanding how Neo1 regulates early Golgi trafficking requires a further investigation of biochemical activity of Neo1 and its interactome within the cells. It is highly possible that a unique interaction partner of Neo1 can enforce a non-redundant and unique role for Neo1. In summary, defining the roles of Neo1 as P4-ATPase would assist us to resolve the flippase and its regulatory network facilitating various vesicular transport routes as well as biosynthetic machineries.

Neo1-Any1-Drs2 axis is required for viability and plasma membrane asymmetry

In a simple eukaryote, S. cerevisiae, there are five different P4-ATPases executing different roles in the endomembrane system. Most strikingly, the Golgi P4-ATPases Neo1 and Drs2 regulate independent trafficking pathways from the Golgi. For instance, Drs2 mainly regulates transport pathways between retrieval pathways from the endosomes to and TGN, while Neo1 regulates the Golgi to ER retrograde transport (3,48). Our previous studies suggested that Neo1 and Drs2 share similar subcellular localizations and substrate preferences, but it remained unclear why they appeared to be functionally non-redundant.

Serendipitously, a novel factor called “Antagonistic Yeast Neo1” (Any1) was identified as a Neo1 antagonist from a genome-wide screen to probe suppressor interactions (114). Any1 is an integral membrane protein with 8 predicted TM segments belonging to the PQ-loop protein

superfamily. In this collaborative study, we observed that Neo1 and Drs2 become functionally redundant in the absence of Any1 (114). Loss of Any1 in neo1ts mutants leads to suppression of growth defects and complete restoration of PE/PS asymmetry. Based on these findings, Any1 might be a phospholipid scramblase that acts against the Golgi P4-ATPases Drs2 and Neo1.

Interestingly, loss of Any1 failed to compensate for loss of both Drs2 and Neo1, and *neo1*Δ*any1*Δ*drs2*Δ cells are inviable. In our recent study, we discovered that PS flippase activity is required in the Golgi/endosomal membranes of *neo1*Δ*drs2*Δ*any1*Δ cells. In the absence of Any1, even the PS-flipping variant Dnf1[N550S] mutant can provide sufficient PS flippase activity required for viability. Contradictory to growth suppression, none of the the single P4-ATPases restore asymmetry in *neo1*Δ*drs2*Δ*any1*Δ cells. We have not tested the suppression of other defects such as protein trafficking defects in *neo1*Δ*drs2*Δ*any1*Δ cells expressing WT Neo1, Drs2 or Dnf1[N550S]. We assume that protein trafficking is not severely perturbed because the cells grow well. However it will be interesting to test how specific trafficking pathways are supported by Drs2, Neo1 or Dnf1[N550S] in this background. In addition, hypomorphic neo1ts alleles are sufficient to provide the flippase activity required for viability at various non-permissive temperatures tested in *neo1*Δ *drs2*Δ *any1*Δ cells. These alleles have not yet tested for the restoration of PS or PE asymmetries in *neo1*Δ *drs2*Δ *any1*Δ cells. Based on these results, execution of PS flip is essential in the Golgi membranes for viability.

A strong genetic interaction between sterol/PI4P exchanger Kes1 and Drs2 has been reported in the literature. Loss of Kes1 activity is sufficient for bypassing the roles of Drs2 in vesicular transport, lateral membrane organization and ergosterol biosynthesis (86,115). Especially, PS flip is required as a part of homeostatic mechanism regulating sterol distribution as well as membrane organization of lipid and protein domains at the TGN (86). We tested if loss of Kes1 can bypass the essential requirement for PS flip in *neo1*Δ *drs2*Δ *any1*Δ cells. Loss of Kes1

failed to suppress the synthetic lethality of *neo1*Δ *drs2*Δ *any1*Δ cells. Strong suppressor of *drs2*Δ, Kes1 has not been in strong strong rescue interaction with neo1Δdrs2Δany1Δ cells expressing non-PS flipping Drs2[QQ→GA]. We assumed that absence of Kes1 might enhance either Dnf1/2 or Dnf3 activities in the Golgi membranes by the elevation of PI4P pools at early and late Golgi membranes. These results provide additional evidence that emphasizes the importance of PS flip in the Golgi/endosomal system.

The lyso-phospholipid flippases Dnf1/2 are functionally segregated from the di-acylated phospholipid flippases Drs2 and Neo1, suggesting these two Golgi flippases primarily transport di-acylated phospholipid. Despite the functional segregation, *drs2*Δ displays a strong synthetic interaction with *dnf1,2*Δ as well as *dnf1*Δ cells (2). On the contrary, hypomorphic neo1ts alleles did not exhibit any synthetic interaction with either *dnf1*Δ or *dnf2*Δ (3). In our study, we detected a strong synthetic lethal interaction between hypomorphic neo1ts alleles and *lem3*Δ (phenocopying dnf1,2Δ) (74). Surprisingly, loss of Any1 suppress the synthetic lethality between *neo1*^{ts} and *lem3*Δ at all temperatures tested. Possibly, loss of Neo1 and Dnf1/2 activities leads to the loss of PE/PS asymmetry to an extent detrimental to cell viability. Upon loss of Any1, membrane asymmetry is sufficiently restored in neo1ts and neo1ts *lem3*Δ *any1*Δ mutants, to allow them to grow as well as *dnf1,2*Δ cells. Clearly, loss of Any1 cannot suppress the PE or PS asymmetry defects in *dnf1,2*Δ or *drs2*Δ cells. Strong suppression of neo1 mutants by the loss of Any1 indicate that there is a stronger functional link between Any1 and Neo1 than Any1 with other Drs2/Dnf P4-ATPases.

In our study, we had defined Any1 as a strong antagonist of Neo1 activity. Genetic interactions imply that Any1 is tightly linked with Neo1 and its interaction partners Mon2 and Dop1. Loss of Any1 leads to the suppression of *neo1*^{ts}, *dop1*^{ts} and *mon2*Δ lethality (114). Conversely, overexpression of Any1 leads to severe growth defects in *neo1*^{ts}, *dop1*^{ts} and *mon2*Δ

mutants, but only a partial growth defect in *drs2*Δ and *dnf1,2*Δ mutant cells. Based on previous findings, Any1 was proposed to be a potential scramblase (114). In the previous work, overexpression of Any1 has been shown to accumulate PS pools in the intracellular localizations, but there was no evidence that overexpression of Any1 alters bilayer distribution of PS or PE at the PM. Surprisingly, overexpression of Any1 leads to only a modest, although significant loss of PE asymmetry in WT and *drs2*Δ cells. If Any1 is a scramblase, we might expect a greater degree of PE and PS exposure when it is overexpressed. However, it is possible that Any1 is a part of a protein complex that has scramblase activity, and overexpression of one subunit may not increase scramblase activity. Consistent with this possibility, a SILAC-based mass spectrometry analysis of Neo1 and Any1 protein interactions recovered Ist2, the yeast ortholog of the TMEM16F scramblase. Possibly, Any1 lacks a stoichiometric interaction partner Ist2 to exert its scramblase activity. Another possibility is that Any1 might influence the activity of Golgi P4-ATPases through direct protein-protein actions. Despite the lack of evidence for Any1 interaction with any P4-ATPase in our high-throughput data, we might detect a protein- protein interaction between Neo1 and Any1 in Golgi-enriched membrane fractions. Biochemical characterizations of Any1 and its interaction partners are required for a more detailed functional characterization of Any1.

Based on our findings, Neo1 seems to transport PS as well as PE, but PS can be considered as essential substrate for maintaining Golgi functions and vesicular transport pathways. Using targeted mutagenesis, we attempted to map PS recognizing residues in Neo1. We targeted and mutated the residues that are both conserved in Neo1/Atp9a/Atp9b/Tat-5 and implicated in the PS recognition in Drs2/Dnf P4-ATPases. We expected that loss of PS recognizing residues would lead to the loss of essential Neo1 activity. None of TM1-2 or TM3-4 Neo1 mutants tested had a loss of function (LOF) phenotype. Except for Neo1 D503N (ATPase-dead mutant), every Neo1 mutant tested complemented the essential Neo1 function (in *neo1*Δ

background) and displayed no loss of PE/PS asymmetry relative to WT cells. In order to test growth phenotypes more restrictively, we tested the growth profiles of Neo1 mutants in the *neo1*Δ*drs2*Δ background. In conjunction with our *neo1*Δ complementation tests, none of Neo1 mutants displayed any growth deficits at different temperatures tested. Possibly, a partial loss of Neo1 PS flippase activity might be compensated by the activities of Dnf1/2 in *neo1*Δ*drs2*Δ background at 30^{o}C or elevated temperatures. Another possibility is that Neo1 might use entirely different transport pathway for its potential substrates PE and PS. For instance, Dnf1[D258E] acts as gain-of-function mutant regarding PS-flip and the reciprocal E→D mutation in Drs2 leads to PS asymmetry defects (65,83). It is possible that that the analagous glutamic acid in Neo1 does not participate in PS transport. Unbiased and rigorous random mutagenesis should be performed to map the PS recognizing residues in Neo1.

Table 4-1. Physical interactors of Any1 and Neo1 from the SGD

Neo1 Interactome		
Gene Systematic Name	Gene Name	Description
YDR264C	AKR1	Palmitoyl transferase involved in protein palmitoylation
YLR431C	ATG23	Peripheral membrane protein required for autophagy and CVT
YJL178C	ATG27	Type I membrane protein involved in autophagy and the Cvt pathway
YBL078C	ATG8	Component of autophagosomes and Cvt vesicles
YDL149W	ATG9	Transmembrane protein involved in forming Cvt and autophagic vesicles
YLR241W	CSC1	Calcium permeable gated cation channel
YDR141C	DOP1	Golgi-localized, leucine-zipper domain containing protein
YJL196C	ELO1	Elongase I, medium-chain acyl elongase
YJL124C	LSM1	Lsm (Like Sm) protein
YBL026W	LSM2	Lsm (Like Sm) protein
YER146W	LSM5	Lsm (Like Sm) protein
YNL297C	MON2	Protein with a role in endocytosis and vacuole integrity
YHR195W	NVJ1	Nuclear envelope protein
YLR208W	SEC13	Subunit of the COPII vesicle coat required for ER-to-Golgi transport
YPR181C	SEC23	GTPase-activating protein, stimulates the GTPase activity of Sar1p
YIL109C	SEC24	Component of the Sec23p-Sec24p heterodimer of the COPII vesicle coat
YBL102W	SFT2	Tetra-spanning membrane protein found mostly in the late Golgi
YBR106W	SND3	Protein involved in SRP-independent targeting of substrates to the ER
YBR097W	VPS15	Serine/threonine protein kinase involved in vacuolar protein sorting
YPL120W	VPS30	Subunit of phosphatidylinositol (PtdIns) 3-kinase complexes I and II
YLR240W	VPS34	Phosphatidylinositol (PI) 3-kinase

Any1 Interactome		
Gene Systematic Name	Gene Name	Description
YDR264C	AKR1	Palmitoyl transferase involved in protein palmitoylation
YMR010W	ANY1	Protein involved in phospholipid flippase function
YDL192W	ARF1	GTPase of the Ras superfamily involved in regulation of coated vesicle formation
YKL004W	AUR1	Phosphatidylinositol:ceramide phosphoinositol transferase
YLR330W	CHS5	Component of the exomer complex
YER157W	COG3	Essential component of the conserved oligomeric Golgi complex
YNR028W	CPR8	Peptidyl-prolyl cis-trans isomerase (cyclophilin)
YDR141C	DOP1	Golgi-localized, leucine-zipper domain containing protein
YDR068W	DOS2	Protein of unknown function
YLR083C	EMP70	Protein with a role in cellular adhesion and filamentous growth
YGL077C	HNM1	Plasma membrane transporter for choline, ethanolamine, and carnitine
YDR497C	ITR1	Myo-inositol transporter
YOR233W	KIN4	Serine/threonine protein kinase
YGR055W	MUP1	High affinity methionine permease
YBL017C	PEP1	Type I transmembrane sorting receptor for multiple vacuolar hydrolases
YJL053W	PEP8	Vacuolar protein component of the retromer
YOR104W	PIN2	Exomer-dependent cargo protein
YLL013C	PUF3	Protein of the mitochondrial outer surface
YPL246C	RBD2	Possible rhomboid protease
YNL287W	SEC21	Gamma subunit of coatomer
YDR100W	TVP15	Integral membrane protein; localized to late Golgi vesicles
YOR069W	VPS5	Nexin-1 homolog; structural component of retromer membrane coat complex
YNL197C	WHI3	RNA binding protein that sequesters CLN3 mRNA in cytoplasmic foci
YCR043C	YCR043C	Putative protein of unknown function

Interestingly, targeted mutagenesis revealed a gain-of-function (GOF) Neo1[Y222S] mutant that can suppress drs2Δ growth and membrane asymmetry defects when expressed in the *neo1*Δ*drs2*Δ background. Rather than causing a loss of PS recognition, this GOF phenotype suggests that the Y222S mutation might actually enhance PS/PE recognition by Neo1. Y222 is a residue in TM1 of Neo1 that is conserved in the Atp9a/Atp9b/Tat-5 orthologs and we mutated this residue to a serine, which is present in this same position in Dnf1. The reciprocal Dnf1[S243Y] mutant can be considered to be a LOF and GOF mutant for certain phenotypes. Dnf[S243Y] displayed a significant increase in NBD-PC and PS uptake relative to WT Dnf1, and transported NBD-PE normally. More intriguingly, Dnf1[S243Y] mutant failed to complement the dnf1,2,3Δdrs2Δ synthetic lethality, unlike other PS-flipping variants Dnf1[N550S] and Dnf1[Y618F]. Dnf1[S243Y] is a very interesting mutant and should be further tested for changes in substrate specificity. For example, Dnf1[S243Y] *dnf2*Δ cells could be tested for edelfosine resistance to determine if this variant can transport this lyso-PC mimicking toxin. Using PS and PE-binding toxins, Dnf1[S243Y] should also be tested for restoration of lyso-PE and lyso-PS membrane asymmetry at the PM. Our lipidomic analyses of flippase mutants suggest that Dnf1 can flip lyso-PI. It is possible that Dnf1[S243Y] failed to complement the *dnf1,2,3*Δ*drs2*Δ synthetic lethality due to its inability to transport lyso-PI and this should be tested. Conversely, it is possible that the Neo1[Y222S] GOF phenotype is caused by an enhancement of lyso-PI transport by Neo1.

However, penetrance of Neo1[Y222S] varies depending on the genetic background and phenotype assayed. Neo1[Y222S] suppresses the cs growth defect of a *drs2*Δ single mutant, but failed to significantly suppress the PS asymmetry defects in the presence of WT Neo1. Thus, the presence of WT Neo1 actually attenuates the GOF phenotype of Neo1[Y222S] mutant with

regard to PS/PE asymmetry. This observation may argue against the possibility that Y222S enhances PS/PE transport by Neo1, as one might expect this type of mutation to be dominant rather than recessive. We also tested whether Y222S altered the subcellular distribution of Neo1. However, localization of Neo1 and Neo1[Y222S] are not drastically different from each other. Therefore, change of localization of Neo1[Y222S] is the least likely reason for the GOF phenotype.

The GOF phenotype of Neo1[Y222S] suggests a molecular link between this phenotype and Any1 because loss of Any1 and Y222S both allow Neo1 to suppress *drs2*Δ. In order to test this link, we examined the GOF phenotype of Neo1[Y222S] in the absence of Any1. Neo1[Y222S] mutant can no longer suppress PE/PS asymmetry defects in *neo1*Δ*drs2*Δ*any1*Δ mutant cells relative to WT Neo1. On the contrary, suppression of cold-sensitivity in *neo1*Δ*drs2*Δ*any1*Δ cells is not dependent on the presence of Any1. This raised the possibility that Any1 is not a lipid scramblase or lipid transporter, but it directly influences Neo1 activity through direct protein-protein interaction. Loss interaction with Any1 and Neo1[Y222S] might confer a GOF phenotype compared to WT Neo1. Both WT Neo1 and Neo1[Y222S] seem to interact with Any1 to the same extent by a co-immunoprecipitation assay. Physical interaction between Neo1 or Neo1[Y222S] and Any1 should be further investigated at endogenous expression levels for Any1 and Neo1. It is also plausible that Neo1[Y222S] alters the consequence of the Any1 interaction rather than disrupting the interaction itself. For example, if Any1 is an allosteric inhibitor of Neo1, perhaps the Y222S mutation in Neo1 prevents it from undergoing a conformational change into the inhibited state.

In summary, further analysis of Neo1 and Neo1[Y222S] interactomes would give us a better understanding how interacting proteins influence the activity of Neo1 and if Y222S alters these interactions. One intriguing possibility to further test is that Neo1[Y222S] gains the ability

to flip lyso-PI as a new substrate and Dnf1[S243Y] loses this activity. Transport of lyso-PI by Neo1[Y222S] might facilitate cellular homeostasis by generating an anionic phospholipid gradient in the Golgi membranes, which could replace the role of PS transport by Drs2. In addition, Neo1[Y222S] should be further explored in vitro to assess the influence of this mutation on lipid transport and substrate-dependent ATPase activity.

Future Directions

My thesis research answers some of key questions about the roles of Neo1 in membrane asymmetry and protein trafficking. In our quest, we discovered a novel factor called "Any1" with the Boone research group. There are still several fundamental questions that should be answered:

What are the primary substrates for the essential Neo1?

How is Neo1 activity regulated?

What is the biochemical function of Any1? Lipid scramblase? Lipid transporter? Neo1 inhibitor?

How does Neo1 control COPI-mediated retrograde trafficking?

How does the Neo1-Drs2-Any1 axis influences lipid biosynthetic machinery?

Are PI, lyso-PI or PIPs substrates for yeast P4-ATPases?

What are the physiological roles of Atp9a/Atp9b in humans?

As mentioned earlier, a study of the evolutionarily conserved Neo1 will lead to more impactful discoveries. Further biochemical and structural studies of Neo1 will help us to decipher de novo ways to modulate P4-ATPase activity for benchside and bedside applications. Hypomorphic mutation in the Drs2 ortholog ATP8A2 causes cerebellar atrophy, mental retardation and disequilibrium syndrome. Our studies suggest it may be possible to find drugs that allow other P4-ATPases to compensate for the loss of ATP8A2 activity.

APPENDIX

Appendix 1. Strains and plasmids used in Chapter 2.

Strain	Genotype	Plasmid	Source
BY4741	MATa *his3Δ1 leu2Δ0 ura3Δ0 met15Δ0*		Invitrogen
BY4742	MATα *his3Δ1 leu2Δ0 ura3Δ0 lys2Δ0*		Invitrogen
SEY6210	MATα *his3Δ1 leu2Δ0 ura3Δ0 lys2Δ0 trp1Δ suc2Δ*		(171)
ZHY124-15B1B	MATα *his3Δ1 leu2Δ0 ura3Δ0 lys2Δ0 trp1Δ suc2Δ ade2Δ neo1-1::HIS3-KanMX*		(3)
ZHY124-34A2A	MATα *his3Δ1 leu2Δ0 ura3Δ0 lys2Δ0 trp1Δ suc2Δ ade2Δ neo1-2::HIS3-KanMX*		(3)
EGY1211-6B	MATα *his3Δ1 leu2Δ0 ura3Δ0 lys2Δ0 trp1Δ suc2Δ sec21-1*		(172)
EGY101-6D	MATα *his3Δ1 leu2Δ0 ura3Δ0 lys2Δ0 trp1Δ suc2Δ ret1-1*		(172)
PFY3273A	MATa *his3Δ1 leu2Δ0 ura3Δ0 met15Δ0 dnf1Δ dnf2Δ dnf3Δ*		(2)
PFY3275F	MATa *his3Δ1 leu2Δ0 ura3Δ0 met15Δ0 dnf1Δ dnf2Δ*		(2)
YWY10	MATa *his3Δ1 leu2Δ0 ura3Δ0 lys2Δ0 neo1Δ::KanMX*	*pRS416-NEO1*	This study
ZHY615M2D	MATα *his3Δ1 leu2Δ0 ura3Δ0 lys2Δ0 drs2Δ*		(2)
ZHY704	MATα *his3Δ1 leu2Δ0 ura3Δ0 lys2Δ0 dnf1Δ dnf2Δ dnf3Δ drs2Δ::LEU2*	*pRS416-DRS2*	(2)
MTY219RR	MATa *his3Δ1 leu2Δ0 ura3Δ0 lys2Δ0 neo1Δ::KanMX*	*pR413-NEO1*	This study
MTY628-15B	MATa *his3Δ1 leu2Δ0 ura3Δ0 lys2Δ0 neo1Δ::KanMX*	*pR413-neo1-1*	This study
MTY628-34A	MATa *his3Δ1 leu2Δ0 ura3Δ0 lys2Δ0 neo1Δ::KanMX*	*pR413-neo1-2*	This study
MTY219RRL	MATa *his3Δ1 leu2Δ0 ura3Δ0 lys2Δ0 neo1Δ::KanMX*	*pRS315-NEO1*	This study
MTY628-15BL	MATa *his3Δ1 leu2Δ0 ura3Δ0 lys2Δ0 neo1Δ::KanMX*	*pRS315-neo1-1*	This study
MTY628-34AL	MATa *his3Δ1 leu2Δ0 ura3Δ0 lys2Δ0 neo1Δ::KanMX*	*pRS315-neo1-2*	This study
MTYD1-219RRL	MATa *his3Δ1 leu2Δ0 ura3Δ0*	*pRS315-NEO1*	This study

		lys2Δ0 neo1Δ::KanMX DNF1::6XHA::His5	
MTYD1-62815BL	MATa	*his3Δ1 leu2Δ0 ura3Δ0 pRS315-neo1-1 lys2Δ0 neo1Δ::KanMX DNF1::6XHA::His5*	This study
MTYD2-219RRL	MATa	*his3Δ1 leu2Δ0 ura3Δ0 pRS315-NEO1 lys2Δ0 neo1Δ::KanMX DNF2::6XHA::His5*	This study
MTYD2-62815BL	MATa	*his3Δ1 leu2Δ0 ura3Δ0 pRS315-neo1-1 lys2Δ0 neo1Δ::KanMX DNF2::6XHA::His5*	This study

RBY3901	ZHY615M2D	*pRS313*	(70)
RBY3904	ZHY615M2D	*pRS313-DRS2*	(70)
MTY40	ZHY615M2D	*pRS313-NEO1*	This study
MTY44	ZHY615M2D	*pRS413-ADH-NEO1*	This study
MTY48	ZHY615M2D	*pRS423-NEO1*	This study
MTY52	ZHY615M2D	*pRS313-Neo1[D503N]*	This study
MTY300	ZHY704	*pRS313*	This study
MTY303	ZHY704	*pRS313-DNF1*	This study
MTY306	ZHY704	*pRS313-DRS2*	This study
MTY309	ZHY704	*pRS313-NEO1*	This study
MTY312	ZHY704	*pRS423-NEO1*	This study
RBY601	PFY3275F	*pRS313*	(70)
RBY604	PFY3275F	*pRS313-DNF1*	(70)
MTY104	PFY3275F	*pRS313-NEO1*	This study
MTY5001	MTY219RR	*pRS416*	This study
MTY5005	MTY628-15B	*pRS416-NEO1*	This study
MTY5009	MTY628-15B	*pRS416*	This study
MTY5017	MTY628-15B	*pRS416-DNF1*	This study
MTY5025	MTY628-15B	*pRS416-DRS2*	This study
MTY6000	MTY628-15B	*pRS416; pRS425*	This study
MTY6004	MTY628-15B	*pRS416-NEO1; pRS425*	This study
MTY6008	MTY628-15B	*pRS416; pRS425*	This study
MTY6012	MTY628-15B	*pRS416-DNF1; pRS425-LEM3*	This study
MTY6016	MTY628-15B	*pRS426-DNF1; pRS425-LEM3*	This study
MTY6020	MTY628-15B	*pRS315-DRS2; pRS426-CDC50*	This study
MTY6024	MTY628-15B	*pRS425-DRS2; pRS426-CDC50*	This study
MTY400	BY4741	*pRS313*	This study
MTY403	PFY3273A	*pRS313-NEO1*	This study
MTY406	PFY3273A	*pRS423-NEO1*	This study
MTY700	YWY10	*pRS313; pRS425*	This study
MTY703	YWY10	*pRS313-NEO1; pRS425*	This study
MTY706	YWY10	*pRS313-DNF1; pRS425-LEM3*	This study
MTY709	YWY10	*pRS423-DNF1; pRS425-LEM3*	This study
MTY712	YWY10	*pRS315-DRS2; pRS423-CDC50*	This study
MTY715	YWY10	*pRS425-DRS2; pRS423-CDC50*	This study
MTY718	YWY10	*pRS313-Neo1[D503N]; pRS425*	This study
MTY6210R	SEY6210	*pSKY5/RER1-0*	This study
MTY15B1BR	ZHY124-15B1B	*pSKY5/RER1-0*	This study
MTY34A2AR	ZHY124-34A2A	*pSKY5/RER1-0*	This study

MTY1211-6BR	EGY1211-6B	*pSKY5/RER1-0*	This study
MTY101-6DR	EGY1211-6D	*pSKY5/RER1-0*	This study

Plasmid	**Notes**	**Source**
pR413-NEO1	*cen, PNEO1, HIS3*	(2)
pR413-neo1-1	*cen, PNEO1, HIS3*	(3)
pR413-neo1-2	*cen, PNEO1, HIS3*	(42)
pRS416-NEO1	*cen, PNEO1, URA3*	This study
pRS416	*cen, URA3*	(51)
pRS425	*cen, LEU2*	(162)
pRS313	*cen, HIS3*	(162)
pRS423	*2μ, HIS3*	(2)
pRS313-DRS2	*cen, PDRS2, HIS3*	This study
pRS313-NEO1	*cen, PNEO1, HIS3*	(2)
pRS413-ADH-NEO1	*cen, PADH, HIS3*	(2)
pRS423-NEO1	*2μ, PNEO1, HIS3*	This study
pRS313-Neo1[D503N]	*cen, PNEO1, HIS3*	This study
pRS315-DRS2	*cen, PDRS2, LEU2*	(2)
pRS425-DRS2	*2μ, PDRS2, LEU2*	(2)
pRS313-DNF1	*cen, PDNF1, HIS3*	(102)
pRS423-DNF1	*2μ, PDNF1, HIS3*	(2,65)
pRS416-DNF1	*cen, PDNF1, URA3*	(33)
pRS426-DNF1	*2μ, PDNF1, URA3*	(33)
pRS423-CDC50	*2μ, PCDC50, HIS3*	(33)
pRS425-LEM3	*2μ, PLEM3, LEU2*	(70)
pSKY5/RER1-0	*cen, PTDH3, URA3*	*(173)*
PYM15	*integrating, HIS5, 6XHA*	*(174)*

Appendix 2. Strains and plasmids used in Chapter 3.

Strain	Genotype	Plasmid	Source
BY4741	MATa *his3Δ1 leu2Δ0 ura3Δ0 met15Δ0*		Invitrogen
BY4742	MATα *his3Δ1 leu2Δ0 ura3Δ0 lys2Δ0*		Invitrogen
PFY3275F	MATa *his3Δ1 leu2Δ0 ura3Δ0 met15Δ0 dnf1Δ dnf2Δ*		(2)
YWY10	MATa *his3Δ1 leu2Δ0 ura3Δ0 lys2Δ0 neo1Δ::KanMX*	*pRS416-NEO1*	This study
ZHY615M2D	MATα *his3Δ1 leu2Δ0 ura3Δ0 lys2Δ0 drs2Δ*		(2)
ZHY704	MATα *his3Δ1 leu2Δ0 ura3Δ0 lys2Δ0 dnf1Δ dnf2Δ dnf3Δ drs2Δ::LEU2*	*pRS416-DRS2*	(2)
MTY10S	YWY10 *ymr010wΔ::natMX4*	*pRS416-NEO1*	(114)
MTY615M2DS	ZHY615M2D *ymr010wΔ::natMX4*		(114)
MTY10 -615M2D	YWY10 *drs2Δ::HygR*	*pRS416-NEO1*	(114)
MTY10 -615M2DS	MTY10S *drs2Δ::HygR*	*pRS416-NEO1*	(114)
MTY10 -615M2DKS	MTY10-615M2DS *kes1Δ::HIS3MX6*	*pRS416-NEO1*	This study
MTY3275S	PFY3275F *ymr010wΔ::HygR*	*pRS416-NEO1*	This study
MTY704S	ZHY704 *ymr010wΔ::natMX4*	*pRS416-DRS2*	This study
MTY10-8600	YWY10 *lem3Δ::HygR*	*pRS416-NEO1*	This study
MTY10-8600-219RR	YWY10 *lem3Δ::HygR*	*pRS313-NEO1*	This study
MTY10-8600-15B	YWY10 *lem3Δ::HygR*	*pRS313-neo1-1*	This study
MTY10-8600-34A	YWY10 *lem3Δ::HygR*	*pRS313-neo1-2*	This study
MTY10-8600S-219RR	YWY10 *lem3Δ::HygR ymr010wΔ::natMX4*	*pRS313-NEO1*	This study
MTY10-8600S-15B	YWY10 *lem3Δ::HygR ymr010wΔ::natMX4*	*pRS313-neo1-1*	This study
MTY10-8600S-34A	YWY10 *lem3Δ::HygR*	*pRS313-neo1-2*	This study

	ymr010wΔ::natMX4		
MTY10-8600S	YWY10 *lem3Δ::HygR ymr010wΔ::natMX4*	*pRS416-NEO1*	This study
MTY10-615M2DS-219RR	MTY10-615M2DS	*pRS313-NEO1*	This study
MTY10-615M2D-15B	MTY10-615M2DS	*pRS313-neo1-1*	This study
MTY10-615M2DS-34A	MTY10-615M2DS	*pRS313-neo1-2*	This study
Y7092	*MATα can1Δ::STE2pr-Sp_his5 lyp1Δ0 his3Δ1 leu2Δ0 ura3Δ0 met15Δ0*		(114)
Y7092-001	Y7092	*pRS416*	This study
Y7092-002	Y7092	*pBY011-YMR010W*	This study
Y14538	*MATα mon2Δ::natMX4 ymr010wΔ::kanMX4 can1Δ::STE2pr-Sp_his5 lyp1Δ::STE3pr-LEU2 his3Δ1 leu2Δ0 ura3Δ0 met15Δ0*		(114)
Y14538-001	Y14538	*pRS416*	This study
Y14538-002	Y14538	*pBY011-YMR010W*	This study
TSQ854	*MATα dop1-1::natMX4 can1Δ::STE2pr-Sp_his5 lyp1Δ::STE3pr-LEU2 his3Δ1 leu2Δ0 ura3Δ0 met15Δ0*		(114)
TSQ854-001	TSQ854	*pRS416*	This study
TSQ854-002	TSQ854	*pBY011-YMR010W*	This study
TSQ188	*MATα neo1-2::natMX4 can1Δ::STE2pr-Sp_his5 lyp1Δ::STE3pr-LEU2 his3Δ1 leu2Δ0 ura3Δ0 met15Δ0*		(114)
TSQ188-001	TSQ188	*pRS416*	This study
TSQ188-002	TSQ188	*pBY011-YMR010W*	This study
MTY3275F-001	PFY3275F	*pRS416*	This study
MTY3275F-002	PFY3275F	*pBY011-YMR010W*	This study
MTY2DM-001	ZHY615M2D	*pRS416*	This study
MTY2DM-002	ZHY615M2D	*pBY011-YMR010W*	This study
MTY10-615M2DS-001	MTY10-615M2DS	*pRS313-NEO1*	This study
MTY10-615M2DS-002	MTY10-615M2DS	*pRS313*	This study

MTY10-615M2DS-003	MTY10-615M2DS	*pRS313- DRS2*	This study
MTY10-615M2DS-004	MTY10-615M2DS	*pRS313- Drs2[QQ→GA]*	This study
MTY10-615M2DS-005	MTY10-615M2DS	*pRS313-Dnf1[N550S]*	This study
MTY10-615M2DKS-001	MTY10-615M2DKS	*pRS313-NEO1*	This study
MTY10-615M2DKS-002	MTY10-615M2DKS	*pRS313*	This study
MTY10-615M2DKS-003	MTY10-615M2DKS	*pRS313- DRS2*	This study
MTY10-615M2DKS-004	MTY10-615M2DKS	*pRS313- Drs2[QQ→GA]*	This study
YHY-10-001	YWY10	*pRS313-NEO1*	This study
YHY-10-002	YWY10	*pRS313*	This study
YHY-10-003	YWY10	*pRS313-Neo1[Y222S]*	This study
YHY10-004	YWY10	*pRS313-Neo1[Y222A]*	This study
YHY10-001FL	YWY10	*pRS313-NEO1-5XFLAG*	This study
YHY10-002FL	YWY10	*pRS313-Neo1[Y222S] -5XFLAG*	This study
YHY-704-001	ZHY704	*pRS313-DRS2*	This study
YHY-704-002	ZHY704	*pRS313*	This study
YHY-704-003	ZHY704	*pRS313-NEO1*	This study
YHY-704-004	ZHY704	*pRS313-Neo1[Y222S]*	This study
YHY-704-005	ZHY704	*pRS313-Neo1[Y222A]*	This study
YHY-704-D001	ZHY704	*pRS313-DNF1*	This study
YHY-704-D002	ZHY704	*pRS313-Dnf1[S243A]*	This study
YHY-704-D003	ZHY704	*pRS313-Dnf1[S243T]*	This study
YHY-704-D004	ZHY704	*pRS313-Dnf1[S243Y*	This study
YHY-615-001	ZHY615M2D	*pRS313-DRS2*	This study
YHY-615-002	ZHY615M2D	*pRS313*	This study
YHY-615-003	ZHY615M2D	*pRS313-NEO1*	This study
YHY-615-004	ZHY615M2D	*pRS313-Neo1[Y222S]*	This study
YHY-615-005	ZHY615M2D	*pRS313-Neo1[Y222A]*	This study
YHY10-615-001	MTY10-615M2D	*pRS313-NEO1*	This study
YHY10-615-002	MTY10-615M2D	*pRS313*	This study
YHY10-615-003	MTY10-615M2D	*pRS313-Neo1[Y222S]*	This study
YHY10-615-004	MTY10-615M2D	*pRS313-Neo1[Y222A]*	This study

YHY10-615-005	MTY10-615M2D	*pRS313-Neo1[N199A]*	This study
YHY10-615-006	MTY10-615M2D	*pRS313-Neo1[Q209G]*	This study
YHY10-615-007	MTY10-615M2D	*pRS313-Neo1[A210Q]*	This study
YHY10-615-008	MTY10-615M2D	*pRS313-Neo1[A210F]*	This study
YHY10-615-008	MTY10-615M2D	*pRS313-Neo1[P212Q]*	This study
YHY10-615-009	MTY10-615M2D	*pRS313-Neo1[Y222S]*	This study
YHY10-615-010	MTY10-615M2D	*pRS313-Neo1[F228V]*	This study
YHY10-615-011	MTY10-615M2D	*pRS313-Neo1[E237D]*	This study
YHY10-615-011	MTY10-615M2D	*pRS313-Neo1[Y222S,F228V]*	This study
YHY10-615-012	MTY10-615M2D	*pRS313-Neo1[Y222S, E237D]*	This study
YHY10-615-013	MTY10-615M2D	*pRS313-Neo1 [Y222S, F228V, E237D]*	This study
YHY10-615-014	MTY10-615M2D	*pRS313-Neo1[N412S]*	This study
YHY10-615-015	MTY10-615M2D	*pRS313-Neo1[E237D]*	This study
YHY10-615-016	MTY10-615M2D	*pRS313-Neo1[R460A]*	This study
YHY10-615-017	MTY10-615M2D	*pRS313-Neo1[R460F]*	This study
YHY10-615-018	MTY10-615M2D	*pRS313-Neo1[R460Y]*	This study
YHY10-615-019	MTY10-615M2D	*pRS313-Neo1[R460Q]*	This study
YHY10-615-020	MTY10-615M2D	*pRS313-Neo1[D503N]*	This study
YHY10-615M2DS-001	MTY10-615M2DS	*pRS313-NEO1*	This study
YHY10-615M2DS-002	MTY10-615M2DS	*pRS313*	This study
YHY10-615M2DS-003	MTY10-615M2DS	*pRS313-Neo1[Y222S]*	This study
YHY10-615M2DS	MTY10-615M2DS	*pRS313-Neo1[Y222A]*	This study

-004			
YHY-E-001	BY4742	*pRS315-mCherry-Tlg1* *pRS413-ADH-GFP-NEO1*	This study
YHY-E-002	BY4742	*pRS315-mCherry-Tlg1* *pRS413-ADH-GFP-Neo1[Y222S]*	This study
YHY-C-001	JHY59	*pRS413-ADH-GFP-NEO1*	This study
YHY-C-002	JHY59	*pRS413-ADH-GFP-Neo1[Y222S]*	
YHY-M-001	JHY60	*pRS413-ADH-GFP-NEO1*	This study
YHY-M-002	JHY60	*pRS413-ADH-GFP-Neo1[Y222S]*	
YHY-T-001	CWY267	*pRS413-ADH-GFP-NEO1*	This study
YHY-T-002	CWY267	*pRS413-ADH-GFP-Neo1[Y222S]*	
ANY1-GFP	*ANY1::GFP::HIS3MX6*		*(156)*
YHY-IP-001	*ANY1::GFP::HIS3MX6*	*pRS313-NEO1*	This study
YHY-IP-002	*ANY1::GFP::HIS3MX6*	*pRS313-NEO1-5XFLAG*	This study

REFERENCES

1. Prezant, T. R., Chaltraw, W. E., Jr., and Fischel-Ghodsian, N. (1996) Identification of an overexpressed yeast gene which prevents aminoglycoside toxicity. *Microbiology* **142 (Pt 12)**, 3407-3414
2. Hua, Z., Fatheddin, P., and Graham, T. R. (2002) An essential subfamily of Drs2p-related P-type ATPases is required for protein trafficking between Golgi complex and endosomal/vacuolar system. *Molecular biology of the cell* **13**, 3162-3177
3. Hua, Z., and Graham, T. R. (2003) Requirement for neo1p in retrograde transport from the Golgi complex to the endoplasmic reticulum. *Mol Biol Cell* **14**, 4971-4983
4. Brett, C. L., Kallay, L., Hua, Z., Green, R., Chyou, A., Zhang, Y., Graham, T. R., Donowitz, M., and Rao, R. (2011) Genome-wide analysis reveals the vacuolar pH-stat of Saccharomyces cerevisiae. *PLoS One* **6**, e17619
5. Takar, M., Wu, Y., and Graham, T. R. (2016) The Essential Neo1 Protein from Budding Yeast Plays a Role in Establishing Aminophospholipid Asymmetry of the Plasma Membrane*. in *J Biol Chem*. pp 15727-15739
6. Wu, Y., Takar, M., Cuentas-Condori, A. A., and Graham, T. R. (2016) Neo1 and phosphatidylethanolamine contribute to vacuole membrane fusion in Saccharomyces cerevisiae. *Cell Logist* **6**, e1228791
7. Wehman, A. M., Poggioli, C., Schweinsberg, P., Grant, B. D., and Nance, J. (2011) The P4-ATPase TAT-5 inhibits the budding of extracellular vesicles in C. elegans embryos. *Curr Biol* **21**, 1951-1959

8. Takatsu, H., Baba, K., Shima, T., Umino, H., Kato, U., Umeda, M., Nakayama, K., and Shin, H. W. (2011) ATP9B, a P4-ATPase (a putative aminophospholipid translocase), localizes to the trans-Golgi network in a CDC50 protein-independent manner. *J Biol Chem* **286**, 38159-38167
9. Barbosa, S., Pratte, D., Schwarz, H., Pipkorn, R., and Singer-Kruger, B. (2010) Oligomeric Dop1p is part of the endosomal Neo1p-Ysl2p-Arl1p membrane remodeling complex. *Traffic* **11**, 1092-1106
10. Takahashi, Y., Fujimura-Kamada, K., Kondo, S., and Tanaka, K. (2011) Isolation and characterization of novel mutations in CDC50, the non-catalytic subunit of the Drs2p phospholipid flippase. *J Biochem* **149**, 423-432
11. Chen, S., Wang, J., Muthusamy, B. P., Liu, K., Zare, S., Andersen, R. J., and Graham, T. R. (2006) Roles for the Drs2p-Cdc50p complex in protein transport and phosphatidylserine asymmetry of the yeast plasma membrane. *Traffic* **7**, 1503-1517
12. Kornberg, R. D., and McConnell, H. M. (1971) Inside-outside transitions of phospholipids in vesicle membranes. *Biochemistry* **10**, 1111-1120
13. Kornberg, R. D., and McConnell, H. M. (1971) Lateral diffusion of phospholipids in a vesicle membrane. *Proc Natl Acad Sci U S A* **68**, 2564-2568
14. Bretscher, M. S. (1972) Asymmetrical lipid bilayer structure for biological membranes. *Nat New Biol* **236**, 11-12
15. Sebastian, T. T., Baldridge, R. D., Xu, P., and Graham, T. R. (2012) Phospholipid flippases: building asymmetric membranes and transport vesicles. *Biochim Biophys Acta* **1821**, 1068-1077
16. Tsai, K. H., and Lenard, J. (1975) Asymmetry of influenza virus membrane bilayer demonstrated with phospholipase C. *Nature* **253**, 554-555
17. Rothman, J. E., and Dawidowicz, E. A. (1975) Asymmetric exchange of vesicle phospholipids catalyzed by the phosphatidylcholine exhange protein. Measurement of inside--outside transitions. *Biochemistry* **14**, 2809-2816
18. Bloj, B., and Zilversmit, D. B. (1976) Asymmetry and transposition rates of phosphatidylcholine in rat erythrocyte ghosts. *Biochemistry* **15**, 1277-1283
19. Schick, P. K., Kurica, K. B., and Chacko, G. K. (1976) Location of phosphatidylethanolamine and phosphatidylserine in the human platelet plasma membrane. *J Clin Invest* **57**, 1221-1226
20. van Meer, G., Voelker, D. R., and Feigenson, G. W. (2008) Membrane lipids: where they are and how they behave. *Nature reviews. Molecular cell biology* **9**, 112-124
21. Mercer, J., and Helenius, A. (2008) Vaccinia virus uses macropinocytosis and apoptotic mimicry to enter host cells. *Science* **320**, 531-535
22. Aoki, Y., Uenaka, T., Aoki, J., Umeda, M., and Inoue, K. (1994) A novel peptide probe for studying the transbilayer movement of phosphatidylethanolamine. *J Biochem* **116**, 291-297

23. Verkleij, A. J., Zwaal, R. F., Roelofsen, B., Comfurius, P., Kastelijn, D., and van Deenen, L. L. (1973) The asymmetric distribution of phospholipids in the human red cell membrane. A combined study using phospholipases and freeze-etch electron microscopy. *Biochim Biophys Acta* **323**, 178-193
24. Seigneuret, M., and Devaux, P. F. (1984) ATP-dependent asymmetric distribution of spin-labeled phospholipids in the erythrocyte membrane: relation to shape changes. *Proc Natl Acad Sci U S A* **81**, 3751-3755
25. Zachowski, A., Henry, J. P., and Devaux, P. F. (1989) Control of transmembrane lipid asymmetry in chromaffin granules by an ATP-dependent protein. *Nature* **340**, 75-76
26. Sune, A., Bette-Bobillo, P., Bienvenue, A., Fellmann, P., and Devaux, P. F. (1987) Selective outside-inside translocation of aminophospholipids in human platelets. *Biochemistry* **26**, 2972-2978
27. Kean, L. S., Fuller, R. S., and Nichols, J. W. (1993) Retrograde lipid traffic in yeast: identification of two distinct pathways for internalization of fluorescent-labeled phosphatidylcholine from the plasma membrane. *J Cell Biol* **123**, 1403-1419
28. Moriyama, Y., and Nelson, N. (1988) Purification and properties of a vanadate- and N-ethylmaleimide-sensitive ATPase from chromaffin granule membranes. *J Biol Chem* **263**, 8521-8527
29. Xie, X. S., Stone, D. K., and Racker, E. (1989) Purification of a vanadate-sensitive ATPase from clathrin-coated vesicles of bovine brain. *J Biol Chem* **264**, 1710-1714
30. Tang, X., Halleck, M. S., Schlegel, R. A., and Williamson, P. (1996) A subfamily of P-type ATPases with aminophospholipid transporting activity. *Science* **272**, 1495-1497
31. Bull, L. N., van Eijk, M. J., Pawlikowska, L., DeYoung, J. A., Juijn, J. A., Liao, M., Klomp, L. W., Lomri, N., Berger, R., Scharschmidt, B. F., Knisely, A. S., Houwen, R. H., and Freimer, N. B. (1998) A gene encoding a P-type ATPase mutated in two forms of hereditary cholestasis. *Nat Genet* **18**, 219-224
32. Marx, U., Polakowski, T., Pomorski, T., Lang, C., Nelson, H., Nelson, N., and Herrmann, A. (1999) Rapid transbilayer movement of fluorescent phospholipid analogues in the plasma membrane of endocytosis-deficient yeast cells does not require the Drs2 protein. *Eur J Biochem* **263**, 254-263
33. Siegmund, A., Grant, A., Angeletti, C., Malone, L., Nichols, J. W., and Rudolph, H. K. (1998) Loss of Drs2p does not abolish transfer of fluorescence-labeled phospholipids across the plasma membrane of Saccharomyces cerevisiae. *J Biol Chem* **273**, 34399-34405
34. Pomorski, T., Lombardi, R., Riezman, H., Devaux, P. F., van Meer, G., and Holthuis, J. C. (2003) Drs2p-related P-type ATPases Dnf1p and Dnf2p are required for phospholipid translocation across the yeast plasma membrane and serve a role in endocytosis. *Mol Biol Cell* **14**, 1240-1254

35. Natarajan, P., Wang, J., Hua, Z., and Graham, T. R. (2004) Drs2p-coupled aminophospholipid translocase activity in yeast Golgi membranes and relationship to in vivo function. *Proc Natl Acad Sci U S A* **101**, 10614-10619
36. Zhou, X., and Graham, T. R. (2009) Reconstitution of phospholipid translocase activity with purified Drs2p, a type-IV P-type ATPase from budding yeast. *Proceedings of the National Academy of Sciences of the United States of America* **106**, 16586-16591
37. Coleman, J. A., Kwok, M. C., and Molday, R. S. (2009) Localization, purification, and functional reconstitution of the P4-ATPase Atp8a2, a phosphatidylserine flippase in photoreceptor disc membranes. *J Biol Chem* **284**, 32670-32679
38. Axelsen, K. B., and Palmgren, M. G. (1998) Evolution of substrate specificities in the P-type ATPase superfamily. *J Mol Evol* **46**, 84-101
39. Palmgren, M. G., and Axelsen, K. B. (1998) Evolution of P-type ATPases. *Biochim Biophys Acta* **1365**, 37-45
40. Palmgren, M. G., and Nissen, P. (2011) P-type ATPases. *Annu Rev Biophys* **40**, 243-266
41. Daleke, D. L., and Huestis, W. H. (1985) Incorporation and translocation of aminophospholipids in human erythrocytes. *Biochemistry* **24**, 5406-5416
42. Hankins, H. M., Baldridge, R. D., Xu, P., and Graham, T. R. (2015) Role of flippases, scramblases and transfer proteins in phosphatidylserine subcellular distribution. *Traffic* **16**, 35-47
43. Fairn, G. D., Schieber, N. L., Ariotti, N., Murphy, S., Kuerschner, L., Webb, R. I., Grinstein, S., and Parton, R. G. (2011) High-resolution mapping reveals topologically distinct cellular pools of phosphatidylserine. *The Journal of cell biology* **194**, 257-275
44. Segawa, K., Kurata, S., Yanagihashi, Y., Brummelkamp, T. R., Matsuda, F., and Nagata, S. (2014) Caspase-mediated cleavage of phospholipid flippase for apoptotic phosphatidylserine exposure. *Science* **344**, 1164-1168
45. Suzuki, J., Denning, D. P., Imanishi, E., Horvitz, H. R., and Nagata, S. (2013) Xk-related protein 8 and CED-8 promote phosphatidylserine exposure in apoptotic cells. *Science* **341**, 403-406
46. Suzuki, J., Imanishi, E., and Nagata, S. (2016) Xkr8 phospholipid scrambling complex in apoptotic phosphatidylserine exposure. *Proc Natl Acad Sci U S A* **113**, 9509-9514
47. Graham, T. R. (2004) Flippases and vesicle-mediated protein transport. *Trends in cell biology* **14**, 670-677
48. Xu, P., Baldridge, R. D., Chi, R. J., Burd, C. G., and Graham, T. R. (2013) Phosphatidylserine flipping enhances membrane curvature and negative charge required for vesicular transport. *J Cell Biol* **202**, 875-886
49. Lee, S., Uchida, Y., Wang, J., Matsudaira, T., Nakagawa, T., Kishimoto, T., Mukai, K., Inaba, T., Kobayashi, T., Molday, R. S., Taguchi, T., and Arai, H. (2015)

Transport through recycling endosomes requires EHD1 recruitment by a phosphatidylserine translocase. *Embo j* **34**, 669-688
50. van der Mark, V. A., Elferink, R. P., and Paulusma, C. C. (2013) P4 ATPases: flippases in health and disease. *Int J Mol Sci* **14**, 7897-7922
51. Onat, O. E., Gulsuner, S., Bilguvar, K., Nazli Basak, A., Topaloglu, H., Tan, M., Tan, U., Gunel, M., and Ozcelik, T. (2013) Missense mutation in the ATPase, aminophospholipid transporter protein ATP8A2 is associated with cerebellar atrophy and quadrupedal locomotion. *Eur J Hum Genet* **21**, 281-285
52. Zhu, X., Libby, R. T., de Vries, W. N., Smith, R. S., Wright, D. L., Bronson, R. T., Seburn, K. L., and John, S. W. (2012) Mutations in a P-type ATPase gene cause axonal degeneration. *PLoS Genet* **8**, e1002853
53. Arashiki, N., Takakuwa, Y., Mohandas, N., Hale, J., Yoshida, K., Ogura, H., Utsugisawa, T., Ohga, S., Miyano, S., Ogawa, S., Kojima, S., and Kanno, H. (2016) ATP11C is a major flippase in human erythrocytes and its defect causes congenital hemolytic anemia. *Haematologica* **101**, 559-565
54. Yabas, M., Teh, C. E., Frankenreiter, S., Lal, D., Roots, C. M., Whittle, B., Andrews, D. T., Zhang, Y., Teoh, N. C., Sprent, J., Tze, L. E., Kucharska, E. M., Kofler, J., Farell, G. C., Broer, S., Goodnow, C. C., and Enders, A. (2011) ATP11C is critical for the internalization of phosphatidylserine and differentiation of B lymphocytes. *Nature immunology* **12**, 441-449
55. Yabas, M., Coupland, L. A., Cromer, D., Winterberg, M., Teoh, N. C., D'Rozario, J., Kirk, K., Broer, S., Parish, C. R., and Enders, A. (2014) Mice deficient in the putative phospholipid flippase ATP11C exhibit altered erythrocyte shape, anemia, and reduced erythrocyte life span. *The Journal of biological chemistry* **289**, 19531-19537
56. Siggs, O. M., Arnold, C. N., Huber, C., Pirie, E., Xia, Y., Lin, P., Nemazee, D., and Beutler, B. (2011) The P4-type ATPase ATP11C is essential for B lymphopoiesis in adult bone marrow. *Nat Immunol* **12**, 434-440
57. Sigurdsson, M. I., Jamshidi, N., Jonsson, J. J., and Palsson, B. O. (2009) Genome-scale network analysis of imprinted human metabolic genes. *Epigenetics* **4**, 43-46
58. Dhar, M., Webb, L. S., Smith, L., Hauser, L., Johnson, D., and West, D. B. (2000) A novel ATPase on mouse chromosome 7 is a candidate gene for increased body fat. *Physiol Genomics* **4**, 93-100
59. Kengia, J. T., Ko, K. C., Ikeda, S., Hiraishi, A., Mieno-Naka, M., Arai, T., Sato, N., Muramatsu, M., and Sawabe, M. (2013) A gene variant in the Atp10d gene associates with atherosclerotic indices in Japanese elderly population. *Atherosclerosis* **231**, 158-162
60. Hicks, A. A., Pramstaller, P. P., Johansson, A., Vitart, V., Rudan, I., Ugocsai, P., Aulchenko, Y., Franklin, C. S., Liebisch, G., Erdmann, J., Jonasson, I., Zorkoltseva, I. V., Pattaro, C., Hayward, C., Isaacs, A., Hengstenberg, C., Campbell, S., Gnewuch, C., Janssens, A. C., Kirichenko, A. V., Konig, I. R.,

Marroni, F., Polasek, O., Demirkan, A., Kolcic, I., Schwienbacher, C., Igl, W., Biloglav, Z., Witteman, J. C., Pichler, I., Zaboli, G., Axenovich, T. I., Peters, A., Schreiber, S., Wichmann, H. E., Schunkert, H., Hastie, N., Oostra, B. A., Wild, S. H., Meitinger, T., Gyllensten, U., van Duijn, C. M., Wilson, J. F., Wright, A., Schmitz, G., and Campbell, H. (2009) Genetic determinants of circulating sphingolipid concentrations in European populations. *PLoS Genet* **5**, e1000672

61. Sigruener, A., Wolfrum, C., Boettcher, A., Kopf, T., Liebisch, G., Orso, E., and Schmitz, G. (2017) Lipidomic and metabolic changes in the P4-type ATPase ATP10D deficient C57BL/6J wild type mice upon rescue of ATP10D function. *PLoS One* **12**, e0178368
62. Natarajan, P., Liu, K., Patil, D. V., Sciorra, V. A., Jackson, C. L., and Graham, T. R. (2009) Regulation of a Golgi Flippase by Phosphoinositides and an ArfGEF. *Nat Cell Biol* **11**, 1421-1426
63. Ding, J., Wu, Z., Crider, B. P., Ma, Y., Li, X., Slaughter, C., Gong, L., and Xie, X. S. (2000) Identification and functional expression of four isoforms of ATPase II, the putative aminophospholipid translocase. Effect of isoform variation on the ATPase activity and phospholipid specificity. *J Biol Chem* **275**, 23378-23386
64. Alder-Baerens, N., Lisman, Q., Luong, L., Pomorski, T., and Holthuis, J. C. (2006) Loss of P4 ATPases Drs2p and Dnf3p disrupts aminophospholipid transport and asymmetry in yeast post-Golgi secretory vesicles. *Mol Biol Cell* **17**, 1632-1642
65. Baldridge, R. D., Xu, P., and Graham, T. R. (2013) Type IV P-type ATPases distinguish mono- versus diacyl phosphatidylserine using a cytofacial exit gate in the membrane domain. *J Biol Chem* **288**, 19516-19527
66. Riekhof, W. R., and Voelker, D. R. (2006) Uptake and utilization of lyso-phosphatidylethanolamine by Saccharomyces cerevisiae. *J Biol Chem* **281**, 36588-36596
67. Naito, T., Takatsu, H., Miyano, R., Takada, N., Nakayama, K., and Shin, H. W. (2015) Phospholipid Flippase ATP10A Translocates Phosphatidylcholine and Is Involved in Plasma Membrane Dynamics*. *J Biol Chem* **290**, 15004-15017
68. Takatsu, H., Tanaka, G., Segawa, K., Suzuki, J., Nagata, S., Nakayama, K., and Shin, H. W. (2014) Phospholipid flippase activities and substrate specificities of human type IV P-type ATPases localized to the plasma membrane. *The Journal of biological chemistry* **289**, 33543-33556
69. Takar, M., Wu, Y., and Graham, T. R. (2016) The Essential Neo1 Protein from Budding Yeast Plays a Role in Establishing Aminophospholipid Asymmetry of the Plasma Membrane. *J Biol Chem* **291**, 15727-15739
70. Baldridge, R. D., and Graham, T. R. (2012) Identification of residues defining phospholipid flippase substrate specificity of type IV P-type ATPases.

Proceedings of the National Academy of Sciences of the United States of America **109**, E290-298
71. Vestergaard, A. L., Coleman, J. A., Lemmin, T., Mikkelsen, S. A., Molday, L. L., Vilsen, B., Molday, R. S., Dal Peraro, M., and Andersen, J. P. (2014) Critical roles of isoleucine-364 and adjacent residues in a hydrophobic gate control of phospholipid transport by the mammalian P4-ATPase ATP8A2. *Proc Natl Acad Sci U S A* **111**, E1334-1343
72. Roland, B. P., and Graham, T. R. (2016) Decoding P4-ATPase substrate interactions. *Crit Rev Biochem Mol Biol* **51**, 513-527
73. Bryde, S., Hennrich, H., Verhulst, P. M., Devaux, P. F., Lenoir, G., and Holthuis, J. C. (2010) CDC50 proteins are critical components of the human class-1 P4-ATPase transport machinery. *J Biol Chem* **285**, 40562-40572
74. Saito, K., Fujimura-Kamada, K., Furuta, N., Kato, U., Umeda, M., and Tanaka, K. (2004) Cdc50p, a protein required for polarized growth, associates with the Drs2p P-type ATPase implicated in phospholipid translocation in Saccharomyces cerevisiae. *Molecular biology of the cell* **15**, 3418-3432
75. Noji, T., Yamamoto, T., Saito, K., Fujimura-Kamada, K., Kondo, S., and Tanaka, K. (2006) Mutational analysis of the Lem3p-Dnf1p putative phospholipid-translocating P-type ATPase reveals novel regulatory roles for Lem3p and a carboxyl-terminal region of Dnf1p independent of the phospholipid-translocating activity of Dnf1p in yeast. *Biochem Biophys Res Commun* **344**, 323-331
76. Coleman, J. A., Vestergaard, A. L., Molday, R. S., Vilsen, B., and Andersen, J. P. (2012) Critical role of a transmembrane lysine in aminophospholipid transport by mammalian photoreceptor P4-ATPase ATP8A2. *Proc Natl Acad Sci U S A* **109**, 1449-1454
77. Toyoshima, C., Iwasawa, S., Ogawa, H., Hirata, A., Tsueda, J., and Inesi, G. (2013) Crystal structures of the calcium pump and sarcolipin in the Mg2+-bound E1 state. *Nature* **495**, 260-264
78. Toyoshima, C., Nakasako, M., Nomura, H., and Ogawa, H. (2000) Crystal structure of the calcium pump of sarcoplasmic reticulum at 2.6 A resolution. *Nature* **405**, 647-655
79. Gourdon, P., Liu, X. Y., Skjorringe, T., Morth, J. P., Moller, L. B., Pedersen, B. P., and Nissen, P. (2011) Crystal structure of a copper-transporting PIB-type ATPase. *Nature* **475**, 59-64
80. Norimatsu, Y., Hasegawa, K., Shimizu, N., and Toyoshima, C. (2017) Protein-phospholipid interplay revealed with crystals of a calcium pump. *Nature* **545**, 193-198
81. Gantzel, R. H., Mogensen, L. S., Mikkelsen, S. A., Vilsen, B., Molday, R. S., Vestergaard, A. L., and Andersen, J. P. (2017) Disease mutations reveal residues critical to the interaction of P4-ATPases with lipid substrates. *Sci Rep* **7**, 10418

82. Nyblom, M., Poulsen, H., Gourdon, P., Reinhard, L., Andersson, M., Lindahl, E., Fedosova, N., and Nissen, P. (2013) Crystal structure of Na+, K(+)-ATPase in the Na(+)-bound state. *Science* **342**, 123-127
83. Baldridge, R. D., and Graham, T. R. (2013) Two-gate mechanism for phospholipid selection and transport by type IV P-type ATPases. in *Proc Natl Acad Sci U S A*. pp E358-367
84. Roland, B. P., and Graham, T. R. (2016) Directed evolution of a sphingomyelin flippase reveals mechanism of substrate backbone discrimination by a P4-ATPase. *Proc Natl Acad Sci U S A* **113**, E4460-4466
85. Roland, B. P., and Graham, T. R. (2016) Decoding P4-ATPase Substrate Interactions. *Crit Rev Biochem Mol Biol* **51**, 513-527
86. Hankins, H. M., Sere, Y. Y., Diab, N. S., Menon, A. K., and Graham, T. R. (2015) Phosphatidylserine translocation at the yeast trans-Golgi network regulates protein sorting into exocytic vesicles. *Mol Biol Cell* **26**, 4674-4685
87. Parsons, A. B., Lopez, A., Givoni, I. E., Williams, D. E., Gray, C. A., Porter, J., Chua, G., Sopko, R., Brost, R. L., Ho, C. H., Wang, J., Ketela, T., Brenner, C., Brill, J. A., Fernandez, G. E., Lorenz, T. C., Payne, G. S., Ishihara, S., Ohya, Y., Andrews, B., Hughes, T. R., Frey, B. J., Graham, T. R., Andersen, R. J., and Boone, C. (2006) Exploring the mode-of-action of bioactive compounds by chemical-genetic profiling in yeast. *Cell* **126**, 611-625
88. Emoto, K., Kobayashi, T., Yamaji, A., Aizawa, H., Yahara, I., Inoue, K., and Umeda, M. (1996) Redistribution of phosphatidylethanolamine at the cleavage furrow of dividing cells during cytokinesis. *Proceedings of the National Academy of Sciences of the United States of America* **93**, 12867-12872
89. Umeda, M., and Emoto, K. (1999) Membrane phospholipid dynamics during cytokinesis: regulation of actin filament assembly by redistribution of membrane surface phospholipid. *Chem Phys Lipids* **101**, 81-91
90. Newton, A. C., and Keranen, L. M. (1994) Phosphatidyl-L-serine is necessary for protein kinase C's high-affinity interaction with diacylglycerol-containing membranes. *Biochemistry* **33**, 6651-6658
91. Yeung, T., Terebiznik, M., Yu, L., Silvius, J., Abidi, W. M., Philips, M., Levine, T., Kapus, A., and Grinstein, S. (2006) Receptor activation alters inner surface potential during phagocytosis. *Science* **313**, 347-351
92. Das, A., Slaughter, B. D., Unruh, J. R., Bradford, W. D., Alexander, R., Rubinstein, B., and Li, R. (2012) Flippase-mediated phospholipid asymmetry promotes fast Cdc42 recycling in dynamic maintenance of cell polarity. *Nat Cell Biol* **14**, 304-310
93. Takatsu, H., Takayama, M., Naito, T., Takada, N., Tsumagari, K., Ishihama, Y., Nakayama, K., and Shin, H. W. (2017) Phospholipid flippase ATP11C is endocytosed and downregulated following Ca2+-mediated protein kinase C activation. in *Nat Commun*. pp

94. Fujii, T., Sakata, A., Nishimura, S., Eto, K., and Nagata, S. (2015) TMEM16F is required for phosphatidylserine exposure and microparticle release in activated mouse platelets. *Proc Natl Acad Sci U S A* **112**, 12800-12805
95. Malvezzi, M., Chalat, M., Janjusevic, R., Picollo, A., Terashima, H., Menon, A. K., and Accardi, A. (2013) Ca2+-dependent phospholipid scrambling by a reconstituted TMEM16 ion channel. *Nat Commun* **4**, 2367
96. Yang, H., Kim, A., David, T., Palmer, D., Jin, T., Tien, J., Huang, F., Cheng, T., Coughlin, S. R., Jan, Y. N., and Jan, L. Y. (2012) TMEM16F forms a Ca2+-activated cation channel required for lipid scrambling in platelets during blood coagulation. *Cell* **151**, 111-122
97. Poulsen, L. R., Lopez-Marques, R. L., Pedas, P. R., McDowell, S. C., Brown, E., Kunze, R., Harper, J. F., Pomorski, T. G., and Palmgren, M. (2015) A phospholipid uptake system in the model plant Arabidopsis thaliana. *Nat Commun* **6**, 7649
98. Holthuis, J. C., and Menon, A. K. (2014) Lipid landscapes and pipelines in membrane homeostasis. *Nature* **510**, 48-57
99. Furuta, N., Fujimura-Kamada, K., Saito, K., Yamamoto, T., and Tanaka, K. (2007) Endocytic recycling in yeast is regulated by putative phospholipid translocases and the Ypt31p/32p-Rcy1p pathway. *Mol Biol Cell* **18**, 295-312
100. Liu, K., Surendhran, K., Nothwehr, S. F., and Graham, T. R. (2008) P4-ATPase Requirement for AP-1/Clathrin Function in Protein Transport from the trans-Golgi Network and Early Endosomes. in *Mol Biol Cell*. pp 3526-3535
101. Dalton, L. E., Bean, B. D. M., Davey, M., and Conibear, E. (2017) Quantitative high-content imaging identifies novel regulators of Neo1 trafficking at endosomes. *Mol Biol Cell* **28**, 1539-1550
102. Liu, K., Hua, Z., Nepute, J. A., and Graham, T. R. (2007) Yeast P4-ATPases Drs2p and Dnf1p Are Essential Cargos of the NPFXD/Sla1p Endocytic Pathway. in *Mol Biol Cell*. pp 487-500
103. Hachiro, T., Yamamoto, T., Nakano, K., and Tanaka, K. (2013) Phospholipid flippases Lem3p-Dnf1p and Lem3p-Dnf2p are involved in the sorting of the tryptophan permease Tat2p in yeast. *J Biol Chem* **288**, 3594-3608
104. Takeda, M., Yamagami, K., and Tanaka, K. (2014) Role of phosphatidylserine in phospholipid flippase-mediated vesicle transport in Saccharomyces cerevisiae. *Eukaryot Cell* **13**, 363-375
105. Nakano, K., Yamamoto, T., Kishimoto, T., Noji, T., and Tanaka, K. (2008) Protein kinases Fpk1p and Fpk2p are novel regulators of phospholipid asymmetry. *Mol Biol Cell* **19**, 1783-1797
106. Roelants, F. M., Baltz, A. G., Trott, A. E., Fereres, S., and Thorner, J. (2010) A protein kinase network regulates the function of aminophospholipid flippases. in *Proc Natl Acad Sci U S A*. pp 34-39

107. Sartorel, E., Barrey, E., Lau, R. K., and Thorner, J. (2015) Plasma membrane aminoglycerolipid flippase function is required for signaling competence in the yeast mating pheromone response pathway. *Mol Biol Cell* **26**, 134-150
108. Yamane-Sando, Y., Shimobayashi, E., Shimobayashi, M., Kozutsumi, Y., Oka, S., and Takematsu, H. (2014) Fpk1/2 kinases regulate cellular sphingoid long-chain base abundance and alter cellular resistance to LCB elevation or depletion. *Microbiologyopen* **3**, 196-212
109. Zhou, X., Sebastian, T. T., and Graham, T. R. (2013) Auto-inhibition of Drs2p, a Yeast Phospholipid Flippase, by Its Carboxyl-terminal Tail*. in *J Biol Chem*. pp 31807-31815
110. Azouaoui, H., Montigny, C., Ash, M. R., Fijalkowski, F., Jacquot, A., Gronberg, C., Lopez-Marques, R. L., Palmgren, M. G., Garrigos, M., le Maire, M., Decottignies, P., Gourdon, P., Nissen, P., Champeil, P., and Lenoir, G. (2014) A high-yield co-expression system for the purification of an intact Drs2p-Cdc50p lipid flippase complex, critically dependent on and stabilized by phosphatidylinositol-4-phosphate. *PLoS One* **9**, e112176
111. Tsai, P. C., Hsu, J. W., Liu, Y. W., Chen, K. Y., and Lee, F. J. (2013) Arl1p regulates spatial membrane organization at the trans-Golgi network through interaction with Arf-GEF Gea2p and flippase Drs2p. *Proc Natl Acad Sci U S A* **110**, E668-677
112. Hanamatsu, H., Fujimura-Kamada, K., Yamamoto, T., Furuta, N., and Tanaka, K. (2014) Interaction of the phospholipid flippase Drs2p with the F-box protein Rcy1p plays an important role in early endosome to trans-Golgi network vesicle transport in yeast. *J Biochem* **155**, 51-62
113. Wicky, S., Schwarz, H., and Singer-Kruger, B. (2004) Molecular interactions of yeast Neo1p, an essential member of the Drs2 family of aminophospholipid translocases, and its role in membrane trafficking within the endomembrane system. *Molecular and cellular biology* **24**, 7402-7418
114. van Leeuwen, J., Pons, C., Mellor, J. C., Yamaguchi, T. N., Friesen, H., Koschwanez, J., Usaj, M. M., Pechlaner, M., Takar, M., Usaj, M., VanderSluis, B., Andrusiak, K., Bansal, P., Baryshnikova, A., Boone, C. E., Cao, J., Cote, A., Gebbia, M., Horecka, G., Horecka, I., Kuzmin, E., Legro, N., Liang, W., van Lieshout, N., McNee, M., San Luis, B. J., Shaeri, F., Shuteriqi, E., Sun, S., Yang, L., Youn, J. Y., Yuen, M., Costanzo, M., Gingras, A. C., Aloy, P., Oostenbrink, C., Murray, A., Graham, T. R., Myers, C. L., Andrews, B. J., Roth, F. P., and Boone, C. (2016) Exploring genetic suppression interactions on a global scale. *Science* **354**
115. Muthusamy, B. P., Raychaudhuri, S., Natarajan, P., Abe, F., Liu, K., Prinz, W. A., and Graham, T. R. (2009) Control of protein and sterol trafficking by antagonistic activities of a type IV P-type ATPase and oxysterol binding protein homologue. *Mol Biol Cell* **20**, 2920-2931

116. de Saint-Jean, M., Delfosse, V., Douguet, D., Chicanne, G., Payrastre, B., Bourguet, W., Antonny, B., and Drin, G. (2011) Osh4p exchanges sterols for phosphatidylinositol 4-phosphate between lipid bilayers. *J Cell Biol* **195**, 965-978
117. Yamamoto, T., Fujimura-Kamada, K., Shioji, E., Suzuki, R., and Tanaka, K. (2017) Cfs1p, a Novel Membrane Protein in the PQ-Loop Family, Is Involved in Phospholipid Flippase Functions in Yeast. *G3 (Bethesda)* **7**, 179-192
118. Jezegou, A., Llinares, E., Anne, C., Kieffer-Jaquinod, S., O'Regan, S., Aupetit, J., Chabli, A., Sagne, C., Debacker, C., Chadefaux-Vekemans, B., Journet, A., Andre, B., and Gasnier, B. (2012) Heptahelical protein PQLC2 is a lysosomal cationic amino acid exporter underlying the action of cysteamine in cystinosis therapy. *Proc Natl Acad Sci U S A* **109**, E3434-3443
119. Zhou, X., Sebastian, T. T., and Graham, T. R. (2013) Auto-inhibition of Drs2p, a yeast phospholipid flippase, by its carboxyl-terminal tail. *J Biol Chem* **288**, 31807-31815
120. Pascon, R. C., and Miller, B. L. (2000) Morphogenesis in Aspergillus nidulans requires Dopey (DopA), a member of a novel family of leucine zipper-like proteins conserved from yeast to humans. *Mol Microbiol* **36**, 1250-1264
121. Guipponi, M., Brunschwig, K., Chamoun, Z., Scott, H. S., Shibuya, K., Kudoh, J., Delezoide, A. L., El Samadi, S., Chettouh, Z., Rossier, C., Shimizu, N., Mueller, F., Delabar, J. M., and Antonarakis, S. E. (2000) C21orf5, a novel human chromosome 21 gene, has a Caenorhabditis elegans ortholog (pad-1) required for embryonic patterning. *Genomics* **68**, 30-40
122. Rachidi, M., Lopes, C., Costantine, M., and Delabar, J. M. (2005) C21orf5, a new member of Dopey family involved in morphogenesis, could participate in neurological alterations and mental retardation in Down syndrome. *DNA Res* **12**, 203-210
123. Gillingham, A. K., Whyte, J. R., Panic, B., and Munro, S. (2006) Mon2, a relative of large Arf exchange factors, recruits Dop1 to the Golgi apparatus. *J Biol Chem* **281**, 2273-2280
124. Beer, K. B., Rivas-Castillo, J., Kuhn, K., Fazeli, G., Karmann, B., Nance, J. F., Stigloher, C., and Wehman, A. M. (2018) Extracellular vesicle budding is inhibited by redundant regulators of TAT-5 flippase localization and phospholipid asymmetry. *Proc Natl Acad Sci U S A* **115**, E1127-e1136
125. Muren, E., Oyen, M., Barmark, G., and Ronne, H. (2001) Identification of yeast deletion strains that are hypersensitive to brefeldin A or monensin, two drugs that affect intracellular transport. *Yeast* **18**, 163-172
126. Singer-Kruger, B., and Ferro-Novick, S. (1997) Use of a synthetic lethal screen to identify yeast mutants impaired in endocytosis, vacuolar protein sorting and the organization of the cytoskeleton. *Eur J Cell Biol* **74**, 365-375
127. Jochum, A., Jackson, D., Schwarz, H., Pipkorn, R., and Singer-Kruger, B. (2002) Yeast Ysl2p, homologous to Sec7 domain guanine nucleotide exchange

factors, functions in endocytosis and maintenance of vacuole integrity and interacts with the Arf-Like small GTPase Arl1p. *Mol Cell Biol* **22**, 4914-4928
128. Bonangelino, C. J., Chavez, E. M., and Bonifacino, J. S. (2002) Genomic screen for vacuolar protein sorting genes in Saccharomyces cerevisiae. *Mol Biol Cell* **13**, 2486-2501
129. Efe, J. A., Plattner, F., Hulo, N., Kressler, D., Emr, S. D., and Deloche, O. (2005) Yeast Mon2p is a highly conserved protein that functions in the cytoplasm-to-vacuole transport pathway and is required for Golgi homeostasis. *J Cell Sci* **118**, 4751-4764
130. Mahajan, D., Boh, B. K., Zhou, Y., Chen, L., Cornvik, T. C., Hong, W., and Lu, L. (2013) Mammalian Mon2/Ysl2 regulates endosome-to-Golgi trafficking but possesses no guanine nucleotide exchange activity toward Arl1 GTPase. *Sci Rep* **3**, 3362
131. Manlandro, C. M., Palanivel, V. R., Schorr, E. B., Mihatov, N., Antony, A. A., and Rosenwald, A. G. (2012) Mon2 is a negative regulator of the monomeric G protein, Arl1. *FEMS Yeast Res* **12**, 637-650
132. Singer-Kruger, B., Lasic, M., Burger, A. M., Hausser, A., Pipkorn, R., and Wang, Y. (2008) Yeast and human Ysl2p/hMon2 interact with Gga adaptors and mediate their subcellular distribution. *Embo j* **27**, 1423-1435
133. Schlitt, T., Palin, K., Rung, J., Dietmann, S., Lappe, M., Ukkonen, E., and Brazma, A. (2003) From gene networks to gene function. *Genome Res* **13**, 2568-2576
134. Zer, C., and Chanfreau, G. (2005) Regulation and surveillance of normal and 3'-extended forms of the yeast aci-reductone dioxygenase mRNA by RNase III cleavage and exonucleolytic degradation. *J Biol Chem* **280**, 28997-29003
135. Saudek, V. (2012) Cystinosin, MPDU1, SWEETs and KDELR belong to a well-defined protein family with putative function of cargo receptors involved in vesicle trafficking. *PLoS One* **7**, e30876
136. Town, M., Jean, G., Cherqui, S., Attard, M., Forestier, L., Whitmore, S. A., Callen, D. F., Gribouval, O., Broyer, M., Bates, G. P., van't Hoff, W., and Antignac, C. (1998) A novel gene encoding an integral membrane protein is mutated in nephropathic cystinosis. *Nat Genet* **18**, 319-324
137. Ruivo, R., Bellenchi, G. C., Chen, X., Zifarelli, G., Sagne, C., Debacker, C., Pusch, M., Supplisson, S., and Gasnier, B. (2012) Mechanism of proton/substrate coupling in the heptahelical lysosomal transporter cystinosin. *Proc Natl Acad Sci U S A* **109**, E210-217
138. Ponting, C. P., Mott, R., Bork, P., and Copley, R. R. (2001) Novel protein domains and repeats in Drosophila melanogaster: insights into structure, function, and evolution. *Genome Res* **11**, 1996-2008
139. Liu, B., Du, H., Rutkowski, R., Gartner, A., and Wang, X. (2012) LAAT-1 is the lysosomal lysine/arginine transporter that maintains amino acid homeostasis. *Science* **337**, 351-354

140. Llinares, E., Barry, A. O., and Andre, B. (2015) The AP-3 adaptor complex mediates sorting of yeast and mammalian PQ-loop-family basic amino acid transporters to the vacuolar/lysosomal membrane. *Sci Rep* **5**, 16665
141. Lee, Y., Nishizawa, T., Yamashita, K., Ishitani, R., and Nureki, O. (2015) Structural basis for the facilitative diffusion mechanism by SemiSWEET transporter. *Nat Commun* **6**, 6112
142. Tao, Y., Cheung, L. S., Li, S., Eom, J. S., Chen, L. Q., Xu, Y., Perry, K., Frommer, W. B., and Feng, L. (2015) Structure of a eukaryotic SWEET transporter in a homotrimeric complex. *Nature* **527**, 259-263
143. Bretscher, M. S. (1972) Phosphatidyl-ethanolamine: differential labelling in intact cells and cell ghosts of human erythrocytes by a membrane-impermeable reagent. *J Mol Biol* **71**, 523-528
144. Gordesky, S. E., Marinetti, G. V., and Love, R. (1975) The reaction of chemical probes with the erythrocyte membrane. *J Membr Biol* **20**, 111-132
145. Emoto, K., and Umeda, M. (2000) An essential role for a membrane lipid in cytokinesis. Regulation of contractile ring disassembly by redistribution of phosphatidylethanolamine. *The Journal of cell biology* **149**, 1215-1224
146. Suzuki, J., Umeda, M., Sims, P. J., and Nagata, S. (2010) Calcium-dependent phospholipid scrambling by TMEM16F. *Nature* **468**, 834-838
147. Kuhlbrandt, W. (2004) Biology, structure and mechanism of P-type ATPases. *Nature reviews. Molecular cell biology* **5**, 282-295
148. van Veen, S., Sorensen, D. M., Holemans, T., Holen, H. W., Palmgren, M. G., and Vangheluwe, P. (2014) Cellular function and pathological role of ATP13A2 and related P-type transport ATPases in Parkinson's disease and other neurological disorders. *Frontiers in molecular neuroscience* **7**, 48
149. Puts, C. F., Panatala, R., Hennrich, H., Tsareva, A., Williamson, P., and Holthuis, J. C. (2012) Mapping functional interactions in a heterodimeric phospholipid pump. *The Journal of biological chemistry* **287**, 30529-30540
150. van der Velden, L. M., Wichers, C. G., van Breevoort, A. E., Coleman, J. A., Molday, R. S., Berger, R., Klomp, L. W., and van de Graaf, S. F. (2010) Heteromeric interactions required for abundance and subcellular localization of human CDC50 proteins and class 1 P4-ATPases. *The Journal of biological chemistry* **285**, 40088-40096
151. Klomp, L. W., Vargas, J. C., van Mil, S. W., Pawlikowska, L., Strautnieks, S. S., van Eijk, M. J., Juijn, J. A., Pabon-Pena, C., Smith, L. B., DeYoung, J. A., Byrne, J. A., Gombert, J., van der Brugge, G., Berger, R., Jankowska, I., Pawlowska, J., Villa, E., Knisely, A. S., Thompson, R. J., Freimer, N. B., Houwen, R. H., and Bull, L. N. (2004) Characterization of mutations in ATP8B1 associated with hereditary cholestasis. *Hepatology* **40**, 27-38
152. Stapelbroek, J. M., Peters, T. A., van Beurden, D. H., Curfs, J. H., Joosten, A., Beynon, A. J., van Leeuwen, B. M., van der Velden, L. M., Bull, L., Oude Elferink, R. P., van Zanten, B. A., Klomp, L. W., and Houwen, R. H. (2009) ATP8B1 is

essential for maintaining normal hearing. *Proceedings of the National Academy of Sciences of the United States of America* **106**, 9709-9714
153. Dhar, M. S., Sommardahl, C. S., Kirkland, T., Nelson, S., Donnell, R., Johnson, D. K., and Castellani, L. W. (2004) Mice heterozygous for Atp10c, a putative amphipath, represent a novel model of obesity and type 2 diabetes. *The Journal of nutrition* **134**, 799-805
154. Xu, P., Okkeri, J., Hanisch, S., Hu, R. Y., Xu, Q., Pomorski, T. G., and Ding, X. Y. (2009) Identification of a novel mouse P4-ATPase family member highly expressed during spermatogenesis. *Journal of cell science* **122**, 2866-2876
155. Chen, C. Y., Ingram, M. F., Rosal, P. H., and Graham, T. R. (1999) Role for Drs2p, a P-type ATPase and potential aminophospholipid translocase, in yeast late Golgi function. *The Journal of cell biology* **147**, 1223-1236
156. Huh, W. K., Falvo, J. V., Gerke, L. C., Carroll, A. S., Howson, R. W., Weissman, J. S., and O'Shea, E. K. (2003) Global analysis of protein localization in budding yeast. *Nature* **425**, 686-691
157. Iwamoto, K., Hayakawa, T., Murate, M., Makino, A., Ito, K., Fujisawa, T., and Kobayashi, T. (2007) Curvature-dependent recognition of ethanolamine phospholipids by duramycin and cinnamycin. *Biophysical journal* **93**, 1608-1619
158. Georgiev, A. G., Sullivan, D. P., Kersting, M. C., Dittman, J. S., Beh, C. T., and Menon, A. K. (2011) Osh proteins regulate membrane sterol organization but are not required for sterol movement between the ER and PM. *Traffic* **12**, 1341-1355
159. Jarmoszewicz, K., Lukasiak, K., Riezman, H., and Kaminska, J. (2012) Rsp5 ubiquitin ligase is required for protein trafficking in Saccharomyces cerevisiae COPI mutants. *PloS one* **7**, e39582
160. Sherman, F. (2002) Getting started with yeast. *Methods in enzymology* **350**, 3-41
161. Gietz, R. D., and Schiestl, R. H. (2007) High-efficiency yeast transformation using the LiAc/SS carrier DNA/PEG method. *Nat Protoc* **2**, 31-34
162. Sikorski, R. S., and Hieter, P. (1989) A system of shuttle vectors and yeast host strains designed for efficient manipulation of DNA in Saccharomyces cerevisiae. *Genetics* **122**, 19-27
163. Heckman, K. L., and Pease, L. R. (2007) Gene splicing and mutagenesis by PCR-driven overlap extension. *Nature protocols* **2**, 924-932
164. Brodsky, J. L., and Schekman, R. (1993) A Sec63p-BiP complex from yeast is required for protein translocation in a reconstituted proteoliposome. *The Journal of cell biology* **123**, 1355-1363
165. Gong, X., and Chang, A. (2001) A mutant plasma membrane ATPase, Pma1-10, is defective in stability at the yeast cell surface. *Proceedings of the National Academy of Sciences of the United States of America* **98**, 9104-9109

166. Daleke, D. L. (2003) Regulation of transbilayer plasma membrane phospholipid asymmetry. *J Lipid Res* **44**, 233-242
167. Lopez-Marques, R. L., Poulsen, L. R., Bailly, A., Geisler, M., Pomorski, T. G., and Palmgren, M. G. (2015) Structure and mechanism of ATP-dependent phospholipid transporters. *Biochim Biophys Acta* **1850**, 461-475
168. Sherman, F. (1991) Getting started with yeast. *Methods Enzymol* **194**, 3-21
169. Van Driessche, B., Tafforeau, L., Hentges, P., Carr, A. M., and Vandenhaute, J. (2005) Additional vectors for PCR-based gene tagging in Saccharomyces cerevisiae and Schizosaccharomyces pombe using nourseothricin resistance. *Yeast* **22**, 1061-1068
170. Nilsson, L., Jonsson, E., and Tuck, S. (2011) Caenorhabditis elegans numb inhibits endocytic recycling by binding TAT-1 aminophospholipid translocase. *Traffic* **12**, 1839-1849
171. Robinson, J. S., Klionsky, D. J., Banta, L. M., and Emr, S. D. (1988) Protein sorting in Saccharomyces cerevisiae: isolation of mutants defective in the delivery and processing of multiple vacuolar hydrolases. *Molecular and cellular biology* **8**, 4936-4948
172. Gaynor, E. C., Chen, C. Y., Emr, S. D., and Graham, T. R. (1998) ARF is required for maintenance of yeast Golgi and endosome structure and function. *Molecular biology of the cell* **9**, 653-670
173. Sato, K., Sato, M., and Nakano, A. (2001) Rer1p, a retrieval receptor for endoplasmic reticulum membrane proteins, is dynamically localized to the Golgi apparatus by coatomer. *The Journal of cell biology* **152**, 935-944
174. Janke, C., Magiera, M. M., Rathfelder, N., Taxis, C., Reber, S., Maekawa, H., Moreno-Borchart, A., Doenges, G., Schwob, E., Schiebel, E., and Knop, M. (2004) A versatile toolbox for PCR-based tagging of yeast genes: new fluorescent proteins, more markers and promoter substitution cassettes. *Yeast* **21**, 947-962